Innovative Methods for the Diagnosis and Treatment of Implant-associated Infections

Inauguraldissertation
Zur
Erlangung der Würde eines Doktors der Philosophie
Vorgelegt der
Philosophisch-Naturwissenschaftlichen Fakultät
der Universität Basel

von

Daniela Baldoni
Aus Avezzano (AQ), Italy

Basel, 2009

Genehmigt von der Philosophisch-Naturwissenschaftlichen Fakultät auf Antrag von:

PD Dr. Andrej Trampuz
Prof. Dr. Werner Zimmerli
Prof. Dr. Stephan Krähenbühl

Basel, 13th October 2009

Prof. Dr. Eberhard Parlow, Dekan

Acknowledgement

I would like to thank my supervisor, Dr. Andrej Trampuz and Prof. Stephan Krähenbühl, for having given me the opportunity to do my thesis in the laboratory of Infectious Diseases, at the Department of Biomedicine, University Hospital of Basel.

A special thank goes also to all our collaborators, who made possible the proceeding of our research with their enthusiasm and support:
Prof. Dr. Werner Zimmerli, University Hospital of Liestal;
Prof. Regine Landmann of the Department of Biomedicine, University Hospital of Basel;
Prof. Roger Schibli and Prof. Robert Waibel, from the department of Radiopharmaceutical Science at PSI;
Prof. Helmut Maecke from the department of Nuclear Medicine, University Hospital of Basel;
Prof. Alberto Signore, University La Sapienza in Rome;
Dr. Manuel Haschke, Department of Pharmacology, University of Basel.

Many thanks to Zarko Rajacic and Brigitte Schneider for their precious help in the lab.

To my lab members, present and past, Andrea Steinhuber, Anne John, Daniela Abgottspon, Sandrine Aeppli, Eline Angevaare, Karin Probst, Gina Rolli and Ivana Majic, thanks for having always contributed in any working day to maintain a friendly atmosphere in the lab.

Finally, I thank my parents, relatives and friends, for their help and patience.

Table of Contents

Table of Tables

Table of Figures

List of Abbreviations

ATCC	American type culture collection
Cbl	cobalamin
CFU	colony forming units
CLSI	clinical laboratory standards institute
C_{max}	maximum (peak) concentration
C_{min}	minimum (trough) concentration
CPM	counts per minute
CT	computed tomography
DTPA	diethylene triamine pentaacetic acid
GC	growth control
%ID	percentage injected dose
i.p.	intraperitoneal injection
ITLC	instant thin layer chromatography
i.v.	intravenous injection
LEVO	levofloxacin
LNZ	linezolid
MBC	minimal bactericidal concentration
MBIC	minimal biofilm inhibitory concentration
MHB	Muller Hinton broth
MHIC	minimal heat inhibitory concentrations
MIC	minimal inhibitory concentration
MSSA	methicillin susceptible *Staphylococcus aureus*
MSSE	methicillin susceptible *Staphylococcus epidermidis*
MRSA	methicillin resistant *Staphylococcus aureus*
MRSE	methicillin resistant Staphylococcus epidermidis
NaCl	sodium chloride solution
OD	optical density
PAMA	picolylamine monoacetic acid
PCR	polymerase chain reaction
PET	positron emission tomography
PFGE	pulsed field gel electrophoresis
p.i.	post-injection
PBS	phosphate buffer solution

p.o.	per os (oral) administration
RH	Relative heat (joules)
RIF	rifampin
Rpm	revolutions per time
SD	standard deviation
SEM	standard error mean
SPECT	single photon emission tomography
TCF	tissue cage fluid
$t_{1/2}$	half life time
t_{max}	time at which C_{max} is achieved
t_{min}	time at which C_{min} is achieved
T/NT	target to non-target ratio
TSB	triptic soy broth

Summary

Indwelling devices and prosthesis are increasingly used in modern medicine practices. Failures of prosthetic joint devices constitute an important complication. Especially, the management of patients with a septic failure is characterized by difficulties in the diagnosis and by frequent treatment failures, with infection relapses. Thus, the goal of our studies was to establish and evaluate innovative methods for the diagnosis, prophylaxis and treatment of prosthetic infections.

The accurate differentiation between septic and aseptic loosening of the implants is difficult. Nuclear medicine methods are promising, non-invasive procedures aiming to visualize the specific accumulation at sites of infection of an injected radiotracer. However, reliable pre-clinical protocols suitable for screening of radiotracers are missing. In our study, we compared in vitro and in the tissue cage mouse model of implant infection: ^{99m}Tc-UBI, ^{99m}Tc-ciprofloxacin, ^{99m}TcN-CIPROCS$_2$ and ^{111}In-DTPA-biotin for targeting *E. coli* and *S. aureus*. Radiochemical purity of the labeled agents ranged between 94 % and 98 %. Stability in serum was high for all tracers. In vitro binding assays displayed a rapid and non-displaceable bacterial binding for all tested agents. Using the tissue cage mouse model, the tested agents accumulated in vivo in infected sites, being ^{99m}Tc-ciprofloxacin and ^{111}In-DTPA-biotin from 4 h p.i. discriminative for both *E. coli* and *S. aureus* infections, whereas ^{99m}Tc-UBI 29-41 and ^{99m}TcN-CiproCS$_2$ discriminated only for *E. coli* infected cages. The measured tissue cage to blood (T/NT) ratios remained lower than 3, a finding that in our opinion may constitute a limiting factor for the use of the tested tracers in patients.

Following, we evaluated the potentials for targeting infections of the novel transcobalamin II non-binder ^{99m}Tc-labeled derivative of Vitamin B$_{12}$ (^{99m}Tc-PAMA(4)-Cbl). Vitamin B$_{12}$ (Cbl) is an essential co-factor, accumulated by rapidly replicating prokaryotic and eukaryotic cells. For comparison, we tested in parallel the labeled native vitamin ^{57}Co-Cbl and the ^{99m}Tc-PAMA(4)-Cbl derivative. In vitro binding to a *S. aureus* and an *E. coli* strain was specific and could be antagonized by addition of unlabeled Cbl. ^{99m}Tc-PAMA(4)-Cbl showed lower in vitro binding than ^{57}Co-Cbl to *E. coli*, but similar binding to *S. aureus*. In vivo, ^{57}Co-Cbl showed gradual accumulation into the cage fluids, and discriminated only for *E. coli* infected cages. On the contrary, ^{99m}Tc-PAMA(4)-Cbl showed a rapid kinetic, it was rapidly cleared from most tissues and was able to discriminate both *S. aureus* and *E. coli* infected from sterile cages at time points longer than 4 h p.i.. Thus, the new ^{99m}Tc-PAMA(4)-Cbl derivative may represent a promising candidate for bacterial imaging in humans.

In addition, we demonstrated the validity of the mouse tissue cage model for screening radiotracers targeting infections. The negative control, ^{99m}Tc-DTPA, showed rapid accumulation and clearance from both sterile and infected cages, whereas, the positive control, ^{67}Gallium citrate, accumulated

selectively in infected cages between 48 h and 72 h p.i.

Early and accurate detection of methicillin-resistant *Staphylococcus aureus* (MRSA) is essential in the hospital and the outpatient setting. We established a calorimetry assay for discrimination of MRSA from methicillin susceptible *S. aureus* (MSSA). The assay consisted of paired heat measurements of batch cultures in pure medium and in medium supplied with cefoxitin. Relative heat was calculated as ratio between the total heat, measured in the presence and absence of cefoxitin. Using a relative heat cutoff of 0.4, 19 of 20 MRSA (95%) and 10 of 10 MSSA (100%) clinical isolates were correctly identified within 5 h. Thus, microcalorimetry may be successfully applied in routine screening for MRSA and potentially be extended to screen resistance patterns of other pathogens and antibiotic agents.

Ga^{3+} is a semi-metal element competing for iron-binding sites of transporters and enzymes. We investigated the activity of gallium maltolate (GaM), against laboratory and clinical strains of MSSA, MRSA and methicillin susceptible or resistant *S. epidermidis* (MSSE, MRSE). The MICs of GaM were higher for *S. aureus* (375-2000 µg/ml) than *S. epidermidis* (94-200 µg/ml). Minimal biofilm inhibitory concentrations (MBIC) were 3000-≥6000 (*S. aureus*) and 94-3000 µg/ml (*S. epidermidis*). In time-kill studies, GaM exhibited a slow and dose-dependent killing mechanism. Sub-inhibitory concentrations of GaM inhibited growth-related heat production measured in a batch calorimeter. The GaM minimal heat inhibitory concentrations (MHIC) correlated well with the MIC values. Thus, GaM exhibited activity against staphylococci, but high concentrations were required. These data supports the potential use of GaM for local application, including treatment of wound infections, MRSA decolonization and implant coating.

Finally, we investigated the efficacy of linezolid, alone and in combination with rifampin (rifampicin), against MRSA in a guinea pig model of foreign-body infection. In vitro, linezolid was bacteriostatic against the tested strain. In time-kill studies, development of rifampin resistance was observed with rifampin alone, but was prevented by the addition of linezolid. After the administration of single intraperitoneal doses, linezolid concentrations into sterile cage fluids remained above the MIC during 12 h. Antimicrobial treatments administered to animals with cage implant infections were given twice daily for 4 days. Linezolid alone reduced planktonic bacteria in cage fluid during treatment. Efficacy in eradication of cage-associated infection was achieved only when linezolid was combined with rifampin, with cure rates being between 50% and 60%. For comparison, the levofloxacin-rifampin combination was tested and demonstrated the highest cure rate (91%). Thus, the linezolid-rifampin combination may be a treatment option for implant-associated infections caused by quinolone-resistant MRSA.

Chapter 1

Introduction

1.1 Bacterial Infections

It is estimated that the adult human body is colonized by 10^{14} microorganisms, which constitute the natural microflora. Bacteria constitute the most common microorganisms forming the normal human flora, and they inhabit inner and outer body surfaces such as skin, mucosae of the upper respiratory tract, the oral cavity, the intestinal tract, and the urogenital tract.

Adherence of bacteria to host epithelial cells is the first step for colonization and distribution on the different body surfaces. The adherence occurs by specific recognition and binding of protein or polysaccharide structures expressed at the surfaces of the host skin and mucosa. Following, the degree of hydration, the pH, the temperature, and the presence or absence of oxygen and nutrients influence the possible growth and persistence of microorganisms on body surfaces, and their heterogeneous distribution in different regions of the human body [1, 2].

The relationship between the colonizing bacteria and the host could be of symbiosis, commensalisms, and parasitism. The first two differ from each other for the presence and the absence, respectively, of benefits between the colonizing agent and the host. Symbiontic or commensal microorganisms inhabit the human body without harming or causing disease. The maintenance of an equilibrium within these microflora populations is of great importance and protects towards the invasion of both opportunistic and exogenous parasites.

Parasitism is based on the benefits acquired by a pathogenic bacterium invading the host and causing an infection. A bacterial infection is the process occurring when the microbe manifests its pathogenicity, and thus its capacity of inducing disease, by invading and causing a damage (locally or systemically) of the host organism. Pathogenicity of a bacterium could be exerted also without the induction of an infection; an example is the ingestion by the host of bacterial toxins previously released in food or water. The expression of “virulence factors” (adhesins, cation-chelators and toxins) enables the pathogen to subvert the host immune defenses, invade the host and cause a disease. Consequently the infection may remain localized at the site of colonization, or, through hematgenous or lymphatic route, spread to new organs and tissues.

Bacterial virulence factors are essential determinants of the pathogen invading mechanism (tropism of an infection, intracellular or extracellular persistence, adherence and growth in biofilms) and the symptoms of the induced disease (release of toxins, activation of the immune system). The virulence of a pathogen is often measured as the minimal inoculum of the invading organism able to cause an infection, and it is a good indicator of the type (local or systemic) and the severity of the clinical symptoms that can be induced. Consequently, the infectious disease could result in an acute infection, whit a short and severe course, or a chronic, low-grade and long lasting infection [1, 2].

Infections can be classified according to the pathogen in:

- Opportunistic infections: infections caused by microbes belonging to the normal host flora and that initiate an infective process consequently to environmental changes, antimicrobial treatment, traumas and injuries, the reduction of the host immune defenses, or the migration to a new body-compartment;
- Exogenous infections: caused by pathogen organisms, which do not belong to the normal flora but are transmitted to healthy hosts from a contaminated environment (food and water) or from infected carriers (humans or animals). The main routes of transmission of exogenous pathogens from an infected carrier are the air and aerosol, sexual intercourse, blood transfusions or animal bites.

Exogenous infections can be classified according to the site of acquirement in:

- Community-acquired infections: when the transmission occurs within the community;
- Healthcare-acquired infections: when the pathogen is transmitted within a hospital or a health-care institution;

Finally, iatrogenic infections are those developed consequently to a medical procedure such as pharmaceutical treatment or surgery, and could be caused either by endogenous or exogenous pathogens.

1.2 Prosthetic joint-associated Infections

Indwelling devices and prosthesis are increasingly used in modern medicine practices for restoring a function of defective body tissues or organs, or for aesthetic purposes. Especially, orthopedic devices for joint replacement constitute the major procedure for patients with joint pain and compromised mobility, or fracture fixation [3].

Unfortunately, failure of prosthetic joints devices can occur and constitute an important complication. Even if the aseptic loosening of the implants is more frequent, septic failures are more severe, causing high morbidity and extensive costs. The management of patients with implant infections is complicated by frequent infection relapses, and thus, extensive studies have been dedicated in the last decades to establish and optimize therapy guidelines [4, 5].

1.2.1 Pathogenesis of prosthetic joint infections

None of the biomaterials used in medicine is totally inert in the body. Thus, the host immune system responds to the presence of an implant with a localized low-grade inflammation, resulting first in the formation of a membrane of fibrinogen, fibronectin and collagen in which the device becomes encapsulated. Secondly, the phagocytic efficacy of infiltrated ploymorphonuclear cells (PMNs) or macrophages in proximity of the foreign-body decreases, a phenomenon named as “frustrated phagocytosis”. These factors create an interface surrounding the device surface, highly favorable for microbial adherence [3, 6-11].

Indeed, implant-associated infections are characterized by the adhesion and the growth of microorganism, mainly opportunistic bacteria, on the surface of the foreign-body. The initial adherence of the pathogen to the implant occurs through unspecific factors (surface tension, surface shape, hydrophobicity and electrostatic forces) or specific factors (adhesins mediated interactions) and it is dependent on the invading pathogen, the host and the biomaterial of the implanted device [4].

The bacterial adherence to the prosthesis surface is followed by an irreversible attachment and maturation in a complex three-dimensional structure known as biofilm (figure 1). In the biofilm the bacterial cells are embedded in a highly hydrated and porous polymeric extracellular matrix, and persist in a stationary growth-phase. Gene expression and phenotype are regulated within the biofilm cells through intercellular signalling described as quorum sensing, which leads to structural and functional heterogeneity of the biofilm. From the mature biofilm, planktonic bacteria detach and depending on their virulence could cause either a local or a systemic infection [7, 9].

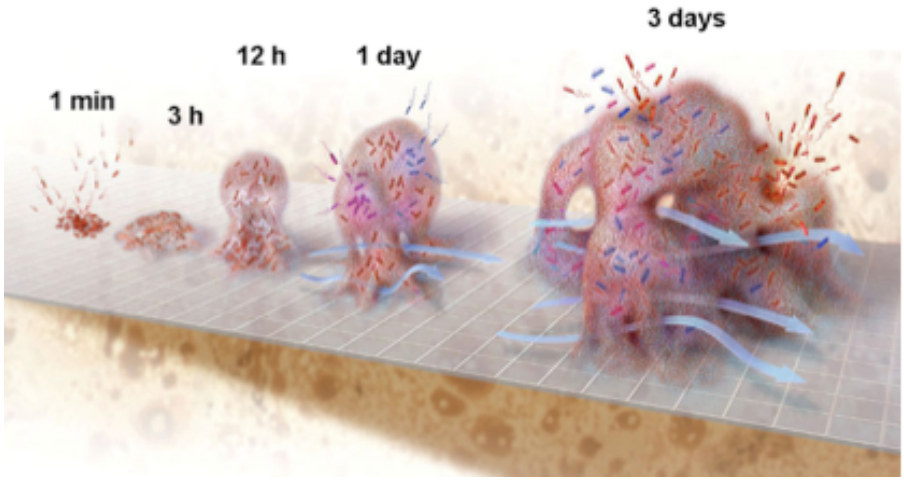

Figure 1. Development of microbial biofilms on an implant surface (illustration adapted from by K. Kasnot, Scientific American, 2001).

The biofilm constitute an excellent survival mechanism for the pathogen, in which bacteria are protected from the immune system and become phenotypically tolerant towards the most used antimicrobial agents. As consequence, the presence of a foreign-body has been reported to increase the virulence of slime-producers opportunistic or exogenous pathogens. Indeed, for strains of staphylococci has been demonstrated that the number of minimal colony forming units (CFU) required to persist and initiate the infectious process in proximity of an implant is dramatically low (≈100 CFU) [5, 6, 9]. Table 1 reports the most common pathogens isolated from prosthetic infections.

Recently, small colony variants (SCV) have been described and isolated from several infection types. SCV bacteria lack functionality of the electron transport cascade, grow slowly and are resistant to most replication phase-dependent and cell-wall-active antimicrobials. Especially, *Staphylococcus aureus* SCV have been reported in prosthetic infection and have been a main risk factor for treatment failures, persistence and relapse of infection [3, 12].

Table 1. Frequency of most common identified microorganisms causing prosthetic joint-associated infections (adapted from Trampuz et al [5])

Microorganism	**Frequency (%)**
Staphylococcus aureus	30-43
Coagulase-negative staphylococci	17-21
Polymicrobial	5-13
Gram-negative bacilli	5-14
Anaerobes	2-5
Enterococci	3-7
Streptococci	11-12
Other/Unknown	5-6

1.2.2 Classification of prosthetic joint infections

Prosthetic joint-infections have been classified depending on the delay of the first symptoms from the date of surgery, as: early, delayed and late infections [4, 5, 13].

Early and delayed prosthetic infections occur either within 3 months or between 3 and 24 months, respectively, after surgery. They constitute the most common cause of implant infection and they are generally caused by inoculation of the implant during the surgery (perioperative), or infection of the wounds shortly after surgery. In early prosthesis infections, highly virulent pathogens such as *S. aureus* and gram-negative bacilli are generally involved. The symptoms recorded are analogue to the ones of an acute infection with local swelling and pain, erythema and fever. On the contrary, when the infective pathogens are low virulent, such as *S. epidermidis* and other coagulase-negative staphylococci, or *Propionibacterium acnes*, the infection usually becomes symptomatic later than 3 months after surgery, and it is defined as delayed. The delayed infections manifest due to a chronic inflammation reaction from the host and the symptoms are hardly distinguished from the ones of an aseptic failure [4, 5, 11, 14].

Finally, late infections manifest 24 months after surgery and are usually caused by haematogenous seeding during bacteremia originated from a distant infection focus, such as infection of the skin, soft tissues, the oral cavity, the urogenital or the respiratory tract. Late infections are mainly caused by high virulent bacteria and present all symptoms of acute infections [3, 13, 15].

1.3 Diagnosis of Prosthetic Joint-associated Infections

The correct diagnosis of prosthetic joint infection, and their differentiation from aseptic failure of the implant, is essential for choosing the optimal treatment procedures. Several pre- and intra-operative tests have been standardized and are currently routinely used (table 2). Early and late infections are often predicted by evidence of clinical symptoms such as fever, swelling and pain, and presence of a sinus tract. The most challenging have become the identification of chronic delayed infections, due to the lack of clinical symptoms discriminative for infections and also reduced specificity of most laboratory tests.

Table 2. Conventional pre-operative and intra-operative tests for the diagnosis of prosthetic joint-associated infections (adapted from Trampuz et al. [16])

Category	Diagnostic test
Pre-operative	
Clinical history and examination	Persistent joint pain; Fever, chills or rigors without known etiology; Erythema, warmth or effusion of the joint; Sinus tract;
Hematological tests	Leukocyte count and differential; erythrocyte sedimentation rate; C-reactive protein level
Synovial fluid aspiration	Leukocyte count and differential; Gram stain and culture
Radiographic imaging	Plain radiography, computer tomography
Radionuclide bone scanning	Scintigraphy by a technetium-99m scan, ^{67}Ga-citrate, ^{111}In-leukocytes, ^{99m}Tc-immunoglobulines
Positron emission tomography	^{18}F-fluorodeoxyglucose
Intra-operative	
Periprosthetic tissue	Hystopathology; Gram stain and culture
Explanted prosthesis	Culture

Based on the criteria to be evaluated, the diagnostic tests could be classified as: indirect, when abnormalities in the patient biochemical and physiologic parameters are used as predictors of infection, and direct, when the indicator for the infection process is the confirmed presence of the invading microbe in the peri-prosthetic fluid and tissues (figure 2). Laboratory cultures and microbiologic methods, histopathology examinations, imaging techniques and sonication of explanted devices have been widely used and evaluated, but there is no single method, which has reached

satisfying accuracy, sensitivity and specificity. Thus, the accurate diagnosis of prosthetic infections is usually achieved by performing both direct and indirect tests [4, 8, 17, 18].

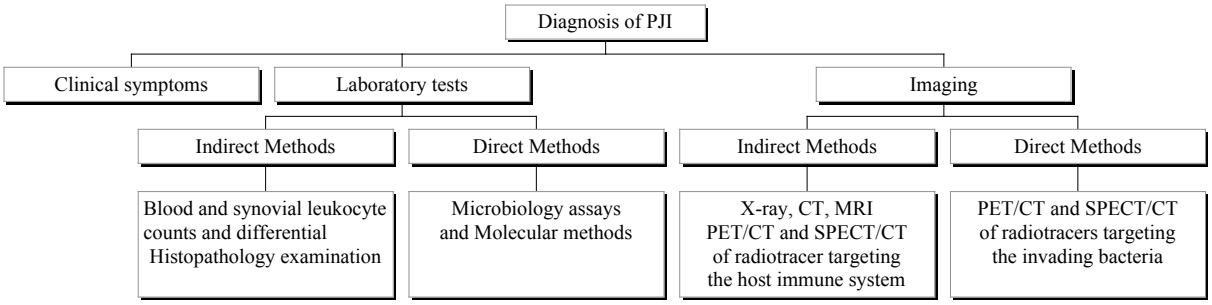

Figure 2. Organization chart of direct and indirect methods adopted for the diagnosis of prosthetic joint infections (PJI).

1.3.1 Laboratory tests

Indirect methods. Conventional laboratory tests for diagnosis of infections such as increased neutrophil counts, elevated C-reactive protein level, and erythrocyte sedimentation rate, constitute simple, low-invasive and fast tests assessing host parameters predicting an ongoing infection.

Leukocyte count and differential in blood and synovial fluid constitute a simple and commonly performed method. However, blood leukocyte counts are usually extremely variable in patients with prosthetic joint failure, and thus, even in repetitive sampling, the discrimination between infections and aseptic inflammation is limited. On the other hand, synovial fluid leukocyte counts is an accurate test, and counts $>1.7\times10^9$ cells/l have been reported having a sensitivity and specificity of 94% and 88%, respectively. Or, in acute infections (early and late infection), a finding of more than 65% granulocytes, has a sensitivity and specificity for infection of 97% and 98%, respectively [17-19].

Histopathology tests of the periprosthetic tissue also constitute valid procedures, and they are based on the staining and differential evaluation of granulocytes' infiltration. However, the tissue specimens are highly heterogeneous, thus, sampling of different areas is recommended [4, 16].

Direct methods. Cultures of blood, synovial fluid or peri-prosthetic tissue specimens in enriched non-selective media, approach the diagnosis of implant-infection by the direct detection of the infective agent. The recovery of the infecting bacteria is followed by standard microbiologic and antimicrobial susceptibility assays.

Synovial fluid or tissue specimens contain a variable and often low number of bacteria, depending on the invading microbe and on its detachment from the biofilm. Replicate specimens cultured in different media, temperature and aerobic-anaerobic conditions increase the recovery of a vast range of organisms in shorter times [18]. Gram stain of synovial fluid or peri-prosthetic tissue specimens gives

already important information about the invading microbes and results in high specificity, ranging from 92% to 100%, but the sensitivity is usually low (< 26%) [4, 17].

When removal of the implant is required, the sonication of the explanted device and the sub-culture of the sonication fluid, have shown a sensitivity of 79%, whereas the conventional cultures of periprosthetic tissue have a sensitivity of 60%. Indeed, the sonication induces the partial dislodgment of the bacterial biofilm from the device surface, helping their recovery from the implant and their growth in culture. As drawback, there is a high risk of contamination of the device during the surgery procedure, which could create artifacts in the final culture results [20].

Microbiology assays have the advantage of giving direct information about the infecting pathogen and thus, are essential for the choice of therapy. However, the sensitivity is generally low and could be further affected by any antimicrobial therapy started before sampling.

Molecular methods, such as broad-range PCR (bacterial 16S rDNA), constitute a sensitive and innovative procedure for the accurate identification of the invading microorganisms. In addition, the characterization of resistance patterns could be accomplished through the identification of specific genetic elements encoding for resistance factors (es. methicillin resistance mecA gene). However, the high costs, the risk of contamination, and the labour-intensive sample preparation have delayed the routine application of molecular methods in the diagnosis of prosthetic joint infections [16].

1.3.2 Imaging and nuclear medicine

Imaging techniques can be classified as either structural or functional. Structural imaging procedures are used to evaluate macroscopic morphological changes and implant loosening [4, 21, 22]. Differently, functional imaging procedures aim to visualize the specific accumulation of an injected gamma-emitter radiotracer at the site of infection. The main characteristics of an ideal radiotracer for diagnosis of infections are:

- well-understood and characterized chemical structure,
- high efficiency of labeling,
- high stability in serum,
- low toxicity or light side effects,
- rapid and specific accumulation at the infection site,
- and fast clearance from all non-infected organs and tissues.

The progresses in positron electron tomography and single photon computed tomography (PET and SPECT) for total body scans, together with the experience gathered in the handling and safety of short half-lives radioisotopes, stimulated the pre-clinical and clinical research towards novel radiolabeled agents. Even if the sensitivity of most radiotracers is high, the main challenge remains the

achievement of a satisfying chemical characterization and infection specificity [23].

Indirect methods. Morphological imaging techniques such as conventional X-ray, CT and MRI constitute standard procedures to evaluate the structural bone and tissue damage, with loose implants or chronically inflamed joints. However, differentiation between aseptic and septic failure cannot always be achieved with these techniques. Additional limits are that metallic devices and prosthesis can produce artefacts both in CT and MRI [4, 21, 22].

The use of radionuclide scintigraphy is more suitable to discriminate between aseptic and septic loosening of prosthetic joints. The gamma-emitter isotope gallium-67 was recognized nearly 40 years ago to accumulate in infection and inflammation sites and thus, it was widely used to enhance the diagnostic accuracy of planar scintigraphy in patients with suspected loose prosthetic joints. However, Gallium-67 has many drawbacks, which limited its applications: it is not specific towards infections, it has a long decay half-life, and a long persistence in non-target tissues. In addition, a delay of 24 h to 72 h from the injection of the ^{67}Ga-citrate solution is needed for achieving good contrast in scintigraphic scans [17, 21, 22, 24, 25].

The gold standard for functional imaging of bacterial infections is the labeled host leukocytes. The leukocytes isolated from the patient are mainly granulocytes, and they can be labeled ex vivo with Indium-111 or technetium-99m. However, the procedure is long and labor-intensive, it involves direct handling of blood products, and it requires highly qualified technicians. In addition, for the diagnosis of prosthesis infections, the labeled leukocytes have been reported having high sensitivity in acute but not in low-grade delayed infections, whereas the specificity was variable or often inconsistent [17, 21, 24, 26]. Alternatively, radiolabeled monoclonal antibodies or antibody's fragments of G or M class, targeting specific receptors expressed on leukocytes during infection, have been synthesized and evaluated. Clinical studies initially reported an accuracy of 95% with Fanolesonab®, a murine monoclonal immunoglobulin M binding to CD15 receptors on leukocytes. However, the studies were withdrawn due to serious, including two fatal, events after administration [27]. Sulesomab®, a techentium-99m labeled Fab' fragment of monoclonal IgG, and the murine monoclonal IgG1 BW 250/183 target the glycoprotein cross-reacting antigen-90 and 95, respectively. They both constitute a valid complementary diagnostic tool, showing sensitivity and specificity of about 85% for detecting prosthesis infections. Especially, the use of antibody fragments, rather than whole monoclonal antibody, has been preferred due to the lower incidence of adverse events [18, 21, 22, 28].

An alternative to immunoglobulines has been the use of radiolabeled cytokines and chemokines (IL-1, IL-2, IL-8, PF4). These radiotracers were mainly tested in pre-clinical studies, while clinical trials were limited by the lack of specificity or the unacceptable side effects [21, 29].

Finally, PET/ CT of F-18 fludeoxyglucose has been evaluated as an auxiliary diagnostic tool for visualizing loosening prosthetic joints. The tracer is sensitive to local increase in blood flow and vascular permeability during inflammation processes, and to the preferential binding to activated

leukocytes [18, 24, 27, 30]. However, no discrimination between infection and aseptic inflammation can be achieved.

Direct methods. The research in the development of tracers targeting directly the infective pathogen, rather than host receptors and physiologic changes, is a novel and challenging issue. A wide and heterogeneous class of radiopharmaceuticals, such as radiolabeled antimicrobial peptides (^{18}F- and ^{99m}Tc-UBI 29-41), synthetic antimicrobial agents (^{99m}Tc- and ^{18}F-ciprofloxacin, ^{99m}Tc-sparfloxacin, ^{99m}Tc-ceftizodime and ^{99m}Tc-eperizolid), bacteriophages, and growth factors (^{99m}Tc- and ^{111}In-biotin) has been described [21, 23, 27, 31]. By binding directly and selectively the infecting organism, such radiotracers represent a promising tool for the discrimination of infection from sterile inflammation. However, the main issue will be to determine if imaging of infection with bacteria-specific radiotracers may represent a feasible procedure. Indeed, the small surface of bacterial cells and their relative low number in chronic/subacute infections, are important limiting factors for visualization of in vivo radiolabeled bacteria. Pre-clinical and clinical studies are still limited, and have sometimes reported conflicting results. Thus, additional optimization is needed, together with the development of standard guidelines for radiotracer labeling and scan interpretations [17, 31, 32].

1.4 Calorimetry in Diagnostic Microbiology

Calorimetry is a sensitive, simple, high reproducible and fast technique in development for clinical and experimental microbiology. The principle is that any dividing microorganism produces heat proportionally to their metabolism (catabolism) and replication rate. As consequence, bacterial culture constitutes a close thermodynamic system, which, at constant pressure and temperature, exchanges heat with its surrounding proportionally to the number of replicating organisms. The heat produced can be recorded in real time, and plotted as heat flow (Watt) versus time (thermogram). The slope of the heat flow curve at each time point depends on the replication rate of the cells, while the area under the heat flow curve is the total heat (Joule), which is proportional to the final number of cells (figure 3) [33-35].

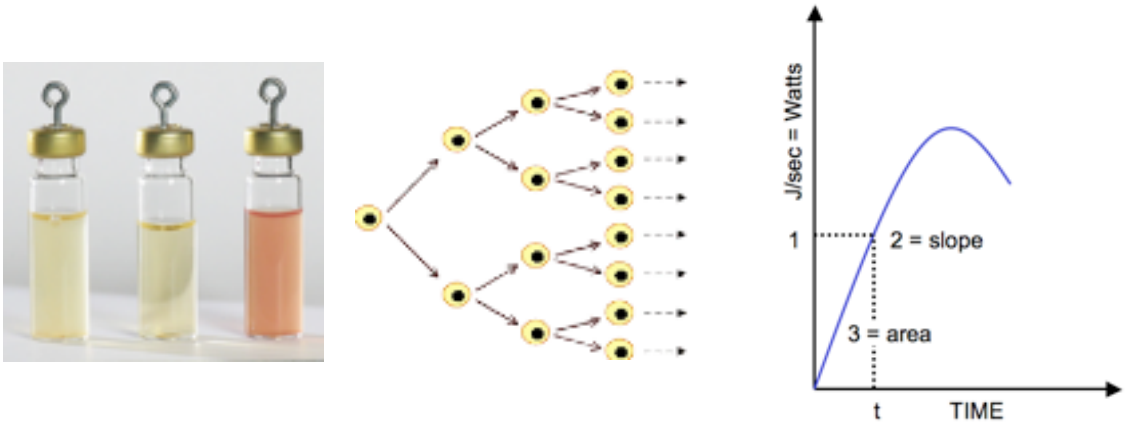

Figure 3. Bacterial cultures in sealed calorimetric ampoules (left) at 37°C are associated to exponential bacterial growth (center), which can be measured and plotted as replication-dependent cumulative heat (right): 1 indicates rate of heat production at time t, proportional to the number of replicating cells, 2 the change in rate of heat production at time t, and 3 the total heat produced by time t.

Heat of bacterial cultures at 37°C can be measured with a batch calorimeter. For clinical microbiology, the isotherm thermopile heat-conduction microcalorimeter is the most commonly reported by experimental studies, due to its high sensitivity and precision.

The calorimeter continuously measures temperature differential between the sample (bacterial culture) and a thermally inert reference (figure 4). A heat sink made of a metal block, connects the sample and the reference vessels through a thermopile ("Peltier effect plates" semiconducting thermoelectric plates). The heat production rate is proportional to the potential between the thermocouple plates generated by the heat flow from the sample vessel through the thermopiles to the metal heat sink [33]. The Thermal Activity Monitor (TAM, Model 3102 TAM III, TA Instruments, New Castle, DE, USA), displayed in figure 4, is an example of batch isothermal thermopile calorimeter, which allows parallel measurements of different samples in 48 channels with a detection

limit of ±0.225 µW.

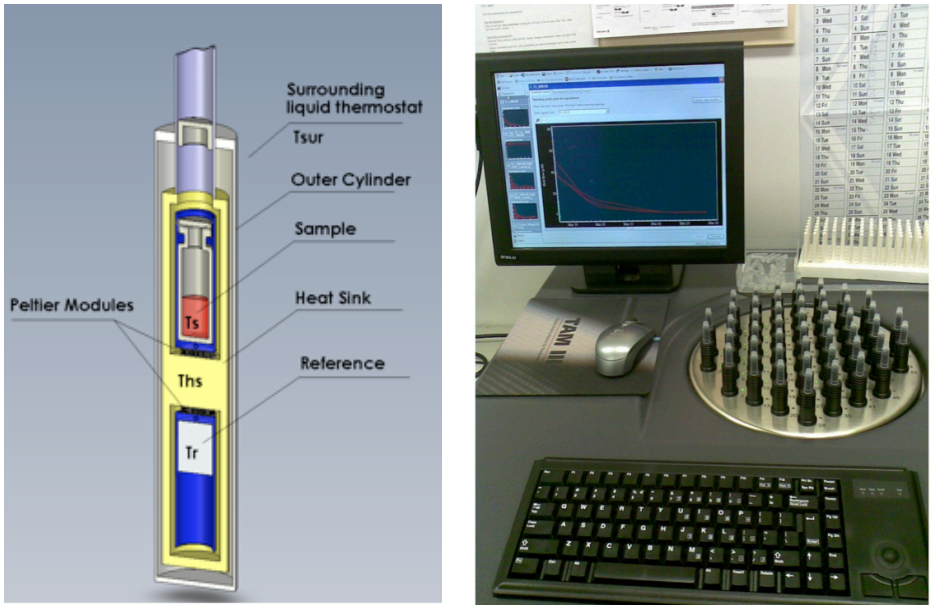

Figure 4. Schematic assembly of batch calorimetric unit of the instrument used in our studies, temperature differences between the sample (Ts) and a thermally inert reference (Tr) is continuously measured in a heat sink (Ths) (left); and TAM, Model 3102 TAM III, TA Instruments, New Castle, DE, USA (right).

In the diagnosis of infections, enriched growth media inoculated with patient specimens (blood, synovial fluid or periprosthetic tissue), with catheter or implant sections, or with implant sonication fluids, can be incubated in a batch isothermal calorimeter and the heat flow monitored as indicator of microbial infection.

The use of selective growth media may allow the recovery of specific microbes, when present in the specimens. In addition, rapid determination of resistance patterns could be performed by incubation of the isolated infective pathogen with test antimicrobials at concentrations correspondent to their resistance cut-off. Susceptible microorganisms are inhibited in their growth and will not lead to any heat measurements; contrarily, resistant bacteria are not inhibited and thus, will produce heat, independently on the presence or absence of the antimicrobial agent [33]. Due to the high sensitivity to the heat produced during bacterial growth, the detection of resistance by calorimetry may be faster than most of culture methods, which are based on the optical evaluation of turbidity associated to the bacterial growth (requiring between 24 h and 48 h of incubation).

Calorimetric methods showed also potentials for early determination of MIC values, or for screening sub-inhibitory concentration of antimicrobial agents against the isolated pathogen. The latter methods allow the early discrimination of the most effective antimicrobials inhibiting heat, and thus, the bacterial catabolism and replication rate [34].

Calorimetric methods have not entered yet into the routine microbiologic procedures, but several studies have been and are conducted to elucidate the benefits and potentials for clinical applications. In

addition, calorimetric techniques have a wide application in experimental microbiology for evaluation of drug-related antimicrobial inhibitory profiles, dose and time dependency of antimicrobials mechanism, antimicrobial post-antibiotic effect on bacterial cultures, potentials of combinations of antimicrobial agents in preventing bacterial growth or development of resistance [34].

1.5 Prevention and Treatment of Prosthetic Joint-associated Infections

The treatment of prosthetic joint-associated infections has the main goal of restoring a pain-free, functional joint. The frequent relapses of the infection and failure of the implants constitute a main cause of morbidity [4]. Within the biofilm, bacteria have shown a 1000-fold higher tolerance, than planktonic bacteria, towards many antimicrobial agents. In addition, the spread of resistant strains has reduced the choice of possible active agents. Methicillin-resistant *S. aureus* (MRSA) and coagulase-negative staphylococci (MRSE) have been associated to increased morbidity and treatment failures, especially when combined to tolerance towards glycopeptides, such as vancomycin [5, 13].

1.5.1 Antimicrobial prophylaxis

Protocols have been developed for the prevention of perioperative infections, which constitute the most frequent cause of prosthetic joint-associated infections. As first, the use of sterile instruments, ultra-clean conditions and of laminar airflow in the operating room, has become standard practice together with the administration of systemic antimicrobial prophylaxis. The antimicrobial agents for prophylaxis should be chosen in each health care centre depending on the most commonly species isolated from healthcare-acquired infections, and their susceptibility-resistance pattern. In general, first- or second-generation cephalosporins, such as cefazolin, cefamandole or cefuroxime, effective against staphylococci and streptococci are the first-choice antimicrobials, when the patient is not allergic or the risk of MRSA infection is minor. Otherwise, vancomycin and teicoplanin can be used. The antimicrobial prophylaxis should be given within 30 and 60 minutes prior to surgery, in order to have periprosthetic tissue levels above the minimal inhibitory concentrations (MICs) at the time of incision and during the whole time of the surgery [5, 13].

In order to reduce the risk of secondary infections, nasal and skin decolonization with mupirocin of patients with indwelling devices and positive for MRSA is recommended by some experts, but no uniform guidelines are accepted. Otherwise, the benefits of antimicrobial prophylaxis in risk of haematogenous infections due to dental surgery, or a secondary localized infection, are unknown. In any case, the early diagnosis and administration of antimicrobial therapy when a bacteremia occurs is essential for reducing the risk of implant-infection.

1.5.2 Antimicrobial coating of implants

A combinatory approach to systemic prophylaxis for the prevention of bacterial perioperative infection is the use of antimicrobial-coated implants and impregnated cement. Several substances have been evaluated, such as: standard antimicrobials (gentamicin, ciprofloxacin, flucloxacillin and

vancomycin), antiseptics (chlorexidine or quaternary ammonia compounds), hydrophilic proteins (albumin, poly-l-lysine), polysaccharides (hyaluronic acid), lysostaphin or inorganic salts (copper, silver ions and silver nitrate, or nitric oxide). Substances having a wide antimicrobial spectrum and a low rate of induction of resistance are recommended. For standard antimicrobial agents it is mandatory that the concentrations released from the implant remain above the MIC, in order to prevent the emergence of resistant strains. Contrarily, inorganic substances active against bacterial adherence are usually not associated with mechanisms of development of resistance [7, 11].

The principle of implant coating would be the local and immediate release of a burst of the antimicrobial agent, followed by a gradual and long-term release. The presence of an anti-biofilm substance covering the surface of the implant would modify the implant-tissue interface and reduce the bacterial adherence mechanisms. In addition, the systemic dose of antimicrobials used for prophylaxis could be lowered, when combined to a coated implant, minimizing the systemic toxicity of the first.

Currently, several research studies about coating procedures (bioactive treatments, simple impregnation and covalent bonding), evaluation of innovative substances and their local and systemic toxicity, are aiming to develop a coating technology for the active prevention of biofilm formation in vivo [4, 7, 11, 36, 37].

1.5.3 Treatment algorithm for prosthetic joint-associated infections

Different treatments of prosthetic joint-infections have been developed and adapted depending on the type of infection (early, delayed or late), the severity (local or systemic) of the clinical symptoms, the stability of the implant and the condition of the periprosthetic tissue. Debridement with implant retention can be used for stable implants, infected by hematogenous route or early after surgery (with symptom duration <3 weeks). Figure 5 shows the algorithm developed by Zimmerli et al. as general guideline for the management of prosthetic joint-associated infections with implant retention [4, 5, 13]. This algorithm was validated in cohort studies of total hip and knee prosthetic infections with an overall efficacy rate of 80% [38].

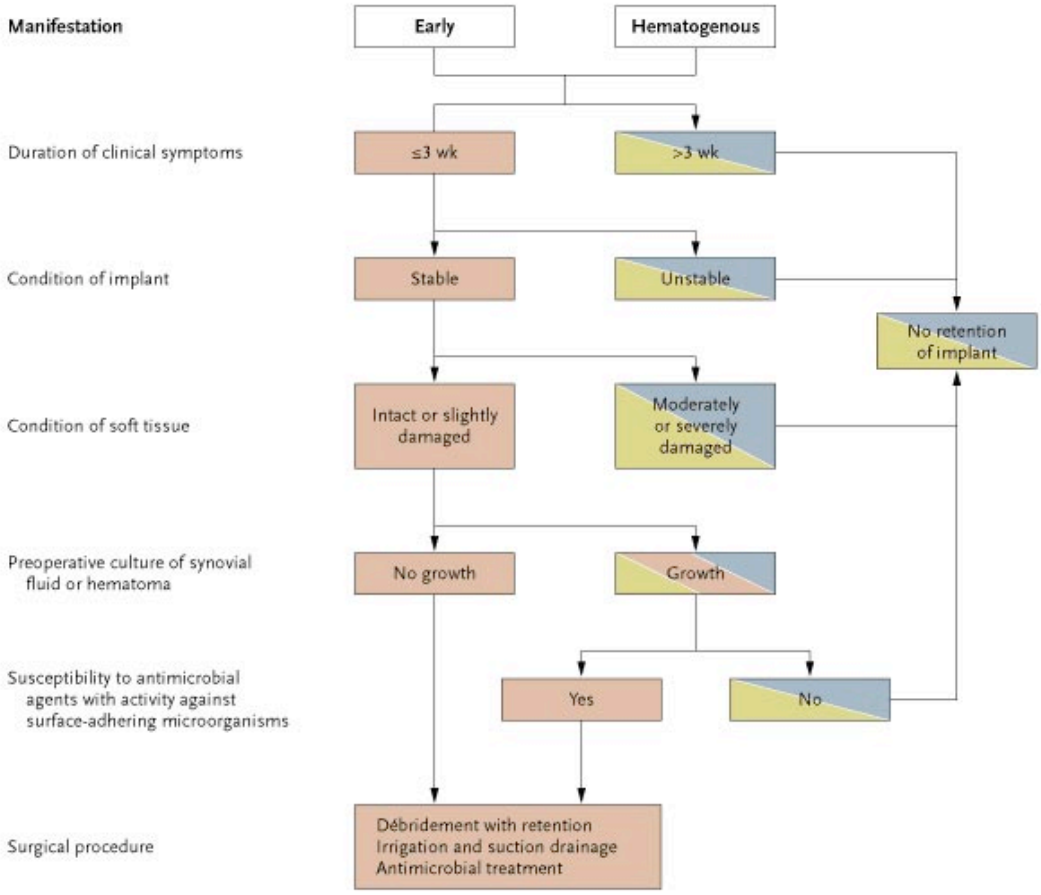

Figure 5. Zimmerli algorithm for the management of patients with prosthetic joint-associated infection qualifying for implant retention (adapted from Zimmerli et al. [4]).

In all other cases (figure 6), a one-stage or two-stage prosthesis exchange is recommended. In two-stage exchanges, a long interval (6-8 weeks) is recommended, if rifampin-resistant staphylococci, quinolon-resistant gram-negative bacilli or small-colony variants of bacteria are involved. In addition, long-term therapy (3 months) with combinations of bactericidal and anti-biofilm antimicrobial agents is mandatory.

Especially, the management of patients with prosthetic joint infections associated with multi-resistant *S. aureus* strains or SCV, may require a two-stage procedure including implant removal without use of spacer [12].

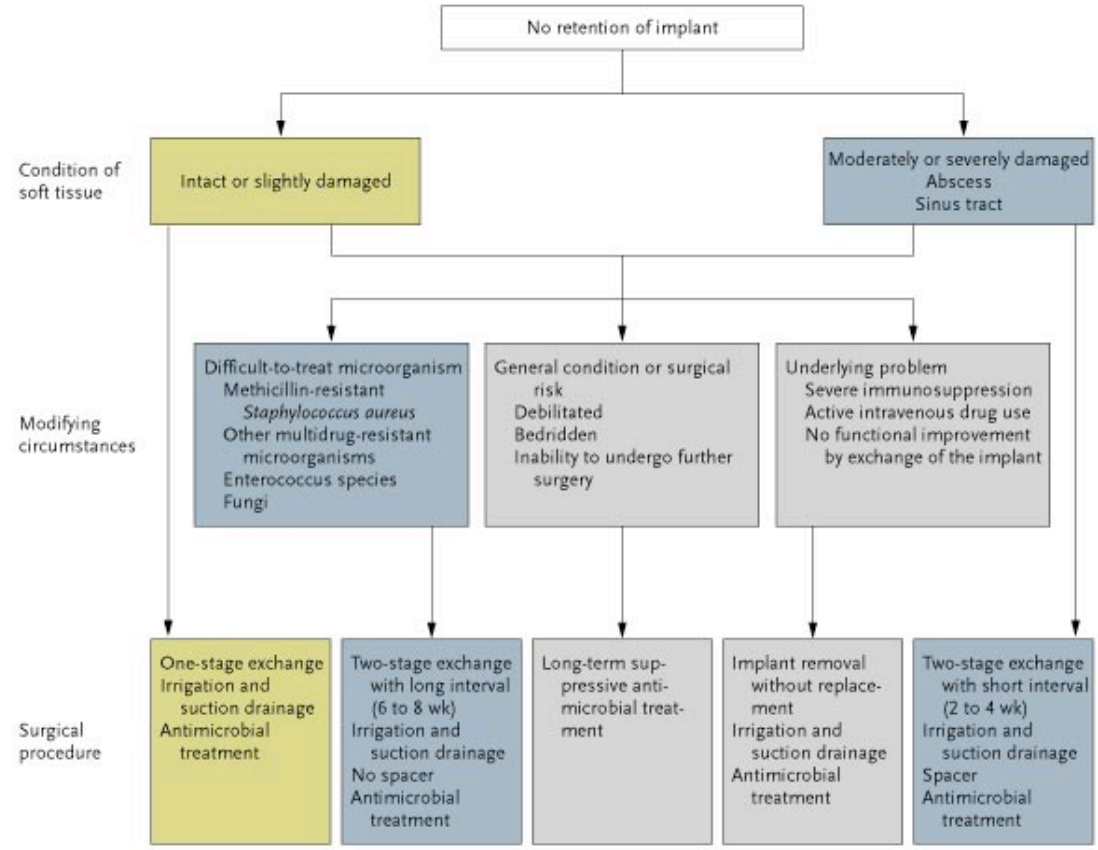

Figure 6. Zimmerli algorithm for the management of patients with prosthetic joint-associated infection qualifying for implant exchange (adapted from Zimmerli et al. [4])

1.6 Antimicrobial Therapy of Prosthetic Joints Infections associated with Staphylococci

1.6.1 Antimicrobial therapy guidelines

Eradication of prosthetic joint infections requires both, surgical and antimicrobial therapy. The eradication of the biofilm constitutes the main challenge. Indeed, in the biofilm, bacteria persist in a stationary growth phase, which makes them tolerant towards most antimicrobial agents. In addition, the polymeric matrix of the biofilm forms a physical protective barrier, which reduces the concentration of antimicrobials reaching the embedded bacterial cells. As consequence, the antimicrobial therapy of prosthetic infections requires bactericidal agents, given in combination and administered for long-term [4, 5, 13]. Further complications have raised consequently the spread of methicillin resistant staphylococci in the hospital setting and in the community [11, 39].

The ideal antimicrobial therapy of prosthetic infection would consist of a combination of agents: acting synergistically, effective against biofilm, bactericidal against stationary phase bacteria, rarely associated to induction of resistance, active at low concentrations, well-tolerated, non-toxic and suitable to be given orally.

The research conducted in the last decades has brought important progresses in the treatment of patients with prosthetic infections upon the establishment of antimicrobial therapy guidelines (table 3).

In pre-clinical and clinical studies rifampin was the only agent, which gave evidence of high efficacy against staphylococcal biofilm, and as consequence, it became mandatory component in any antimicrobial regimen against staphylococcal prosthetic infection. The high incidence of development of rifampin-resistance, when the agent was used in monotherapy, stimulated the development of effective and well-tolerated rifampin combinations with other anti-staphylococcal antimicrobials [40-42].

Nowadays, rifampin-containing regimens are administered for totally 3 months. The first choice for treating methicillin-susceptible staphylococcal infections is the rifampin combination with a beta-lactam. In case of hypersensitivity to beta-lactams or in case of methicillin-resistant staphylococcal infection, rifampin combinations with ciprofloxacin have shown good activity and safety profiles [43]. Moreover, newer fluoroquinolone agents (levofloxacin, moxifloxacin) have displayed higher anti-staphylococcal activity in vitro than ciprofloxacin, and are now under evaluation for long-term safety data. Unfortunately, the use of fluoroquinolones against MRSA prosthetic infections has been limited by the spread of resistance towards these agents. Thus, in alternative, glycopeptides such as vancomycin and teicoplanin could be used, even if associated to frequent adverse events and low efficacy rates. Extensive pre-clinical and clinical research have been evaluating the potentials of new rifampin combinations with the oxazolidindione linezolid, the lipopeptide daptomycin, the

lipoglycopeptide dalbavancin, the streptogamin quinupristin/ dalfopristin and the glycylcycline tigecycline. However, systematic studies should be conducted to evaluate their applicability to staphylococcal prosthetic joint infections and safety in long-term combination therapies [4, 5, 13]

Table 3. Antimicrobial treatment of staphylococcal prosthetic infections (adapted from Zimmerli et al. [5])

Microorganism	Antibacterial agent	Route
Methicillin-susceptible staphylococci		
	Rifampin plus (flu)cloxacillin for 2 weeks followed by	PO/IV
	Rifampin plus ciprofloxacin or levofloxacin for 10 weeks	PO
Methicillin-resistant staphylococci		
	Rifampin plus (vancomycin or daptomycin) for 2 weeks, followed by	PO/IV
	Rifampin plus ciprofloxacin or levofloxacin or fusidic acid or cotrimoxazole or minocycline, for 10 weeks	PO

PO: *per os,* oral administration route

IV: intravenous administration route

1.6.2 Rifampin

Rifampin (figure 7) is a semisynthetic bactericidal antibiotic belonging to the group of ryfamicins. The mechanism of antimicrobial action is the binding to the beta-subunit of the bacterial RNA-polymerase followed by blockage of DNA transcription into messenger RNA, and as consequence, of the protein synthesis [44].

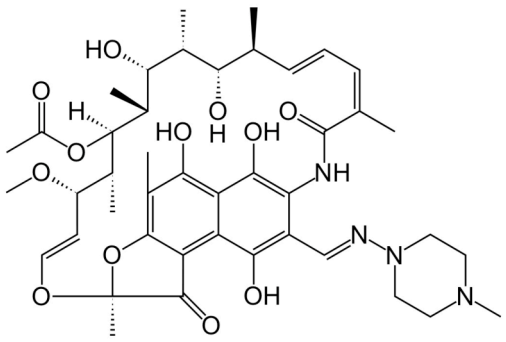

Figure 7. Chemical structure of rifampin.

Rifampin is bactericidal against most of gram-positive bacteria, growing both intra- and extra-cellularly, and is the first choice in the combined therapy of *Mycobacterium* infections. Especially, because of its activity against staphylococcal biofilms, rifampin became an essential component of

combined regimens for the treatment of methicillin-susceptible and methicillin-resistant staphylococci [43]. The development of rifampin resistance is determined by one-step point-mutations in the rpoB gene encoding for the beta-subunit protein binding pocket of the bacterial ribosome. The mutation is associate to the complete loss of activity by rifamycins [44]. Thus, monotherapy is not possible, whereas antimicrobial combinations able to increase rifampin potency and prevent occurrence of resistance, represent the only treatment option for difficult infections [5, 42].

Rifampin is available as intravenous and oral formulations, the latter having high bioavailability (90% to 95%). Peak serum concentrations are achieved in healthy volunteers between 2 and 4 h after administration and the serum half-life ranges from 1.5 to 5 h. Binding to serum protein is over 90%. The metabolism is hepatic and consists of hydrolysis of the ester functional group and deacetylation, followed by elimination through the faeces. The renal elimination of rifampin is lower than 30% of the administered dose.

Rifampin up-regulates the expression and function of hepatic CYP450 and thus, may reduce the half-life of any other drug co-administered and metabolized by this enzyme family.

Most common mild adverse effects are fever, gastrointestinal disturbances, rashes, breathlessness feeling and immunological reactions (development of anti-rifampin antibodies). Severe adverse effects are rare, but hepatic toxicity, with liver failure has been reported [44]. Moreover, novel rifamycin derivatives with reduced activation of the CYP450 and thus, with reduced drug-drug interactions, have shown efficacy against staphylococcal infections and biofilms. The derivative ABI-043 was a promising candidate with similar treatment efficacy than rifampin in the tissue cage animal model of *S. aureus* prosthetic joint infection [42].

1.6.3 Fluoroquinolones

Fluoroquinolones (figure 8) are a family of synthetic broad-spectrum bactericidal antimicrobials, which share with their precursor, the 4-quinolone nalidixic acid, the mechanism of action. The bacterial target of fluoroquinolone agents is the DNA gyrase, or topoisomerase IV, essential for the double-strand supercoiling and relaxation during DNA replication. Binding and inhibition of the DNA-gyrase results in DNA fragmentation and rapid cell death [45]. A limitation in the use of fluoroquinolone in the clinical practice has been the arising emergence of resistance. The main resistance mechanism consists of the over-expression of efflux pumps on the bacterial plasmatic membranes, encoded within the bacterial genome or in genetic mobile elements. Additional resistance mechanisms consist of: plasmid-mediated proteins able to bind the bacterial DNA-gyrase and to protect from fluoroquinolones activity, or mutations in the structure of the DNA gyrase resulting in decreased fluoroquinolones binding affinity [45, 46].

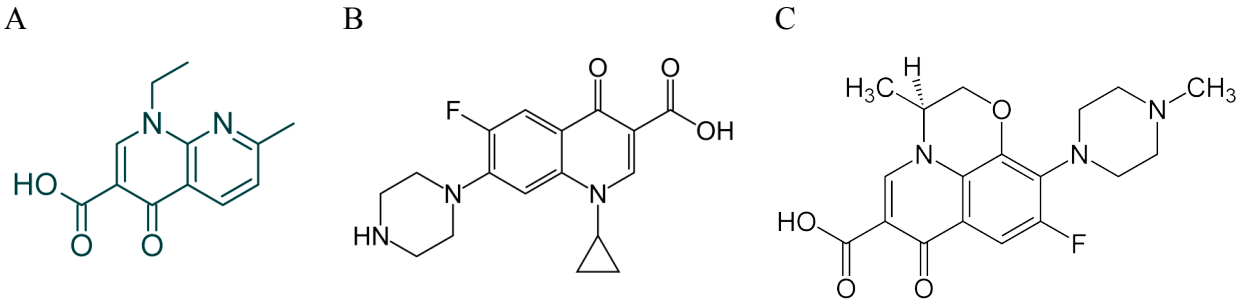

Figure 8. Chemical structure of the 4-quinolone nalidixic acid (A), and the fluoroquinolones ciprofloxacin (B) and S-levofloxacin (C).

Ciprofloxacin is a broad-spectrum fluoroquinolone and it has been extensively studied for treatment of prosthetic staphylococcal infections. Within the new generation of extended-spectrum fluoroquinolones, levofloxacin displayed improved bactericidal activity and consistent post-antibiotic effect against Gram-positive aerobes including *S. aureus* and MRSA.

Novel fluoroquinolones have favourable pharmacokinetic profiles, especially, excellent tissue penetration and convenient once-daily dosing [45]. Indeed, levofloxacin is well absorbed after oral administration, with 99% bioavailabilty, and it is mainly eliminated unchanged in the urine. Possible activity on liver enzymes, including inhibition of CYP450, was exerted from ciprofloxacin and earlier fluoroquinolones, but not by levofloxacin. Fluoroquinolones are usually well-tolerated agents, with severe adverse event occurring rarely and mainly associated to central nervous system, hepatic and tendon toxicity. Safety of long-term therapies has been evaluated for the second- and the third generation agents such as ciprofloxacin and levofloxacin (mycobacterium treatment), but it is still unknown for newer agents [47, 48].

1.6.4 Linezolid

Linezolid (figure 9) is a synthetic antimicrobial belonging to the class of oxazolidinoni, with a bacteriostatic or bactericidal dose-dependent antimicrobial mechanism against Gram-positive bacteria.

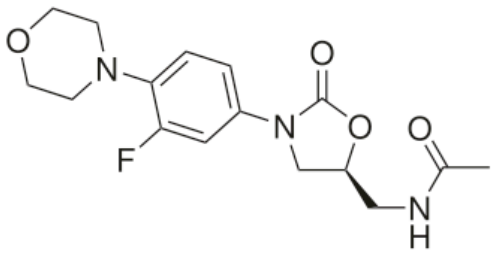

Figure 9. Chemical structure of linezolid.

The antimicrobial mechanism consists of inhibition of the bacterial protein synthesis.

Oxazolidinoni bind to the 23S portion of the ribosome 50S subunit, and they prevent the formation of the initiation complex between the ribosome, the tRNA and the mRNA. Cross-resistance with other protein synthesis inhibitors is rare. Development of resistance to linezolid is uncommon, because the protein binding site is in a highly conserved region of the bacterial ribosome [49]. However, the first linezolid-resistant isolates of *S. aureus* and *Enterococcus faecalis* have been reported between the 1999 and the 2001, and they were associated to point mutations of the genes coding for the 23S ribosomal RNA [39, 50, 51]. In order to avoid the spread of resistance, the main indication of linezolid is limited to the treatment of MRSA and multi-resistant Gram-positive bacteria in uncomplicated ad complicated infections (skin, soft-tissue, and lower respiratory infections, endocarditis, bone and joint infections) [52]. The potentials for treatment of staphylococcal prosthesis infections are uncertain, and further evaluation of linezolid in this setting is necessary [53, 54].

Linezolid has a good bioavailability (close to 100%) when given orally, a low protein binding (31%), high tissue penetration and a half-life between 3 and 5 hours. The hepatic metabolism does not involve the CYP 450 microsomial enzymes, and consist of the oxidation of the morpholine ring followed by renal and faecal elimination of the inactive metabolites [55]. Even if no evidence of CYP450 metabolism has been found, case-report have described a decreased serum concentration of linezolid when given in combination with rifampin, and it was potentially associated to the rifampin induction of hepatic microsomial enzymes [56, 57].

Linezolid is well tolerated in short-term antimicrobial therapy, with the most common adverse effects being diarrhoea, headache and nausea [39]. In long-term therapies, bone marrow suppression, with reversible anaemia, leucopenia, pancytopenia, and thrombocytopenia have been reported and associated with mitochondrial toxicity. In ex vivo studies, linezolid showed inhibitory activity towards mammalian mitochondrial protein synthesis, due to the similarities between bacterial and mitochondria ribosomes [58]. In addition, lactic acidosis, peripheral neuropathy and optic neuropathy have been occasionally reported [39, 59, 60].

1.6.5 Glycopeptides, lipoglycopeptides and lipopeptides

Vancomycin and teicoplanin are both antibiotics belonging to the class of glycopeptides, time-dependent bactereostatic agents active against Gram-positive bacteria. Especially, glycopeptides became agents of choice for the treatment of methicillin-resistant staphylococci. The mechanism of antimicrobial action relies on the inhibition of the bacterial cell wall biosynthesis. The binding to the D-Alanyl-D-Alanyl moieties of the NAM/NAG-peptides inhibits the peptidoglycan cross-linking, fundamental step guaranteeing the integrity of the cell wall.

The emergence of glycopeptide-resistant isolates created big concernments in their clinical use. Vancomycin-resistant enterococci (VRE), vancomycin -intermediate *S. aureus* (VISA), vancomycin-resistant *S. aureus* (VRSA), and vancomycin-resistant *Clostridium difficile* represent a growing

problem [39]. Indeed, the increase in glycopeptide MIC strictly correlated with the increase of failures of vancomycin-containing regimens. Bacterial resistance has been correlated to several mechanisms, one of which relies on the substitution of the D-Alanyl-D-Alanyl fragment with a D-Alanyl-D-Lactate or D-Alanyl-D-Serine, mediated by the acquisition of transposons coding for enzymes catalyzing the elimination of the native precursors. The new substitutes present decreased binding affinity to vancomycin. Intermediate resistant isolates have been described having a thicker peptidoglycan, which would confer lower susceptibility to cell-wall active drugs.

Different resistance categories have been identified for vancomycin in *S. aureus* and enterococci, and in most cases no cross-resistance with teicoplanin and dalbavancin (lipoglycopeptide) was observed.

Vancomycin is administered parenterally because of the low bioavailability, it has a low binding to plasma proteins and it is excreted unmodified by the kidney, essentially by glomerular filtration [44]. Teicoplanin share with vancomycin the mechanism of antibacterial action and the spectrum of activity, but due to its longer serum half-life, it can be administered once daily. Adverse events associated with vancomycin and teicoplanin therapy are severe thrombocytopenia (due to the induction of platelet reactive antibodies), nephrotoxicity, rash and erythema, red man syndrome, dizziness and/or ototoxicity.

Dalbavancin belongs to the class of lipoglycopeptides. Similarly to vancomycin, dalbavancin binds the D-Alanyl-D-Alanyl peptide fragment and compromise the bacterial cell-wall integrity. In addition, a mechanism of polymerization and insertion into Gram-positives plasmatic membranes has been reported but not yet completely understood. Dalbavancin displayed higher in vitro antibacterial activity than vancomycin and teicoplanin against staphylococci and especially MRSA [61-63]. Due to its high lipophylicity, dalbavancin has a serum half-life of 8.5 days in healthy volunteers, allowing once-weekly i.v. dosing; it is highly bound to plasma proteins (93%), excreted into faeces via bile or eliminated via the renal route.

In pre-clinical and clinical safety studies dalbavancin was well tolerated. Mild and rare adverse events were pyrexia, headache and gastrointestinal symptoms, whereas no renal or hepatic toxicity were observed. Dalbavancin is not a substrate of CYP450 and thus, could be given in combination with rifampin without dose-adjustment [39, 64, 65].

Daptomycin is a cyclic lipopeptide antimicrobial agent, with fast dose-dependent bactericidal activity against Gram-positive bacteria. The mechanism of bacterial killing consists of Ca^{2+}-dependent polymerization and insertion in the bacterial plasmatic membranes resulting in the disruption of its functionality, and in the cell death without lyses. The formation of pores into the plasmatic membrane cause loss of potassium, and thus, rapid membrane depolarization with following inhibition of protein, DNA and RNA synthesis [39]. Development of resistance is a rare event both in vitro and in vivo, but

resistant MRSA have been isolated from patients who received long-term daptomycin treatment.

After intravenous administration, daptomycin binding to plasma protein is 90%-96%, the serum half-life is about 8 h and is mostly eliminated into the urine [44]. The main severe adverse event observed in pre-clinical and clinical studies is the dose-dependent neuropathy resulting in skeletal-muscle toxicity, which could constitute a limitation for long-term therapies at high doses [66]. Due to its rapid killing and the efficacy displayed in preclinical studies, daptomycin may become a first-choice agent, in combination with rifampin, against MRSA prosthetic joint infections [67, 68].

1.7 Experimental Models of Prosthetic Joint-associated Infections

In the last 30 years, experimental research has been addressed towards the development of in vitro and in vivo models able to mimic the pathogenesis of prosthetic infections. The main characteristics of implant associated infections are: i) localized and persistent infection, ii) infection inducible with as much as 100 CFU bacterial inocula, iii) bacteria adhering to an inert body and forming biofilms and iv) absence of spontaneous clearance of the infection. Within the most studied animal models, the tissue cage animal model of foreign-body infection has contributed consistently to the development of standard guidelines for the management of patients with implanted prosthesis [69].

1.7.1 Tissue cage infection model

The tissue cage infection model has been widely studied with the purposes of investigating the pathogenesis of foreign-body infections, and of screening antimicrobial agents for therapy optimization. The model was evaluated in several animal species, such as: mice, guinea pigs, rats, rabbits, dogs and caves. The guinea pig tissue cage model perfectly respected the main features characterizing prosthesis infections in humans. The only limitation was that guinea pigs do not tolerate long-term antimicrobial therapies or the antimicrobial agents clindamicin and beta-lactams [6, 40-42, 67, 69-72]. Differently, mice and rats showed a good tolerance to beta-lactams and to long-term antimicrobial therapy, and thus, they may be the best choice when testing the latter conditions. However, the disadvantages of the mice and rat tissue cage models were a higher rate of spontaneous clearance of the cage infection than in guinea pigs, and a higher bacterial inoculum required for the establishment of the infection process [73-77].

The tissue cage infection model relies on the subcutaneous and aseptic implantation into the flank of the animals of Teflon cylinder cave tubes (tissue cages), regularly perforated with 130 holes throughout their whole surface (figure 10).

During the two weeks after surgery, the implanted cages become surrounded by a richly vascularized granulation tissue (lymphocytes, fibroblasts and collagen fibers) and filled with interstitial fluid. The composition of the tissue cage interstitial fluid in guinea pigs, in comparison to serum or heart-puncture collected blood, showed a lower pH, a higher pO_2 and pCO_2, and nearly half of protein (g/l) content [69].

A localized tissue cage infection could be induced with *S. aureus* Wood 46 by percutaneous inoculation of ≥ 100 CFU directly into the cage. In alternative, systemic intravenous inoculation of bacteria was attempted in order to simulate a haematogenous infection. In the latter infection route, an inoculum of 5×10^7 CFU injected i.v. resulted in a transient bacteremia of 10^2-10^3 CFU/ml at 5 min after injection, and it was successful in establishing a selective infection in 50% of the tissue cages,

with no microbial evidence of infection elsewhere [40].

A B

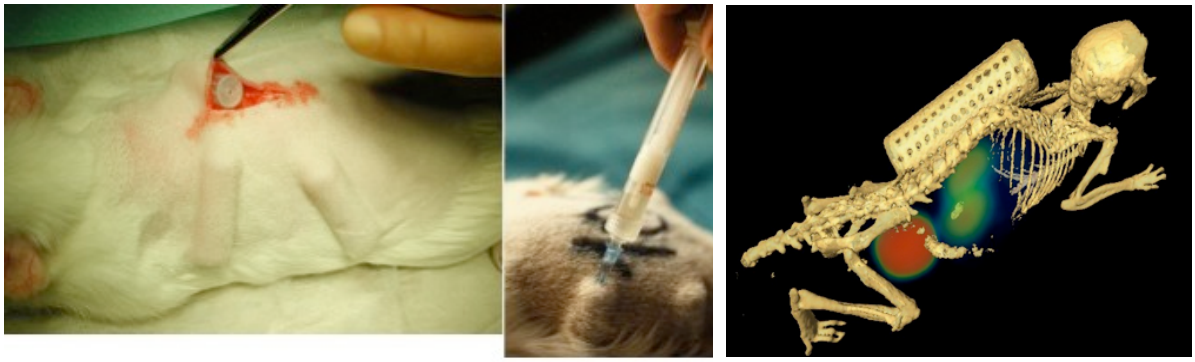

Figure 10. (A) Implantation of the Teflon cages in the flanks of a guinea pig (left), and the percutaneous cage puncture (right), which is used to inoculate bacteria or to sample cage fluid. (B) SPECT/CT scan of a tissue cage implanted C57Bl/6 mouse, after injection of the unspecific Technetium-99m radionuclide (radioactivity detected in the kidneys and in the bladder).

Being the tissue cage fluid easy-to-sample by subcutaneous aspiration, many parameters can be continuously and simultaneously investigated, such as: the number and the ex-vivo activity of cage fluid granulocytes, the kinetic of bacterial growth during the cage infection, the pharmacokinetic of antimicrobial agents into the cage fluids, and the number of planktonic viable bacteria during antimicrobial treatment.

The studies conducted with the guinea pig tissue cage model were initially addressed to determine the fitness of the host inflammatory cells in the tissue cage fluids. The median granulocyte content into aspirated cage fluid was about 8×10^5 PMNs/ml before inducing an infection, and it was shown to increase upon *S. aureus* infection proportionally to the injected bacterial inoculum [71].

The bactericidal activity, ingestion rate, oxidative methabolism, and enzyme content of primary and secondary granules of the cage fluid PMNs were evaluated ex vivo. All tests showed reduced antibacterial activity of isolated cage fluid PMN, when compared to blood or peritoneal exudate PMN. On the contrary, the antibacterial activities of tissue cage PMN were comparable to the ones measured in both: ex vivo PMN of an experimental system reproducing chronic exudates, and the ex vivo exudates PMN pre-incubated in plasma with Teflon fibers. As consequence, it has been postulated that the foreign non-phagocytosable body induces a chronic and protracted stimuli of the local PMN resulting in their loss of activity. Contrarily, the opsonization activity of tissue cage fluid was proven to be intact within the first ours of infections. Thus, the reduced killing activity of the cage fluid PMN could be addressed as one of the driving reasons for the enhanced virulence displayed by bacteria in the presence of a foreign-body [6, 71].

Systematic studies were conducted for the optimization of antimicrobial therapies against implant

infections. Antimicrobials agents, administered either alone or in combination, were tested against established *S. aureus*, *S. epidermidis* and *E. coli* tissue cage infections, in one or twice-daily four-day regimens. The treatment efficacies against planktonic bacteria were evaluated on the last day of treatment (before administration of the last antimicrobial dose), and five days after the end of treatment. The cure rates against biofilm bacteria were evaluated by aseptic explantation of the cages and their subcultures in growth medium. Evidence of bacterial growth from the cage subcultures indicated the treatment failures.

The main findings were that most of the tested antimicrobials (glycopeptides, lipopeptides and fluoroquinolones) had low in vivo activity against biofilm infections, whereas rifampin resulted to be the only agent highly effective against staphylococcal biofilms. Especially, when rifampin was administered in combination either with glycopeptides (vancomycin or teicoplanin) or with fluoroquinolones (ciprofloxacin), higher cure rates of tissue cage infections were achieved, due to either in vivo synergism mechanisms or to prevention of development of rifampin resistance [41, 69, 72, 78]. Following, clinical studies have confirmed rifampin-containing regimens to be the optimal antimicrobial therapies against staphylococcal prosthetic infections [13, 43].

1.7.2 In vitro tests predicting for in vivo efficacy against prosthetic joint infections

The minimal inhibitory concentration (MIC) and the minimal bactericidal concentration (MBC) of an antimicrobial agent against bacterial isolates are generally good predictors for treatment outcomes when dealing with skin and soft-tissue infections. Especially, pharmacokinetic/ pharmacodynamic (PK/PD) parameters such as: the peak level of the agent at the site of infection versus the MIC (C_{max}/MIC), the area under the concentration-time curve of the agent versus the MIC (AUC/MIC), and the time-length of the agent concentration at the site of infection above the MIC (t>MIC), can be good predictors for treatment efficacies. Indeed, the evaluation of PK/ PD parameters helps to define the dose- or time-dependency of in vivo antimicrobial mechanisms, which is important for choosing the correct antimicrobial and the dose regimens [79-81].

Antimicrobial therapies of patients diagnosed with device-associated infections reported several failures, even when the infecting bacteria were susceptible to the antimicrobial agents in standard microbiology tests. As mentioned before, biofilms have enhanced tolerance towards many antimicrobial agents, due to both the stationary metabolic phase of the bacterial cells, and the physic barrier created by the extracellular matrix in which bacterial cells are embedded. Standard microbiology susceptibility parameters, such as MIC and MBC, are evaluated against bacteria in a logarithmic replication phase, and thus, these assays do not constitute good predictors for the treatment of implant infection.

In order to be effective against biofilm infections, an antimicrobial agent should be able to diffuse through the biofilm extracellular matrix, and it should be bactericidal against stationary phase bacteria

at concentrations achievable within the biofilm. As consequence, experimental microbiology assays were developed for testing the bactericidal activity of antimicrobial agents against bacteria in a stationary growth phase, or against in vitro pre-formed biofilms. These tests comprehend: minimal bactericidal concentrations (MBC_{stat}) and kill curve studies of stationary phase bacteria, bactericidal activity against biofilms pre-formed on sinter-glass beads, or slides, and the Calgary device biofilm method for determination of minimal biofilm inhibitory concentrations (MBIC) [41, 82]. Zimmerli *et al*. demonstrated that, in vitro bactericidal activity against biofilm and stationary phase bacteria, generally, well-correlates to the cure rates achieved by antimicrobial therapies in the guinea pig model of tissue cage infection [41, 72, 78, 83, 84].

As consequence, the evaluation of PK/ PD parameters, based on in vitro susceptibility assays conducted against adherent and stationary phase bacteria, may represent an essential step to predict the potentials of new antimicrobial regimens against prosthetic-associated infections.

1.8 AIM OF THE STUDY

The aim of the present study was to develop and evaluate in vitro and in vivo innovative methods for the diagnosis and treatment of bacterial implant associated infections.

1) Nuclear medicine studies aimed to evaluate novel radiopharmaceuticals, testing their in vitro binding and in vivo accumulation at sites of infection, for targeting implant associated infections. The potentials to target bacterial cells of ^{99m}Tc-UBI 29-41, ^{99m}Tc-Ciprofloxacin, ^{99m}Tc-bis-ciprofloxacin and ^{111}In-Biotin were evaluated in vitro and in the mouse tissue cage model of infection, using a *S. aureus* and an *E. coli* bacterial strain (Chapter 2).

2) The vitamin B_{12} derivative ^{99m}Tc-PAMA4-Cbl had been previously developed from Waibel et al. [85] and displayed improved biodistribution parameters (shorter serum half-life, low accumulation in non-target tissues, fast clearance) than the native Cobalt-57 radiolabeled vitamin B_{12}. We aimed to test the potentials of the ^{99m}Tc-PAMA4-Cbl derivative for targeting infections in vitro and in the mouse tissue cage model of infection, using as controls the Co-57 Vitamin B_{12}, ^{67}Ga-citrate (positive control) and ^{99m}Tc-DTPA (negative control) (Chapter 3).

3) The ex vivo, fast recognition of MRSA constitutes a key issue for the management of implant infections. Calorimetric measurements of bacterial growth-related heat could constitute an innovative method for early detection of resistance patterns. The aim of the project was to develop an assay able to correlate the *S. aureus* methicillin resistance, with the heat production of cultures in the absence and in the presence of a beta-lactam, using laboratory stains and clinical isolates (Chapter 4).

4) The introduction of non-conventional antimicrobials, for the prophylaxis, implant coating or treatment of implant infections, may bring enormous advantages for limiting emergence of resistance and infection relapses. The aim of this work was to test the activity of gallium, a semi-metallic element competing with iron, against methicillin susceptible and resistant *S. aureus* and *S. epidermidis*. The in vitro susceptibility of laboratory strains and clinical isolates was characterized towards gallium maltolate (GaM), a gallium formulation highly stable, soluble and suitable for oral administration (Chapter 5).

5) Linezolid is a promising antmicrobial with ant-staphylococcal activity, used for the treatment of MRSA infections. However, limited studies have been reported regarding the efficacy of linzolid against MRSA implant associated infections. Thus, we aimed to describe the antimicrobial activity of linezolid, alone or combined with rifampin, against a laboratory strain of MRSA in vitro and in the

guinea pig tissue cage model of foreign-body infection (Chapter 6).

Chapter 2

Comparison of Technetium-99m Labeled UBI 29-41, Ciprofloxacin, Ciprofloxacin Dithiocarbamate (CiproCS_2) and Indium-111 Biotin for Targeting Experimental *Staphylococcus aureus* and *Escherichia coli* Foreign Body Infections

D. Baldoni[1], F. Galli[2], A. Trampuz*[1,3], A. Signore*[2]

[1]Infectious Diseases Research Laboratory, Department of Biomedicine, University Hospital, Basel, Switzerland

[2]Nuclear Medicine Unit, 2nd Faculty of Medicine, University "Sapienza", Roma, Italy and

Dept of Nuclear medicine & Molecular Imaging, University Medical Center Groningen,

University of Groningen, The Netherlands [6]Institute of Nuclear Medicine, University Hospital, Basel, Switzerland

[3]Infectious Diseases Service, Department of Internal Medicine, University Hospital and University of Lausanne, Lausanne, Switzerland

*Authors equally contributed

Keywords: Tissue cage model, infection, UBI 29-41, ciprofloxacin, biotin

To be submitted in the European Journal of Nuclear Medicine and Molecular Imaging

2.1 Abstract

Diagnosis of implant-associated infection is challenging. Several radiopharmaceuticals have been described but direct comparisons are limited. Here we compared in vitro and in an animal model ^{99m}Tc-UBI, ^{99m}Tc-ciprofloxacin, ^{99m}TcN-ciproCS$_2$ and ^{111}In-DTPA-biotin for targeting *E. coli* (ATCC 25922) and *S. aureus* (ATCC 43335).

Methods: Stability controls were performed with the labeled tracers during 6 h in saline and serum. The in vitro binding to viable or killed bacteria was evaluated at 37° C and 4° C. For in vivo studies, Teflon cages were subcutaneously implanted in mice, followed by percutaneous infection. Bioistribution of i.v. injected radiolabeled tracers were evaluated during 24 h in cages and dissected tissues.

Results: Radiochemical purity of the labeled agents ranged between 94 % and 98 %, with high stability both in saline and in human serum. In vitro binding assays displayed a rapid but poor bacterial binding for all tested agents. However, results are difficult to interpret because similar binding kinetic occurred also with heat-killed and ethanol-killed bacteria. In the tissue cage model, infection was detected at 4 h p.i.: ^{99m}Tc-ciprofloxacin and ^{111}In-DTPA-biotin accumulation was higher in both *E. coli* and *S. aureus* infected than in sterile cages, whereas ^{99m}TcN-ciproCS$_2$ and ^{99m}Tc-UBI only distinguished for *E. coli* infected cages. However, cage fluid or tissue cage to blood (T/NT) ratios did not achieve values >2. All tested radiotracers were mostly cleared from non-target tissues between 12 h and 24 h p.i.

Conclusion: ^{99m}Tc-UBI, ^{99m}Tc-ciprofloxacin, ^{99m}TcN-ciproCS$_2$ and ^{111}In-DTPA-biotin are promising agents for in vivo targeting of living bacteria. ^{99m}Tc-ciprofloxacin and ^{111}In-DTPA-biotin showed high sensitivity and accumulated in both *E. coli* and *S. aureus* infected cages. The low T/NT ratios may constitute a limiting factor for the application of the tested tracers in patients.

2.2 Introduction

Implanted devices are increasingly used in modern medicine to alleviate pain or improve compromised function. Implant associated infections constitute a major complication leading to high morbidity, extensive patient care and costs [4]. The early discrimination between infective and aseptic implant failures is essential for choosing the appropriate therapy procedures. However, standard laboratory methods such as tissue cultures and direct microscopy are either slow or have low sensitivity [17, 86]. Thus, the development of a sensitive and specific diagnostic tool for detection of foreign body infections remains an important and challenging issue.

Imaging techniques for visualization of an injected radiopharmaceutical have been increasingly used for evaluation of loosening prostheses. The gold standard consisted of ex-vivo radiolabeled autologous leukocytes [87]. In alternative, an indirect approach is the injection of radiolabeled monoclonal antibodies or antibody fragments targeting specific leukocytes antigens or receptors. However, these methods are characterized by a long and labor-intensive in vitro labeling procedure the first, and the frequent emergence of toxicity episodes the second. In addition, sensitivity and specificity reported in pre-clinical and clinical studies have been often contradictory or not satisfying [17, 22, 88].

In the last years, diverse and novel agents able to target directly the infecting pathogens, rather than inflammatory cells, have been widely investigated. The antimicrobial peptide UBI 29-41 was labeled with technetium-99m and showed preferential accumulation at sites of experimental soft-tissue or foreign body associated infections. In clinical studies radiolabeled UBI 29-41 was investigated as an infection-specific agent allowing imaging of infectious foci in humans already 30 min after administration [89-94]. In addition, synthetic antimicrobials have been evaluated and proposed as potential infection-specific radiotracers. ^{99m}Tc-ciprofloxacin, belonging to the fluoroquinolone class of antibacterials, was pioneering this field and is the most extensively investigated. Promising in the pre-clinical setting, in clinical studies ^{99m}Tc-ciprofloxacin reported controversial frequency of false-positive cases, with specificity ranging between 41% and 83%. However, an increased specificity has been described when imaging was delayed from 1 h to 4 h or 24 h after administration of the tracer. Indeed, the delayed imaging would allow the clearance of aseptic inflamed lesions, whereas the radioactivity is retained in infection sites [22, 23, 95-101].

The suboptimal radiochemical yield and the little understanding in the chemical structure of ^{99m}Tc complexes of ciprofloxacin stimulated the research towards better chemically defined derivatives. Recently, a promising candidate, ciprofloxacin dithiocarbamate (ciproCS$_2$), has shown a fast and effective labeling, occurring by binding of two ciproCS$_2$ molecules to a nitrido technetium-99m and resulting in a highly stable compound. Pre-clinical studies conducted with the ^{99m}TcN-ciproCS$_2$ displayed in vitro bacterial binding and accumulation into infections sites higher than the precursor

ciprofloxacin [102]. Further evaluation would be recommended for a better characterization of this new tracer both in the pre-clinical and in the clinical settings.

Radiolabeled growth factors may also behave as specific agents accumulated by bacteria due to their high replication rate. Recently, indium-111 labeled biotin displayed high potentials for the diagnosis of vertebral osteomyelitis infections. When compared to clinical, radiological or laboratory tests, the SPECT/CT imaging of administered ^{111}In-DTPA-biotin achieved a sensitivity of 84-100% and specificity of 84-98% [103]. However, confirmatory clinical studies are required for confirming the diagnostic potentials of this radiotracer.

The aim of our study was to compare the performance of ^{99m}Tc-UBI, ^{99m}Tcciprofloxacin, ^{99m}TcN-ciproCS$_2$ and ^{111}In-DTPA-biotin for targeting experimental *S. aureus* and *E. coli* infection in a tissue-cage mouse model of foreign body infection. The tissue-cage model is a well-studied and well-understood model of reproducible, localized and persistent infection [71, 77, 104]. After subcutaneous aseptic implantation on the back of the mice, perforated Teflon cages fill with a vascularized granulation tissue and exudate, originating from an unspecific local inflammation process around the foreign body. Percutaneous injection of bacteria into cages causes a persistent infection, in which bacteria grow in adherent and planktonic growth phases. The advantage of this model is the easy sampling of cage fluid, performed in successive time points without harming the animals, allowing an accurate determination of planktonic bacterial load or concentration of administered radiotracers.

2.3 Materials and Methods

Labeling procedures.

^{99m}Tc-UBI 29-41

Lyophilized kits were reconstituted under aseptic conditions with $Na^{99m}TcO_4$, as previously described [90]. Briefly, the kits consisted of two vials: vial n°1 contained 40 µl of NaOH and vial n°2 contained 25 µg of UBI 29-41 and 12 µg of $SnCl_2$. One ml of a 555 MBq/ml 0.9 % saline solution of$Na^{99m}TcO_4$, eluted from a $^{99}Mo/^{99m}Tc$ generator, was transferred to vial 1. Thus, the content of vial 1 was resuspended and transferred to vial 2. After 15 min at room temperature, 5 ml of 0.9 % saline solution were added to vial 2 (stock solution, SS) and radiochemical purity analyzed with a Sep-Pak C-18 Cartridge (Waters Instruments, USA). The column was preconditioned with 5 ml ethanol, 0.1 ml of the tracer solution was loaded and, first the free $^{99m}TcO_4$ was eluted 5 ml HCl 1 mM, then the ^{99m}Tc-UBI 29-41 was eluted with 3 ml of ethanol/saline (1:1) followed by 3 ml of HCl 0.1 M/methanol (15:85). The colloidal forms remained on the column.

High-performance liquid chromatography (HPLC) was carried out with a Jupiter 4 n column (250 × 4.6 mm^2, 4 µm, Phenomenex, USA), connected to both radioactivity and UV-photodiode detectors. As mobile phases 0.1% TFA/water (solvent A) and 0.1 % TFA/acetonitrile (solvent B) were used at a flow rate of 0.75 ml/min starting with a mixture of solvent A/B of 95/5 % for 3 minutes. Following, a mobile phase gradient started during 10 min to a final ratio solvent A/B of 50/50 %. The latter mobile phase was kept for further 10 min, when the ratio was changed to solvent A/B of 30/70 % during 3 min and to the starting ratio solvent A/B of 95/5 % during the last 3 min. Instant thin layer chromatography (ITLC, Pall Life Sciences, USA) silica gel strips were used with saline or with mobile phase ethanol/ water/ ammonium (2:5:1) as eluent, for measuring the free pertechnetate or colloids, respectively. Stability of the ^{99m}Tc-UBI 29-41 was evaluated by resuspending 100 µl of the SS in saline and performing ITLC at different time points during 6 h.

^{99m}Tc-ciprofloxacin

^{99m}Tc-ciprofloxacin (1-cyclopropyl-6-fluoro-4-oxo-7-piperazin-1-yl-quinoline-3-carboxylic acid) was prepared using a lyophilized kit, as previously described [105, 106]. The kit consisted of 3 vials: vial n°1 contained 20 mg of ciprofloxacin, vial n°2 30 mg of L-tartarat acid and vial n°3 50 mg of $SnCl_2$. First, vial 1 was reconstituted with 5 ml of sterile saline solution 0.9 %, vial 2 with 10 ml of water for injection and vial 3 with 10 ml of HCl 0.1M. Vial 2 and 3 were further diluted 1:20 with water for injection in oxygen free vials. Labeling was performed in a fourth oxygen free vial (reaction vial), in which were transferred 250 µl from vial 1 and 50 µl from 1:20 dilutions of vial 2 and 3, and finally 500 µl of a $Na^{99m}TcO_4$ solution with activity of 740 MBq were transferred to the reaction vial. After 20 min at room temperature the solution in reaction vial was filtered trough a 0.22 µm Millipore

and diluted 1:10 in saline (stock solution, SS) to obtain a ciprofloxacin concentration of 125 µg/ml and an activity of 87 MBq/ml. The latter was further processed for quality controls. Radiochemical purity was evaluated by ITLC using as solvents aceton or ethanol/water/ammonium 25% (20:50:10) for free pertechnate or colloids, respectively. Stability of the ^{99m}Tc-ciprofloxacin was evaluated by resuspending 100 µl of the SS in 900 µl saline or serum and performing ITLC at different time points during 6 h.

^{99m}TcN-ciproCS$_2$

The kit was obtained from A. Duatti et al. (University of Ferrara, Italy) and consisted of 3 vials: vial n°1 contained 5 mg of succinic acid dihydrazide (SDH), 5 mg of ethylenediamine tetraacetic acid (EDTA), 0.1 mg of $SnCl_2$ and phosphate buffer 0.1 M; vial n°2 contained 12 mg of 1-cyclopropyl-6-fluoro-1,4-dihydro-4-oxo-7-(1-piperazinyl-N-dithiocarbamate)-3-quinolinecarboxylic acid sodium salt, (abbreviated as ciprofloxacin dithiocarbamate or ciproCS$_2$); vial n°3 contained 15 mg of γ-cyclodextrin.

Briefly, 1 ml of $^{99m}TcO_4^-$ (740 MBq) was added to vial 1 and after 30 minutes of incubation at room temperature, 100 µl of a 0.5 M carbonate buffer (pH=9.5) were added. Then, 15 ml of normal saline were added to vial 3 and 12 ml of the obtained solution were added to vial 2 and finally 1 ml was transferred to vial 1. The mixture was incubated at room temperature for 20 minutes. The final solution had a concentration of 0.5 mg/ml of ^{99m}TcN-ciproCS$_2$. The final stock solution (SS) was prepared by diluting 1:5 of the labeling solution with normal saline obtaining a final concentration of 100 µg/ml and a specific activity of 74 MBq/ml. Quality controls were performed by both instant thin layer chromatography (ITLC), thin layer chromatography (TLC) and reverse phase high-performance liquid chromatography (HPLC). ITLC silica gel strips and TLC silica gel strips (Baker-flex®, J.T. Baker, USA) were used as stationary phase. Regarding the former the mobile phase consisted in normal saline, while for the latter a methanol/0.5 M ammonium acetate (80:20 v/v) solution was used to determine the amount of free $^{99m}TcO_4^-$ and unreacted ^{99m}Tc-nitrido intermediate. The amount of colloids was determined using ITLC albumin absorbed strips as stationary phase and an ethanol/water/ammonium (2:5:1) solution as mobile phase. High-performance liquid chromatography (HPLC) was carried out using a method previously described [103]. Radiochemical purity was determined by HPLC using a Phenomenex Jupiter 4 n column and 0.1% TFA/water (solvent A) and 0.1 % TFA/acetonitrile (solvent B) as mobile phases at a flow rate of 0.75 ml/min, starting with a solvent ratio of A/B = 95/5 for 10 minutes. Then, a gradient started over 15 min to a final ratio A/B = 5/95 and held constant for 3 minutes then back to 95/5 during the last 2 min. Stability of the ^{99m}TcN-ciproCS$_2$was evaluated by resuspending 100 µl of the SS in 900 µl saline or serum and performing TLC analyses at different time points during 6 h.

^{111}In-biotin

A Diethylenetriaminepentaacetic acid α,ω-bis-biocytinamide (DTPA-biotin) (SIGMA-ALDRICH, USA) solution of 500 µg/ml was prepared in Acetate buffer 0.05 M, pH 5.5 and sterile filtered with Millipore 0.2 µm filters. Labeling was performed as previously described [103]. Briefly 1 ml of DTPA-biotin sterile solution (500 µg) was mixed to 110 MBq of Indium-111 Chloride at room temperature for 15 minutes (stock solution, SS). Radiochemical purity was determined by high-performance liquid chromatography (HPLC). HPLC was carried out using a Phenomenex Jupiter 4 n column. As mobile phases 0.1% TFA/water (solvent A) and 0.1 % TFA/acetonitrile (solvent B) were used at a flow rate of 0.75 ml/min starting with a mixture of solvent A/B of 95/5 % to a final ratio solvent A/B of 70/30 % during 25 minutes. Stability of the ^{111}In-Biotin was evaluated by resuspending 100 µl of the SS in 900 µl saline or serum and performing quality controls at different time points during 6 h.

Microorganisms. The laboratory strains *E. coli* (ATCC 25922) and *S. aureus* (ATCC 35556, methicillin-susceptible) were used. Bacteria were stored at -70°C using a cryovial bead preservation system (Microbank, Pro-Lab Diagnostics, Richmond Hill, ON, Canada). Single cryovial beads were cultured overnight on Columbia sheep blood agar plates (Becton Dickinson, Heidelberg, Germany). Bacterial cultures were prepared by resuspending two to three colony forming units (CFUs) in 5 ml of Tryptic soy broth (TSB) and incubating overnight for 18-20 h at 37°C. For in vitro studies, overnight cultures were diluted 1:100 in TSB and further incubated at 37°C to mid-logarithmic phase. Following, when an optical density (OD_{600}) between 0.3 and 0.4 was achieved, cultures were centrifuged and bacterial pellets concentrated 10× in the appropriate volume of phosphate buffer solution (PBS) or a 0.1% acetic acid and 0.05 % Tween 80 supplemented PBS (incubation buffer solution, IBS) for testing ^{99m}Tc-UBI 29-41. Hundred µl of resuspended bacterial cultures were mixed with 900 µl of tracer solution, reaching a final load of ≈ 1×10^8 CFU/ml.

For in vivo studies, overnight cultures were washed three times and re-suspended in 5 ml of sterile saline 0.9%. Appropriate dilutions (inocula of 5×10^5 CFU and 1×10^7 CFU injected per mouse-cage of *S. aureus* and *E. coli*, respectively) of the washed overnight cultures were prepared and used for mice inoculation.

In vitro binding studies. Binding of the test radiotracers to *E. coli* and *S. aureus* was investigated in vitro. Mid-logarithmic phase bacterial cultures were 10× concentrated and aliquoted into Eppendorf vials, together with the test tracers. Vials were incubated for 1 h at 37°C, in the presence and in the absence a 100-fold excess of unlabelled tracer. Temperature dependency was evaluated by adapting bacterial aliquots for 1 h at 4°C before addition of the tracers, followed by further incubation for 1 h at 4°C. Bacterial colony forming units were evaluated before and after 1 h incubation in the presence of

tracer. For this purpose, 50 µl were 10-fold serial diluted in sterile saline and spread on Columbia agar plates. After overnight incubation at 37°C, plates were counted and the exact $\log_{10}$CFU/ml calculated.

For measuring tracers' binding to non-viable bacteria, cultures were exposed to 70 % ethanol solution at 4°C or in the buffer solution to 99°C for 30 min (*E. coli*) or 1 h (*S. aureus*). Ethanol exposed cultures where washed before performing the binding tests. To confirm the non-viability of the resuspended heat-killed or ethanol-killed bacteria, 100 µl were spread on Columbia blood agar plates and the CFU enumerated after 24 h of incubation at 37°C. Colony counts <10 CFU/ml were considered valid for further binding evaluation.

For testing ^{99m}Tc-UBI 29-41, freshly prepared stock solutions (SS) were diluted 1:20 with the incubation buffer solution (IBS, phosphate buffer solution 0.02 M supplemented with 0.1 % acetic acid and 0.05 % Tween 80), to a final concentration of 210 ng/ml, 2.3 MBq/ml. Following, Eppendorf vials were filled with 800 µl of IBS, 100 µl of bacterial suspension and 100 µl of diluted tracer.

The SS of ^{99m}Tc-Ciprofloxacin and ^{99m}TcN-ciproCS$_2$ were diluted in PBS 1:10 and 1:40, respectively, from which 100 µl were transferred to Eppendorf vials containing 800 µl of PBS and 100 µl of bacterial suspensions.

In the ^{111}In-DTPA-biotin binding assay, the labeled SS was diluted 1:1000 (0.45 µg/ml DTPA-Biotin, 0.1 MBq/ml) in PBS, and 500 µl transferred to vials pre-filled with 500 µl of bacterial cultures resuspended in PBS or a biotin depleted minimal medium.

The % radiotracer bound to bacterial cells was calculated by incubating the different radiopharmaceuticals with the bacteria suspensions for different time points between 5 min and 1 h. Probes were then centrifuged for 5 minutes at 13,500 rpm at 4°C. Pellets were washed with 500 µl of cooled buffer solution. Supernatants and re-suspended pellets were counted in a multi-well NaI γ-counter (Cobra; Packard) and the counts per minutes (CPM) recorded. The percentage of radiolabeled agents in the pellets was calculated as percentage of the CPM_p/CPM_0-ratio per 8.0 $\log_{10}$CFU/ml, where CPM_p were the CPM associated to pellets and CPM_0 the total CPM of the radiolabeled agent added per vial.

Tissue-cage infection model in mice. C57Bl/6 mice from in-house breeding or purchased from Charles River (CR, Germany) were housed in the Animal Facility of the Department of Biomedicine, University Hospital Basel, Switzerland, at a mean temperature of 23 ± 2°C, 50-55% relative humidity, and 12-h light/dark cycle. Drinking water and standard laboratory food pellets (CR) were provided *ad libitum.* At the age of 12 weeks, one sterile polytetrafluoroetylene (Teflon) cage (32 × 10 mm), perforated by 130 regularly spaced holes of 1 mm diameter, was aseptically implanted into the back of each mouse, as previously described [74, 104] (figure 11). Each cage was weighted and numbered before implantation, in order to normalize the final cage-associated CPM measurements with the weight of the cage tissue only. Two weeks after surgery, clips were removed from healed wounds and

sterility of the cage was confirmed by plating of percutaneously aspirated cage fluid on Columbia blood agar plates. On the following day, 5×10^5 CFU of *E. coli* or 5×10^6 CFU of *S. aureus* resuspended in 200 µL of 0.9% NaCl, were injected into the cages. Cages in control animas were injected with sterile 0.9% NaCl. Experiments were performed in accordance to the regulations of Swiss veterinary law. The Institutional Animal Care and Use Committee approved the study protocol.

Figure 11. CT picture of a C57Bl/6 mouse with subcutaneous implanted tissue cage.

Biodistribution studies. In biodistribution studies, 100 µl of test radiopharmaceuticals were administered i.v. into the mice lateral tail vein, 24 h and 48 h after induction of *E. coli* and *S. aureus* infection, respectively. In particular, the injected stock solutions were: ^{99m}Tc-UBI 29-41 (9.3 MBq, 0.40 µg per mouse), ^{99m}Tc-ciprofloxacin (7.4 MBq, 13 µg per mouse), ^{99m}TcN-ciproCS2 (7.4 MBq, 10 µg per mouse) and ^{111}In-biotin (0.6 MBq, 0.5 µg per mouse). Each tracer was injected in at least 10 to 12 mice per sterile/ infected testing group.

Bacterial counts into cage fluids were evaluated by plating 10-fold serial dilutions of fluids collected on the day of tracer injection and plates were incubated for 24 h at 37°C and the CFU counted.

Distribution of tracers into the infected/sterile cage fluids was determined at 30 min, 1 h, 2 h, 4 h, 8 h, 12 h and 24 h p.i. of the radiopharmaceuticals. Hundred µl of aspirated fluids were resuspended in 1 ml PBS and counted in a gamma counter. The percentage of injected dose (% ID_{TCF}/ml) was calculated as measured CPM normalized per 1 ml cage fluid and divided by the CPM_0 of the injected dose. Distribution into organs, tissues and explanted cages was measured at 30 min, 4 h and 24 h p.i. Mice were sacrificed with an intra-peritoneal injection of 50-80 µl saline solution of pentothal (100 mg/ml). Blood was collected by cardiac puncture and animals were perfused with 0.9% NaCl solution for around 5 min. Following, tissues were dissected, weighted and collected into test tubes for γ-counter

(blood, heart, liver, spleen, stomach, kidneys, lungs, intestine, muscle, bone and cage). The percentage of injected dose (% ID_{tissue}/g) was calculated as CPM associated to each organ divided by its weight in grams and by the CPM_0 of the injected dose.

Statistical analysis. Comparisons of in vitro binding results and in vivo biodistribution data were performed using the Student t test for continuous variables. All results were given as mean values ± SEM, unless otherwise indicated. Differences were considered significant when P values were <0.05. All calculations were performed using Prism 4.0a (GraphPad Software, La Jolla, CA, USA).

2.4 Results

Quality controls and stability assays (table 4)

^{99m}Tc-UBI 29-41

The labeling efficiency of ^{99m}Tc-UBI 29-41 determined by ITLC and HPLC was 97 %, while the radioactivity associated with colloid or hydrolyzed ^{99m}Tc species was less than 1.6 %. The compound was stable in saline up to 6 h, but its stability decreased to 12 % after 6 h in serum.

^{99m}Tc-ciprofloxacin

The labeling efficiency of ^{99m}Tc-ciprofloxacin determined by ITLC and HPLC was 93 %, with an amount of colloids not greater than 5 %. The compound was stable in serum up to 6 h, whereas in saline its radiochemical purity decreased up to 58 % after 6 h.

^{99m}Tc-ciproCS$_2$

The labeling efficiency of ^{99m}TcN-ciproCS$_2$ determined by HPLC and TLC was approximately 97 %, with an amount of unreacted ^{99m}Tc-nitrido intermediate not greater than 3%. The compound was stable in saline and serum up to 6 h, without any decrease of the radiochemical purity.

^{111}In-DTPA-biotin

^{111}In-DTPA-biotin presented a labeling efficiency of 96% determined by HPLC and was highly stable in saline and serum up to 6 h, without any decrease of the radiochemical purity.

Table 4. Radiochemical purity of ^{99m}Tc-UBI 29-41, ^{99m}Tc-Ciprofloxacin, ^{99m}TcN-CiproCS$_2$ and ^{111}In-DTPA-biotin immediately after labeling, and during 6 h incubation in saline or serum of a 1:10 dilution of the labeling solution.

	Labeling Efficiency	Stability Control (Saline)			Stability Control (Serum)		
		1 h	3 h	6 h	1 h	3 h	6 h
^{99m}Tc-UBI 29-41	97%	96%	97%	94%	34%	18%	12%
^{99m}Tc-Ciprofloxacin	94%	83%	71%	58%	94%	92%	92%
^{99m}TcN-CiproCS2	98%	96%	97%	97%	96%	97%	97%
^{111}In-DTPA-biotin	96%	96%	95%	95%	96%	96%	95%

In vitro binding studies. The in vitro binding of ^{99m}Tc-UBI 29-41, ^{99m}Tc-ciprofloxacin, ^{99m}TcN-CiproCS$_2$ and ^{111}In-DTPA-biotin to the *E. coli* and *S. aureus* test strains was independent on temperature or bacterial viability. No competition occurred when binding was measured in the presence of 100-fold excess of unlabelled compounds. In addition, for the ^{99m}Tc-UBI 29-41 and ^{99m}Tc-ciprofloxacin, trends of higher binding to ethanol or heat killed than viable bacteria were

observed, with the exception of ^{99m}Tc-ciprofloxacin binding to *S. aureus* which remained constant in all tested conditions. The highest in vitro bacterial binding was observed with ^{99m}TcN-CiproCS_2. Percentages of binding per 8.0 $\log_{10}$ CFU/ml were calculated and are reported in Table 5.

Bacterial viability was tested for the cultures exposed to the tracer solutions during 1 h. Both *S. aureus* and *E. coli* cultures were not affected by the presence of any of the tracers and bacterial counts remained equal to control vials during 1 h of incubation. Whereas, in competition experiments, *E. coli* counts at 1 h incubation decreased when exposed to the 100-fold excesses of unlabeled ciprofloxacin and CiproCS_2 by ≈0.8 and ≈3.5 $\log_{10}$CFU/ml, respectively.

Table 5. In vitro binding assay reported as % CPM/CPM_0 (means ± SD) measured after 1 h incubation of the tracers with the *S. aureus* or *E. coli* bacterial strain.

	37°C	4°C	EtOH Killed	Heat Killed	100x Cold 37°C
			^{99m}Tc-UBI 29-41		
E. coli	0.94 ± 0.082	0.61 ± 0.15	3.34 ± 0.35	12.02 ± 0.52	1.01 ± 0.079
S. aureus	0.36 ± 0.045	0.28 ± 0.050	15.90 ± 0.87	10.20 ± 2.53	1.02 ± 0.13
			^{99m}Tc-Ciprofloxacin		
E. coli	2.60 ± 0.032	1.6 ± 0.16	4.35 ± 0.20	4.81 ± 0.22	1.18 ± 0.052
S. aureus	1.43 ± 0.073	1.11 ± 0.047	2.12 ± 0.25	0.52 ± 0.040	1.038 ±0.11
			^{99m}TcN-CiproCS_2		
E. coli	32.51 ± 3.47	55.46 ± 4.98	48.34 ± 6.14	53.11 ± 6.47	95.41 ± 2.39
S. aureus	91.10 ± 3.67	95.14 ± 4.15	93.14 ± 4.03	92.56 ± 7.97	98.86 ± 3.19
			^{99m}Tc-DTPA-Biotin		
E. coli	0.23 ± 0.058	0.10 ± 0.032	0.088 ± 0.037	0.10 ± 0.038	0.21 ± 0.088
S. aureus	0.14 ± 0.024	0.25 ± 0.022	0.069 ± 0.024	0.050 ± 0.015	0.063 ± 0.037

Biodistribution studies. The *E. coli* and *S. aureus* mean ± SD load into cage fluids was 9.4 ± 0.82 log CFU/ml and 6.3 ± 0.62 log CFU/ml, respectively. No clinical or pathological signs of systemic infection (hematogenous dissemination) were observed during organ dissection. Thus, the cage fluid infections were considered persistent and localized.

Accumulation of the radiolabeled agents into cage fluids was measured at 30 min, 2 h, 4 h, 8 h, 12 h and 24 h p.i., the % ID_{TCF}/ml calculated were plotted versus time and the kinetic profiles are reported in figure 12. ^{99m}Tc-UBI 29-41 and ^{111}In-DTPA-biotin (figure 12A and 12D) displayed a similar kinetic into cage fluids, with peak values measured at 30 min p.i. of 3.26 ± 1.45 and 3.55 ± 0.92, respectively, followed by fast clearance and already at 12 h p.i. %ID/ml became <0.1. Similarly, ^{99m}Tc-ciprofloxacin (figure 12B) peaks of 2.94 ± 1.01 %ID were achieved in cage fluids at 30 min p.i.

Differently, the penetration of ^{99m}TcN-ciproCS$_2$ (figure 12C) into cage fluids was lower than the other tested agents, with a slow kinetic and peak values in sterile fluids between 8 and 12 h of 0.23 ± 0.01.

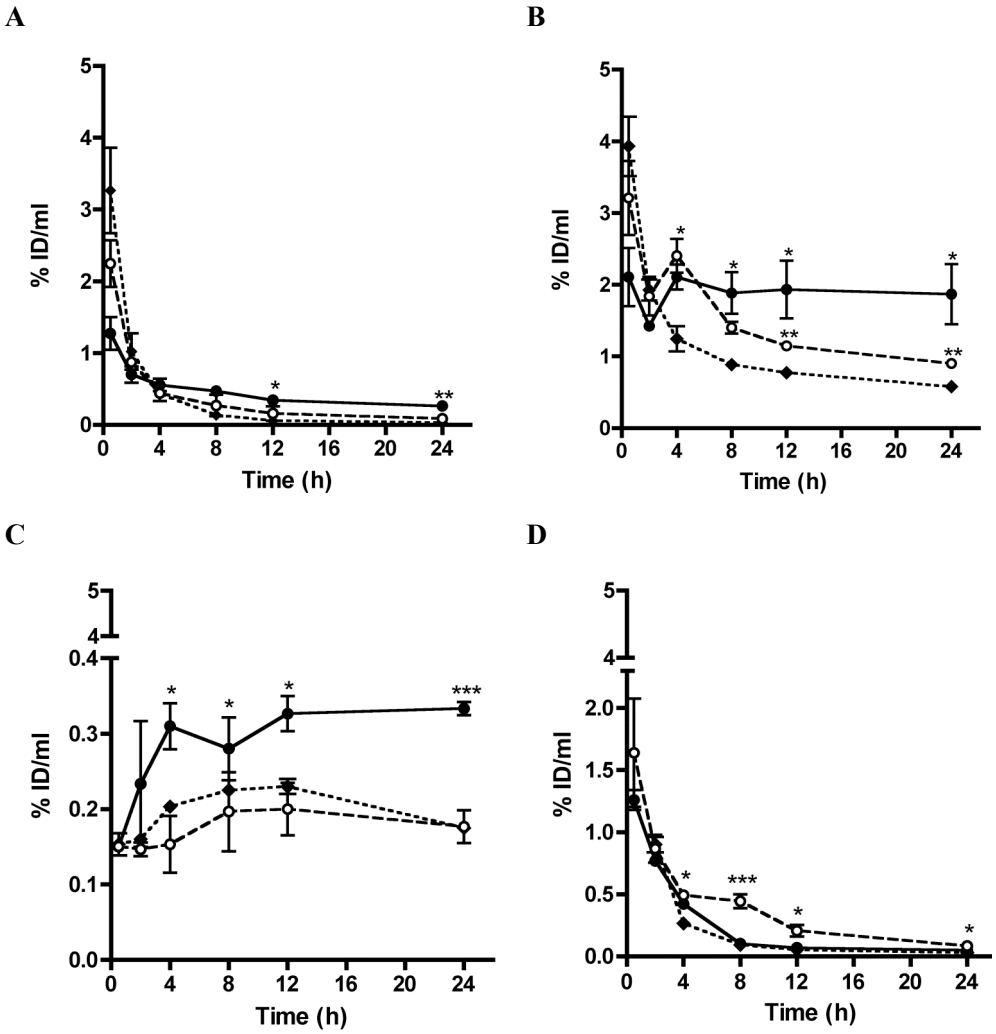

Figure 12. Distribution profiles of ^{99m}Tc-UBI 29-41 (A), ^{99m}Tc-ciprofloxacin (B),^{99m}TcN-CiproCS$_2$ (C) and ^{111}In-DTPA-Biotin (D) at 30 min, 2, 4, 8, 12 and 24 h p.i. into cage fluids sterile (black diamonds and dotted lines), *S.aureus* (empty circles and dashed lines) or *E. coli* (close circles and continuous lines) infected. Data represent % ID/ ml of tissue fluid, expressed as means ± 1 SEM of three to five mice per testing group. Significant differences between infected and control cage fluids are indicated as follow: * P < 0.05, ** P < 0.005, ***P < 0.0005

Radiopharmaceutical accumulation into dissected tissues, organs and cage tissues was evaluated at 4 h and 24 h p.i. %ID/ g measured from total body biodistribution are reported in table 6a, and plots of the cage associated %ID/ g are displayed in figure 13. Distributions of the radiotracers into cage tissues well correlated to the one measured in the cage fluids. In table 6b are reported the cage-fluid and the cage-tissue to blood %ID ratios for all tracers at 4 h and 24 h p.i..

Preferential accumulation of ^{99m}Tc-UBI 29-41 in *E. coli* infected than in sterile cages was measured between 12 h (P=0.045) and 24 h p.i. (P=0.0069) (figure 13A). The agent was fast cleared from blood and calculated cage fluid or tissue cages to blood ratios ranged between 1.60 - 6.00 % in sterile

animals and 4.50 – 18.35 % in infected animals (table 6b). At 24 h p.i. cage-fluid to blood ratios were significantly lower in non-infected than in both *E. coli* (P=0.0008) and *S. aureus* (P=0.035) infected animals (table 6).

The uptake of ^{99m}Tc-ciprofloxacin in both *S. aureus* and *E. coli* infected cage fluids and tissues (figure 12B and 13B) were higher than in sterile ones at any time point between 4 h and 24 h p.i. (P<0.05). Both cage and cage fluids to blood ratios were highly discriminative for infections already from 4 h p.i. (table 6b).

^{99m}TcN-ciproCS$_2$ did not differentiate between sterile and *S. aureus* infection (figure 12C and 13C), whereas %ID, cage-fluid to blood and tissue-cage to blood ratios became significantly higher in *E. coli* infected animals from 4 h p.i. (P=0.028) to 24 h p.i. (P=0.0003).

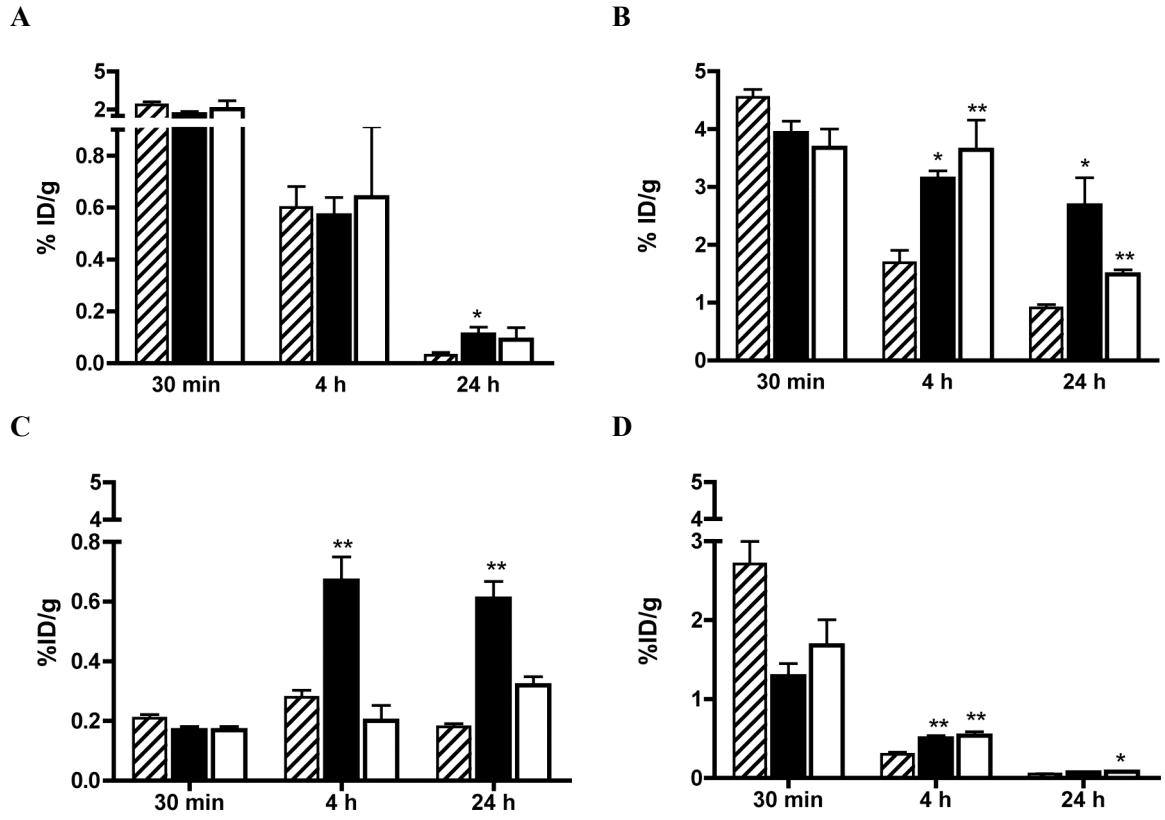

Figure 13. Distribution of ^{99m}Tc-UBI 29-41 (A), ^{99m}Tc-ciprofloxacin (B),^{99m}TcN-CiproCS$_2$ (C) and ^{111}In-DTPA-biotin (D) at 4 and 24 h p.i. into explanted cages sterile (dashed bars), *E.coli* (close bars) or *S. aureus* (open bars) infected. Data represent % ID/g of tissue, expressed as means ± 1 SEM of three to five mice per testing group. Significant differences between infected and control cages are indicated as follow: * P < 0.05, ** P < 0.005, ***P < 0.0005

^{111}In-biotin accumulated in *S. aureus* infected cages more than in sterile animals at any time after 4 h (P=0.0089) p.i. (figure 12D and 13D). %IDs were significantly higher in *E. coli* infected than in explanted cages at 4 h p.i. (P=0.028) but not at 24 h p.i., while the accumulation in *E. coli* infected cage fluids was equal than the one in sterile animals. On the other hand, the ratios of cage-fluid and tissue-cage to blood were discriminative for both *E. coli* and *S. aureus* infections from 4 h to 24 h p.i.

(table 6b).

As previously described, in biodistribution studies both ^{99m}Tc-UBI 29-41 and ^{99m}Tc-ciprofloxacin accumulated in the kidneys, which constitute the main elimination route. In addition, ^{99m}Tc-ciprofloxacin showed liver uptake, probably due to hepatic metabolism [89, 91, 92]. In accordance to J. Zhang et al. [102] ^{99m}TcN-CiproCS_2 distributed mainly in liver and intestine, secondarily in spleen, lungs and kidneys. ^{111}In-biotin showed a low accumulation in all organs and tissues, as it was cleared from blood already at 4 h p.i. A slight accumulation into kidneys indicated the latter being involved in the tracer elimination.

All tested radiopharmaceuticals were cleared from most organs and tissues at 24 h p.i. (table 6a).

Table 6. a Biodistribution after i.v. injection of ^{99m}Tc-UBI 29-41, ^{99m}Tc-ciprofloxacin,^{99m}TcN-CiproCS2 and ^{111}In-DTPA-biotin expressed as means (±SD) %ID/g of tissue and target-to-non target cage ratios (T/NT).

	^{99m}Tc-UBI 29-41		**^{99m}Tc-ciprofloxacin**		**^{99m}TcN-CiproCS$_2$**		**^{111}In-DTPA-biotin**	
	4 h	24 h	4 h	24 h	4 h	24 h	4 h	24 h
Blood	0.06(±0.01)	0.02(±0.00)	0.71(±0.17)	0.55(±0.05)	3.35(±0.31)	0.75(±0.03)	0.03(±0.00)	0.02(±0.00)
Heart	0.14(±0.01)	0.02(±0.01)	2.16(±0.63)	1.01(±0.04)	0.64(±0.09)	0.20(±0.02)	0.06(±0.01)	0.01(±0.00)
Liver	0.77(±0.02)	0.17(±0.07)	7.34(±3.76)	3.14(±0.27)	21.13(±0.93)	8.51(±1.29)	0.08(±0.01)	0.07(±0.02)
Stomach	1.09(±0.18)	0.23(±0.16)	2.11(±0.74)	1.26(±0.14)	0.67(±0.36)	0.31(±0.12)	0.06(±0.04)	0.03(±0.01)
Spleen	0.38(±0.10)	0.09(±0.03)	1.94(±0.85)	1.35(±0.05)	7.76(±0.96)	2.48(±0.75)	0.09(±0.02)	0.07(±0.01)
Kidneys	40.18(±1.88)	5.80(±2.90)	15.42(±1.95)	9.94(±0.40)	3.78(±0.65)	0.87(±0.17)	1.48(±0.31)	1.00(±0.21)
Lungs	0.62(±0.06)	0.05(±0.03)	1.61(±0.36)	1.09(±0.14)	5.62(±2.99)	0.51(±0.18)	0.04(±0.01)	0.38(±0.70)
Intestine	0.71(±0.07)	0.13(±0.07)	2.71(±1.03)	0.84(±0.14)	14.50(±3.87)	1.12(±0.13)	0.18(±0.06)	0.08(±0.04)
Bone	0.09(±0.01)	0.03(±0.01)	3.15(±0.46)	3.64(±0.25)	1.58(±0.27)	0.68(±0.05)	0.06(±0.00)	0.04(±0.00)
Muscle	0.05(±0.02)	0.01(±0.00)	0.62(±0.17)	0.38(±0.06)	0.82(±0.09)	0.22(±0.03)	0.03(±0.01)	0.01(±0.01)
[a]*E. coli*/ sterile TC	1.01(±0.12)	2.83(±1.28)	1.86(±0.14)	2.93(±0.91)	2.35(±0.48)	2.29(±0.36)	1.76(±0.19)	1.47(±0.21)
[a]S. aureus/ sterile TC	1.31(±0.65)	2.17(±1.42)	2.16(±0.53)	1.63(±0.14)	0.71(±0.30)	1.22 (±0.19)	1.91(±0.27)	1.89(±0.36)

[a]Ratios between %ID/g measured in infected and sterile cages. TC = tissue cage.

Table 6.b ^{99m}Tc-UBI 29-41, ^{99m}Tc-ciprofloxacin,^{99m}TcN-ciproCS2 and ^{111}In-DTPA-biotin cage fluids or explanted cages to blood %ID ratios expressed as means (±SD).

		Sterile TC		***E. coli* TC**		***S. aureus* TC**	
		Fluids	**Cages**	**Fluids**	**Cages**	**Fluids**	**Cages**
^{99m}Tc-UBI 29-41	4 h	4.39(±1.07)	6.00(±1.35)	5.68(±2.21)	6.03(±0.70)	4.50(±1.92)	7.83(±3.91)
	24 h	1.90(±1.11)	4.00(±1.73)	18.35(±2.91)	11.33(±5.13)	4.82(±1.87)	8.67(±5.69)
^{99m}Tc-ciprofloxacin	4 h	0.26(±0.06)	0.35 (0.08)	0.44(±0.06)	0.65(±0.05)	0.53(±0.03)	0.76(±0.18)
	24 h	0.52(±0.03)	0.81(±0.09)	1.66(±0.65)	2.38(±0.74)	0.80(±0.05)	1.33(±0.11)
^{99m}TcN-ciproCS$_2$	4 h	0.22(±0.02)	0.31(±0.04)	0.35(±0.06)	0.74(±0.15)	0.14(±0.09)	0.22(±0.09)
	24 h	0.82(±0.04)	1.25(±0.07)	1.59(±0.08)	2.87(±0.45)	0.85(±0.17)	1.52(±0.24)
^{111}In-Biotin	4 h	4.69(±1.42)	4.72(±0.86)	7.44(±1.31)	8.89(±0.95)	9.51(±0.29)	9.61(±1.36)
	24 h	2.26(±0.38)	5.33(±0.58)	3.82(±0.85)	7.00(±1.00)	6.24(±1.17)	9.00(±1.73)

2.5 Discussion

Several classes of radiopharmaceutical have been developed, with the common aim of targeting either host or bacterial cells specifically involved in the infective process. We compared four well-known and promising radiotracers for targeting bacterial infections in a tissue-cage mouse model of implant-associated infection. First, we evaluated the radiotracers in vitro in a competitive binding assay with laboratory strains of *E. coli* and *S. aureus*, followed by study of their biodistribution in sterile and infected animals.

The labeling kits demonstrated a high labeling efficiency and high stability both in saline and serum, with exception of ^{99m}Tc-ciprofloxacin, whose radiochemical purity decreased in saline to ≈ 60 % during 6 h. In serum, the stability of ^{99m}Tc-UBI cannot be assessed by ITLC, but in previous studies the tracer was reported to maintain a radiochemical purity of 85 % to 90 % during 24 h incubation in human serum [107].

The correlation of the in vitro binding results with the binding to bacteria in vivo is unclear. The different uptake mechanism and kinetics of radiopharmaceuticals to bacteria may result being highly affected by the conditions adopted in the in vitro tests. In our studies, the in vitro binding of the four radiotracers to *E. coli* and *S. aureus* was poorly satisfactory. All radiopharmaceuticals showed strain differences and generally similar capacity to bind to both alive and dead bacteria. Furthermore, not always we were able to displace the bound radiopharmaceutical by an excess of unlabelled compound, due to the lack of a receptor-mediated binding mechanism and to the killing induced by the high concentration of unlabelled compound to be added in excess.

Indeed, the initial interaction of antimicrobial peptides, as UBI 29-41, to microbial plasmatic membranes is only guided by electrostatic interaction between the positively charged peptide and the negatively charged lipid bacterial membranes. Following, the amphipathic nature of antimicrobial peptides induces hydrophobic interactions, and insertion through the membranes with formations of pores. Then, the pores mediate internalization and accumulation of antimicrobial peptides in the bacterial cytoplasm, where they presumably specifically bind to intracellular targets [89, 108].

Similarly, ciprofloxacin, a fluoroquinolone antimicrobial targeting bacterial DNA-gyrase, has been described to be taken up by Gram positive and Gram negative bacteria in a non-saturable mode, as simple diffusion through non specific protein channels or directly through the phospholipids bilayer. Bacterial uptake of ciprofloxacin is reduced at lower temperatures, which is in accordance with our results. The ciprofloxacin binding to bacteria may be affected by the phase of bacterial growth, the culture medium or the degree of aeration during growth. In addition, the active efflux system across the cytoplasmic membrane and the washing step performed after exposure of the bacterial cultures to the radiolabeled ciprofloxacin may play key roles in the final binding percentage [109]. Previously, by using the same ^{99m}Tc-ciprofloxacin kit preparation applied in our study, Sierra et al. reported an in

vitro binding to *S. aureus* of 22-23%, which is 10-fold higher than what we could measure [105]. However, Sierra et al. tested a bacterial density of OD_{600} = 1.5, which is three times higher than the one we used in the in vitro binding studies. In our in vitro studies, we chose a bacterial density with OD_{600} 0.5 because corresponding to ≈ 8 $\log_{10}$CFU/ml, which is the highest bacterial counts achieved in vivo in the mouse cage fluid. Indeed, bacterial densities like ours have been used in in vitro assays in previous studies and led to a binding percentage similar to the one we report [110, 111].

Differently from the other tested agents, biotin is a vitamin and was reported to have a specific, temperature and energy dependent receptor-mediated binding to *E. coli* [112]. However, our results showed that the binding of ^{111}In-DTPA-biotin was not dependent on bacterial viability. A possible explanation for this discrepancy is the different concentration of biotin and bacteria that we used in our experiments.

The distribution studies of ^{99m}Tc-UBI 29-41, ^{99m}Tc-ciprofloxacin and ^{111}In-DTPA-biotin performed in the mouse tissue cage model showed a rapid penetration into the cage tissues and fluids followed by an exponential clearance. The peak concentrations were higher in sterile than infected cages, but clearance of sterile cages occurred earlier than infected, thus giving the possibility to discriminate between sterile inflammation and infection with late acquired images. Differently, the penetration of ^{99m}TcN-ciproCS$_2$ into cage fluids followed a slow kinetic and peak concentrations were achieved between 8 h and 12 h p.i..

In contrast with the low binding obtained in vitro, a significantly higher accumulation of the tracers into infected tissue cages was achieved between 4 h and 12 h p.i.. ^{99m}Tc-ciprofloxacin and ^{111}In-DTPA-biotin were discriminative for both *E. coli* and *S. aureus* infections. In previous pre-clinical and clinical studies, ^{99m}Tc-UBI 29-41 was reported to be accumulated preferentially at infection sites between 30 min and 4 h p.i. [89, 94, 113-115]. However, the tissue cage model did not support early time points due to delayed clearance of the non-infected cages. Indeed, at 30 min p.i., the radiotracers showed comparable concentrations in sterile and infected cages and became discriminative for *E. coli* infected cages between 12 h and 24 h p.i..^{99m}TcN-ciproCS$_2$ displayed low penetration into all cages, with peak values between 7- and 20-fols lower than the ones measured with the other tested radiotracers. Contrarily to the in vitro binding results, which led to higher binding affinity to *S. aureus* then to *E. coli*, ^{99m}TcN-ciproCS$_2$ was able to discriminate only for *E. coli* and not for *S. aureus* infected cages.

The T/NT (cage fluids, or tissue cage to blood) ratios of ^{99m}Tc-ciprofloxacin and ^{111}In-DTPA-biotin at 4 h were higher than for ^{99m}Tc-UBI 29-41 and ^{99m}TcN-CiproCS$_2$. At 24 h T/NT ratios > 2 where observed with ^{99m}Tc-UBI 29-41, ^{99m}Tc-ciprofloxacin and ^{99m}TcN-CiproCS$_2$ in *E. coli* infected cages, whereas in *S. aureus* cages and in all ^{111}In-DTPA-biotin injected mice the radioactivity was mainly cleared. T/NT ratio >3 were not achieved at any time and with any bacteria, a finding that in our opinion may constitute a limiting factor for their use in human to detect residual infection during or after therapy.

Conclusions

We report here for the first time, a comparison between four different radiopharmaceuticals developed for imaging of bacterial infections. We compare in vitro labeling stability of published formulated kits, in vitro binding to different strains of bacteria, in vivo biodistribution in a reliable and reproducible animal model of foreign body infection.

All compounds showed in vivo discrimination for infected sites, and thus, they constitute promising option for diagnosis occult implant infections. While ^{99m}Tc-ciprofloxacin and ^{111}In-DTPA-biotin accumulated in both *E. coli* and *S. aureus* infected cages, ^{99m}Tc-UBI 29-41 and ^{99m}TcN-ciproCS$_2$ preferentially discriminated for *E. coli* infected cages.

Chapter 3

Evaluation of a Novel ^{99m}Tc-labeled Vitamin B_{12} Derivative for Targeting *Escherichia coli* and *Staphylococcus aureus* in vitro and in Experimental Foreign Body Infection

D. Baldoni[1], R. Waibel[2], Peter Bläuenstein[2], H. Treichler[3], H. Maecke[4], A. Signore[5], R. Schibli[2], A. Trampuz[1, 6]

[1]Infectious Diseases Research Laboratory, Department of Biomedicine, University Hospital, Basel, Switzerland

[2]Center for Radiopharmaceutical Science, Paul Scherrer Institute, Villigen PSI, Switzerland

[3]Ringgackerstrasse 1, Känerkinden, Switzerland

[4]Institute of Nuclear Medicine, University Hospital, Basel, Switzerland

[5]Nuclear Medicine Unit, 2nd Faculty of Medicine, University "Sapienza", Roma, Italy and Dept of Nuclear medicine & Molecular Imaging, University Medical Center Groningen, University of Groningen, The Netherlands

[6]Infectious Diseases Service, Department of Internal Medicine, University Hospital and University of Lausanne, Lausanne, Switzerland

Running title: Vitamin B_{12} derivatives for diagnosis of infection

Submitted at the Journal of Nuclear Medicine (October 2009)

3.1 Abstract

Vitamin B_{12} (Cbl) is accumulated by rapidly replicating prokaryotic and eukaryotic cells. We investigated the potential of a ^{99m}Tc-labeled Cbl derivative (^{99m}Tc-PAMA(4)-Cbl) for targeting infections caused by *Escherichia coli* and *Staphylococcus aureus*. In vitro binding assays were followed by biodistribution studies in a mouse model of foreign body infection.

Methods: *E. coli* (ATCC 25922) and *S. aureus* (ATCC 43335) were used as test strains. ^{57}Co-Cbl, ^{67}Ga-citrate and ^{99m}Tc-DTPA served as reference compounds. The in vitro competitive binding of ^{57}Co-Cbl or ^{99m}Tc-PAMA(4)-Cbl, and unlabeled Cbl, to viable or killed bacteria, was evaluated at 37°C and 4°C. A cage mouse model of infection was used for biodistribution of intravenous ^{57}Co-Cbl, ^{99m}Tc-PAMA(4)-Cbl and reference compounds in cage and dissected tissues of infected and non-infected mice.

Results: Maximum binding (mean ± SD) of ^{57}Co-Cbl to viable *E. coli* was 81.7 ± 2.6% and to *S. aureus* 34.0 ± 6.7%, at 37°C; no binding occurred to heat-killed bacteria. Binding to both test strains was displaced by 100- to 1000-fold excess of unlabeled Cbl. The in vitro binding of ^{99m}Tc-PAMA(4)-Cbl was 100-fold lower than of ^{57}Co-Cbl for *E. coli*, whereas was equal to the one of ^{57}Co-Cbl for *S. aureus*. In vivo, ^{99m}Tc-PAMA(4)-Cbl showed peak %ID values between 1.33 and 2.3, at 30 min p.i. Significantly higher retention occurred in cage fluids infected with *S. aureus* at 4 h and with *E. coli* at 8 h p.i. than in non-infected animals. Accumulation into infected cages was also higher than the one of ^{99m}Tc-DTPA, which showed similar biodistribution in infected and sterile mice.

^{57}Co-Cbl gradually accumulated in cages with peaks %ID between 3.58% and 4.83% achieved from 24 h to 48 h. Discrimination for infection occurred only in *E. coli* infected mice, at 72 h p.i.

^{67}Ga-citrate, which showed a gradual accumulation into cage fluids during 12 h, was discriminative for infection from 48 to 72 h p.i. ($P<0.05$).

Conclusion: Cbl displayed rapid and specific in vitro binding of the test strains. ^{99m}Tc-PAMA(4)-Cbl was rapidly cleared from most tissues and discriminated between sterile and infected cages, being a promising candidate for imaging infections in humans.

3.2 Introduction

Bacterial infections are an important cause of morbidity and mortality worldwide. The accurate diagnosis of infection (or its exclusion) is the first crucial step in the management of these patients. Imaging techniques constitute a non-invasive and attractive approach that, in the last decades, has gained on importance by combining visualization of radiopharmaceuticals and morphological imaging, with PET/CT and SPECT/CT imaging [24, 32]. In various types of infections, including prosthetic joint infections, radionuclide imaging techniques become essential when the diagnosis remains unclear [4]. The current standard method is based on labeling white blood cells isolated from patients [87, 116-118]. Other agents have been developed in the past decade, such as radiolabeled antimicrobials (ciprofloxacin, sparfloxacin, ceftizoxime, isoniazid, ethambutol, fluconazole), antimicrobial peptides (29-31 UBI, human beta-defensin-3), cytokines (IL-8), ^{18}F-FDG, growth factors and bacteriophages [24, 30, 93, 97, 119-121]. However, in pre-clinical and clinical studies these agents showed several limitations, in particular insufficient specificity for diagnosing infection, making them unsuitable in the clinical practice [22, 31, 32].

Vitamins are essential growth factors, which are required in fast replicating cells, such as bacteria or fungi and may be used in a labeled form for specific targeting infection. Vitamin B_{12} or cobalamin (Cbl) is an important hydrophilic enzyme cofactor. In bacteria, Cbl catalyzes transmethylation and rearrangement reactions by binding to Cbl-dependent enzyme isoforms, directly or indirectly responsible for the synthesis of ATP, amino acids and nucleotides [122] Comparative genomic analysis revealed a wide distribution of genetic elements involved in the regulation or uptake of Cbl derivatives [122]. Cbl transport systems were studied mainly in enteric bacteria, where the best structurally characterized was in *E. coli.* The *E. coli* Cbl uptake is mediated by an external membrane transporter (BtuB, TonB-dependent), which transfer Cbl to a periplasmatic protein (BtuF) and finally across the inner membrane (BtuCD, ABC ATP-dependent) [123-125]. Gram-positive bacteria, as *S. aureus*, do not have an outer membrane, and thus completely lack the BtuB carrier. However, elements analogue to the *E. coli* BtuCD inner-membrane transporter system were reported in *S. aureus* and *S. epidermidis* strains, and described as less specific carriers of Cbl and closely related molecules as heme and siderophores [122]. The latter findings supported previous in vitro studies of ^{57}Co-Cbl uptake mechanism, which reported high avidity of binding to several pathogen bacteria in different culture conditions [126, 127].

The distinctive uptake mechanism in bacterial and animal cells may represent the basis for development of radiolabeled Cbl derivatives for specific targeting bacterial infections and for reduced systemic accumulation in vivo. Cbl distributes through the blood circulation upon binding to the transport protein transcobalamin II (TC II). The Cbl-TC II complex is rapidly internalized through binding to the transcobalamin II receptor (RTC II) and megalin receptor, mainly expressed in humans

in the kidneys, liver, intestine lumen, glands and absorptive epithelia [128, 129]. A second family of proteins, transcobalamin I (TC I or haptocorrins, or R-type Cbl-binders), bind free Cbl and cobinamides in the blood. The TC I protein family was mainly found in secondary granules of granulocytes and in salivary glands, and its release has a protective function of reducing pathogen colonization and growth [130, 131].

A ^{57}Co-Cbl oral formulation was initially developed and used in humans for diagnosis of vitamin B_{12} malabsorption syndromes [132]. A similar intravenous formulation showed potential targeting of tumor cells [133]. However, the long half-life of the isotope ^{57}Co-Cbl, together with its systemic non-specific accumulation and persistence in several organs, limited the maximal injectable dose to 1 µCi. This dose limit prohibits the use of ^{57}Co-Cbl for imaging purposes. Therefore, vitamin B_{12} analogues were synthesized and labeled with isotopes such as ^{111}In and ^{99m}Tc. An ^{111}In-labeled Cbl derivative, diethylentriamine-pentaacetat adenosylcobolamin (^{111}In-DAC), showed promising results for the diagnosis of various malignancies. Interestingly, in the same study, ^{111}In-DAC derivative accumulated in the right wrist of one patient, who was diagnosed a staphylococcal septic arthritis [134]. However the high unspecific accumulation of the ^{111}In-DAC in non-target tissues made this tracer inappropriate for routine clinical application.

The Cbl derivative ^{99m}Tc-PAMA(4)-Cbl has been recently developed and tested for imaging of malignancies (figure 14) [85, 135]. This conjugate carries mono-anionic ligands with a NNO donor set and can be efficiently labelled with $[^{99m}Tc(OH_2)_3(CO)_3]^+$ at yields > 95% under mild conditions (50°C, 60 min) [135]. Importantly, ^{99m}Tc-PAMA(4)-Cbl has abolished binding to the major Cbl-transport protein TC II. As a consequence, significantly lower uptake in non-targeted tissue and organs was demonstrated in mice bearing different tumour types.

In this study we evaluated the potential of ^{99m}Tc-PAMA(4)-Cbl for specific targeting *E. coli* and *S. aureus* in vitro and in a cage model of foreign body infection in mice [71]. The results were compared with the TCII binding molecule ^{57}Co-Cbl.

The infection model of subcutaneously implanted cages has been used in mice for investigating pathophysiology and treatment efficacy of implant-associated infection [74, 77, 104]. The kinetic and histology of the infected cage closely resemble a human infection of prosthesis with bacteria adherent to the foreign body, infiltration of granulocytes and pus. The model allows the induction of a localized persistent infection, characterized by a high and reproducible bacterial density of 10^7-10^9 colony forming units (CFU) per ml cage fluid. Cages fill with inflammatory fluid (exudate) surrounded by a highly vascularized tissue. To determine appropriateness of the animal model for testing radiotracers, the distribution of ^{67}Ga-citrate, an agent accumulating unspecifically at the site of aseptic inflammation and infection, was used as control. In addition, biodistribution studies with ^{99m}Tc-DTPA were performed to evaluate the local vascularization of infected and non-infected cages.

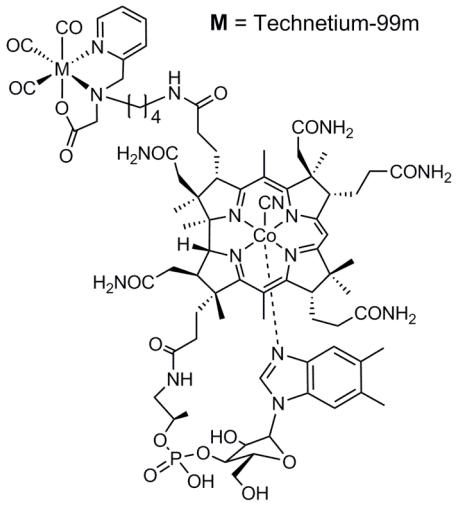

Figure 14. Chemical structure of ^{99m}Tc-PAMA(4)-Cbl

3.3 Material and Methods

Radiolabeled tracers. ^{99m}Tc-PAMA(4)-cyanocobalamin (^{99m}Tc-PAMA(4)-Cbl) was synthesized and labeled as described elsewhere [85]. Five GBq of pertechnetate (1.2 ml) were added to the kit and heated for 20 min. The alkaline solution was neutralized with a 1 M HCl solution and additionally buffered 1 M MES. This solution was added to 30 µg of the lyophilized Cbl-b-(butyl)-PAMA-OEt. The reaction mixture was kept at 75°C for 75 min. The product was purified over a RP-8 column (X-Terra RP8 5µm 30x150 mm) using a gradient of solvent A (10 % Ethanol, 90 % 0.1 M Acetate buffer) and B (70% Ethanol/water). The collected fraction of about 1 ml was diluted with phosphate buffer pH 7.4 up to 10 ml. Aliquots of the product were distributed according to the needs. Briefly, DTPA (Pentacis®, IBA Molecular, Switzerland) was labeled in 10 ml of sterile 0.9% saline with 3.05 GBq of sodium-^{99m}Tc-pertechnetat, according to the manufacturer instructions, with a labeling efficiency of 98.6%. ^{57}Co-cyanocobalamin (^{57}Co-Cbl) 0.39 MBq/50 ng/ml was purchased by MP Biomedicals (Diagnostic Division, Orangeburg, NY, USA). ^{67}Gallium citrate solution for injection was purchased at a radiochemical concentration of 17.17 MBq/ml (Mallinckodt Schweiz AG, Radiopharma, Wollerau, Switzerland).

Test microorganisms. Laboratory strains *E. coli* (ATCC 25922) and *S. aureus* (ATCC 35556, methicillin-susceptible) were used. Bacteria were stored at -70°C using a cryovial bead preservation system (Microbank, Pro-Lab Diagnostics, Richmond Hill, ON, Canada). Single cryovial beads were cultured overnight on Columbia sheep blood agar plates (Becton Dickinson, Heidelberg, Germany).

For in vitro binding studies, overnight cultures were prepared in snap-lid tubes from two to three CFU in 5 ml of a synthetic minimal medium depleted of vitamin B_{12}. After 18-20 h incubation at 37°C and 200 rpm, the cultures were diluted 1:100 in the same medium and further incubated at 37°C to mid-logarithmic phase in sealed tubes, without shaking.

For in vivo studies, overnight cultures were prepared in 5 ml tryptic soy broth (TSB), incubated at 37°C without shaking for 18-20 h. Bacterial suspensions were then washed three times, re-suspended in 5 ml of sterile 0.9% saline and diluted.

***In vitro* binding studies.** The in vitro binding and internalization profiles of ^{57}Co-Cbl and ^{99m}Tc-PAMA(4)-Cbl to *E. coli* and *S. aureus* were characterized. Stock solutions of the radiotracers were prepared at concentration of 0.004 MBq/ml (0.350 – 0.700 ng/ml, 0.3 – 0.5 pmol/ml) for ^{57}Co-Cbl and ≈1 MBq/ml (≈ 0.5 ng/ml, ≈ 0.3 pmol/ml) for ^{99m}Tc-PAMA(4)-Cbl in phosphate buffer solution (PBS). In competition studies, 10-fold dilutions between 3 µg/ml and 0.003 µg/ml of unlabeled Cbl (Sigma-Aldrich, Steinheim, Germany) were added to the stock radiotracer solutions.

Bacterial cultures in the logarithmic phase at OD_{600} between 0.4 and 0.6 were centrifuged and re-

suspended in equal volume of sterile PBS. Five hundred µl of re-suspended cultures were transferred to Eppendorf tubes and used for the measurement of binding to viable bacteria at 37°C. For testing binding at 4°C, bacterial suspension in PBS were let equilibrate for 1 h at 4°C before adding of the tracers. In order to evaluate the binding to killed bacteria, bacterial cultures were either exposed to heat at 99°C or to 70% ethanol at 4°C for 30 min (*E. coli*) or 60 min (*S. aureus*). The bacterial suspensions were then centrifuged, re-suspended in PBS and used for further studies. The PBS resuspended heat-killed or ethanol-killed bacteria were sampled on Columbia blood agar plates and the CFU enumerated after 24 h of incubation at 37°C. Colony counts remained <10 CFU/ml.

Five hundred µl of each tracer solution was added to the 500 µl of bacterial suspensions. Binding assays were performed in quadruplicate vials per testing conditions. Afterwards, vials were centrifuged for 5 minutes at 13,500 rpm and 4°C, and pellets washed with 500 µl of cooled PBS. Supernatants and re-suspended pellets were counted in a multi-well NaI γ-counter (Cobra; Packard, USA) and the counts per minutes (CPM) recorded. The percentage of radiolabeled Cbl in the pellets was calculated as percentage of the CPM_p/CPM_0-ratio per $\log_{10}$ 8.0 CFU/ml, where CPM_p were the CPM associated to pellets and CPM_0 the total CPM of the radiolabeled Cbl added per vial.

In vitro binding of the radiotracers was measured after 5, 30, 60, 120 min (*E. coli* and *S. aureus*) and 180 min (*S. aureus*) of incubation at 37°C and 4°C.

Competition binding studies were measured for cultures incubated for 1 h (*E. coli*) and 3 h (*S. aureus*), at 37°C and 4°C, simultaneously with 10-fold serial dilution of unlabeled Cbl and either ^{57}Co-Cbl or ^{99m}Tc-PAMA(4)-Cbl. In addition, competition with unlabeled Cbl was studied on bacterial cultures previously incubated with ^{57}Co-Cbl or ^{99m}Tc-PAMA(4)-Cbl for 20 min (*E. coli*) or 2 h (*S. aureus*), and further exposed to the unlabelled-labeled Cbl mixtures for 10 min (*E. coli*) or 1 h (*S. aureus*).

Tissue-cage infection model in mice. C57Bl/6 mice from in-house breeding or purchased from Charles River Laboratories GmbH (Sulzfeld, Germany) were housed in the Animal Facility of the Department of Biomedicine, University Hospital, Basel, Switzerland. Experiments were performed in accordance to the regulations of Swiss veterinary law. The Institutional Animal Care and Use Committee approved the study protocol. Drinking water and standard laboratory food pellets (CR) were provided *ad libitum.* To reduce interference of high vitamin B_{12} level in mice, animals randomized for Cbl biodistribution studies were fed with a vitamin B_{12}-reduced diet (Provimi Kliba AG, Kaiseraugst, Switzerland) beginning at the age of 10 weeks. At the age of 12 weeks, one sterile polytetrafluoroetylene (Teflon) tube (32 x 10 mm), perforated by 130 regularly spaced holes of 1 mm diameter, was aseptically implanted into the back of each mouse, as previously described [71, 77]. Each cage was weighted and numbered before implantation. Two weeks after surgery, clips were removed from healed wounds and sterility of the cage was confirmed by culture of aspirated cage

fluid. On the following day, 5×10^5 CFU of *E. coli* or 5×10^6 CFU of *S. aureus*, resuspended in 200 µL of 0.9% saline, were injected into cages. Sterile 0.9% saline was injected in cages in animals used as negative controls.

Biodistribution studies. Biodistribution studies were performed in control and infected mice, 24 h (for *E. coli*) or 48 h (for *S. aureus*) after infection. The bacterial counts in cage fluid were enumerated by plating 10-fold serial dilutions of cage fluid, collected on the day of tracer injection, and incubated for 24 h at 37°C.

Hundred µl of isotonic saline solution containing ≈10 MBq of ^{99m}Tc-PAMA(4)-Cbl and 0.25 mg/ ≈10 MBq of ^{99m}Tc-DTPA were injected into the lateral tail vein of each mouse, randomized for a minimum of nine mice per infection group (*E. coli*, *S. aureus* or sterile mice) per tracer. Distribution of tracers into the cage fluids was determined at 30 min, 1 h, 2 h, 4 h, 8 h, 12 h and 24 h. Distribution into organs, tissues and explanted cages was measured at 30 min, 4 h and 24 h after injection.

One hundred µl of isotonic saline solution containing 1.2 - 2.3 ng/ 0.014 MBq ^{57}Co-Cbl or 0.83 pg/ 0.172 MBq of ^{67}Gallium citrate were injected into the lateral tail vein of each mouse, randomized for a minimum of four mice per infection group (*E. coli*, *S. aureus* or control mice) per tracer. Cage fluids were measured at 1 h, 6 h, 24 h, 48 h and 72 h after injection. Animals were sacrificed at 72 h and the total-body biodistribution was determined.

The two different experimental sets up of biodistribution were adapted to the known tracer binding/ non-binding to plasma protein, long persistence in organs and tissues and half-life of the labeling radioisotope.

Accumulation of tracers in the cage fluid was measured by re-suspending 100 µl of aspirated fluid in 1 ml PBS and counted in gamma counter. The percentage of injected dose (% ID_{TCF}/ml) was calculated as measured CPM normalized per 1 ml cage fluid and divided by the CPM_0 of the injected dose. For determination of tracer biodistribution, mice were sacrificed with an intraperitoneal injection of 50-80 µl saline solution of pentothal (100 mg/ml). Blood was collected by cardiac puncture and mice were perfuse with 0.9% saline for around 5 min. Following, tissues were dissected, weighted and collected into test tubes for γ-counter (blood, heart, liver, spleen, stomach, kidneys, lungs, intestine, muscle, bone and cage). The percentage of injected dose (% ID_{tissue}/g) was calculated as CPM associated to each organ divided by its weight in grams and by the CPM_0 of the injected dose.

Statistical Analysis. Comparisons of in vitro binding results and in vivo biodistribution data were performed using the Student's t test for continuous variables. All results were given as mean values ± SEM, unless otherwise indicated. P values of <0.05 were considered significant. All calculations were performed using Prism 4.0a (GraphPad Software, La Jolla, CA, USA).

3.4 Results

***In vitro* binding studies.** Binding of ^{57}Co-Cbl to viable *E. coli* and *S. aureus* was time-dependent. *E. coli* showed a rapid binding with plateau reached already 10 minutes after incubation in a temperature independent fashion (figure 15A). With *S. aureus*, ^{57}Co-Cbl displayed a slower binding kinetic and no plateau was reached even after 3 h of incubation (figure 15B). In addition, the binding of *S. aureus* to ^{57}Co-Cbl was temperature-dependent (approximately 3-fold higher at 37°C than at 4°C). The maximum binding (mean ± SD) was measured at 37°C and was 81.7 ± 2.6% for *E. coli* and 34.0 ± 6.7% for *S. aureus*. Binding of ^{57}Co-Cbl to ethanol-killed *E. coli* was lower than the one observed in viable bacteria, while no binding was measured with heat-killed *E. coli*. In contrast, ^{57}Co-Cbl did not show any binding to both ethanol-killed and heat-killed *S. aureus*.

Binding of ^{99m}Tc-PAMA(4)-Cbl to *E. coli* was low, and ranged between 0.1 and 0.3% in all the tested conditions (living bacteria as well as ethanol- and heat-killed bacteria, data not shown). In contrast, ^{99m}Tc-PAMA(4)-Cbl binding to viable *S. aureus* at 37°C and 3 h incubation was 11.43 ± 1.7%, and, similarly to the one obtained with the ^{57}Co-Cbl, it was characterized by a slow temperature-depe ndent kinetic of binding to viable cultures and no binding to both ethanol-killed and heat-killed bacteria (figure 15C).

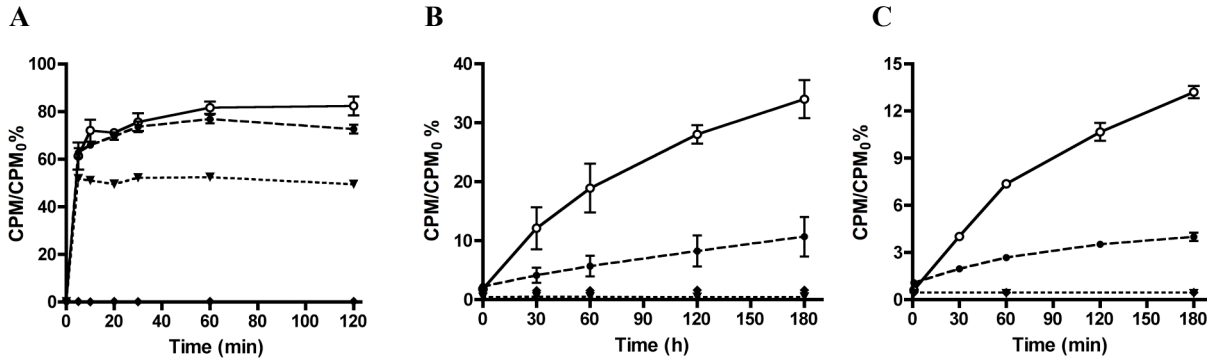

Figure 15. Kinetic of vitro binding (mean CPM/CPM$_0$% ± SD) of ^{57}Co-cyanocobalamin to *E. coli* (A) and *S. aureus* (B) at different incubation times. Kinetic of vitro binding (mean CPM/CPM$_0$% ± SD) of ^{99m}Tc-PAMA(4)-Cbl to *S. aureus* (C) at different incubation times. At 37°C (open circles, continuous line), 4°C (closed circles, dashed line), ethanol-killed bacteria (closed triangles, dotted line) and heat killed bacteria (closed diamonds, dashed-dotted line). Note, X- and Y- axis are scaled depending on the bacterium or tracer tested.

^{57}Co-Cbl could be displaced by non-radioactive Cbl in a concentration-dependent manner. A 1000-fold concentration of unlabeled Cbl was required to show an inhibition of binding to *E. coli* at 37°C, while at 4°C and in ethanol-killed bacteria, a 10-fold cold vitamin B_{12} excess was sufficient to reduce the maximal binding to 50% (figure 16A). The *S. aureus* binding to ^{57}Co-Cbl was reduced already by 10-fold excess of unlabeled Cbl at both 37°C and 4°C; with 1000-fold excess of unlabeled Cbl, binding of the ^{57}Co-Cbl was completely blocked (figure 16B). Similarly, already 1-fold of unlabeled

Cbl decreased the binding of ^{99m}Tc-PAMA(4)-Cbl to *S. aureus* (figure 16C).

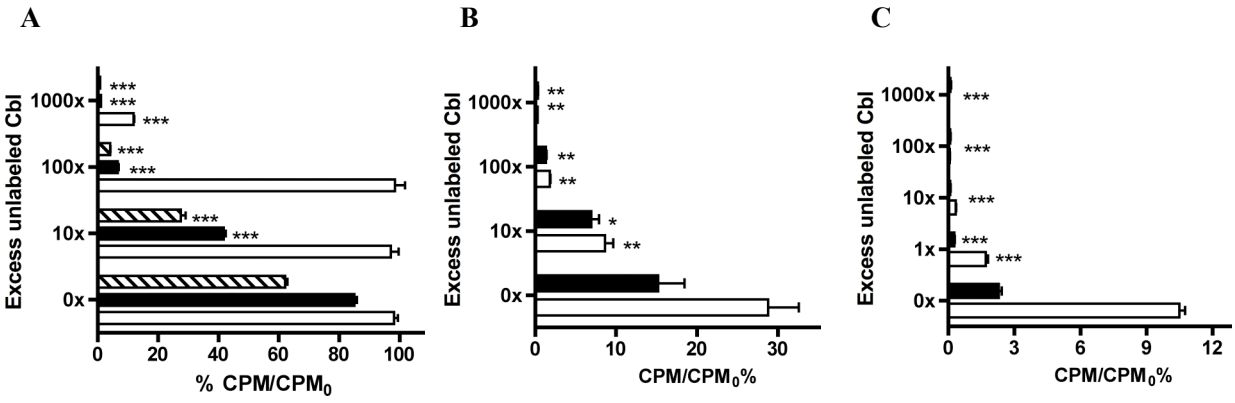

Figure 16. In vitro displacement of binding of ^{57}Co-Cbl to viable and non-viable *E. coli* (A) and to *S. aureus* (B); in vitro displacement of binding of ^{99m}Tc-PAMA(4)-Cbl to *S. aureus* (C); viable bacteria at 37°C (empty bar) or 4°C (filled bar) and non-viable bacteria after ethanol fixation (diagonal hatched bars, *E. coli* only). Significant differences between binding in the absence and in the presence of cold Cbl (at different concentrations) are indicated as follow: * P < 0.05, ** P < 0.005, ***P < 0.0005. Note, X- and Y- axis are scaled depending on the bacterium or tracer tested.

The rate of internalization of ^{57}Co-Cbl and ^{99m}Tc-PAMA(4)-Cbl by the test microorganisms was measured in an in vitro competition assay (figure 17).

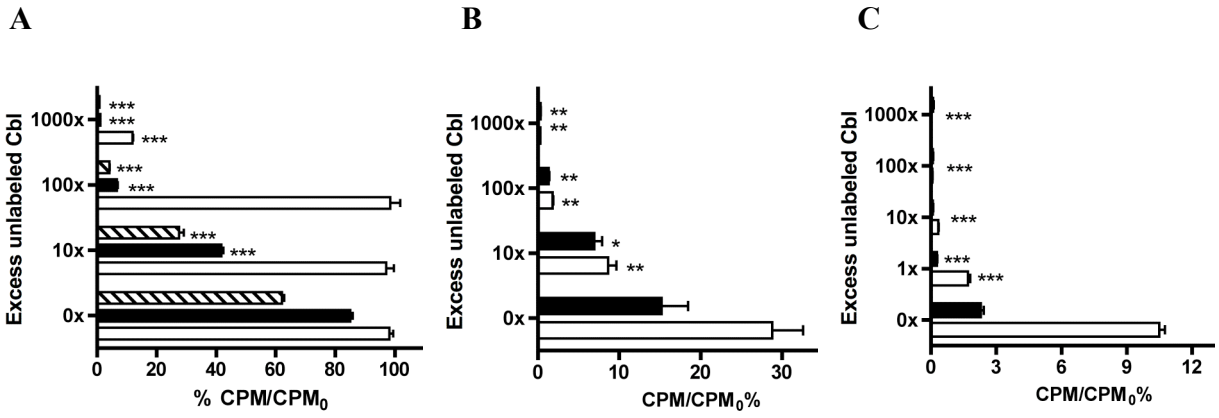

Figure 17. In vitro displacement of binding by non-labeled Cbl added after pre-incubation of ^{57}Co-Cbl and *E. coli* (A), ^{57}Co-Cbl and *S. aureus* (B) and of ^{99m}Tc-PAMA(4)-Cbl and *S.aureus* (C). Viable bacteria at 37°C (empty bars), at 4°C (filled bars) and non-viable bacteria after ethanol fixation (diagonal hatched bars, *E. coli* only). Significant differences between binding in the absence and in the presence of cold Cbl (at different concentrations) are indicated as follow: * P < 0.05, ** P < 0.005, ***P < 0.0005. Note, X- and Y- axis are scaled depending on the bacterium or tracer tested.

At 37°C, the binding of ^{57}Co-Cbl to *E. coli* achieved after 20 minutes incubation was unchanged upon following addition of the unlabeled Cbl. Differently, at 4°C the binding showed a slight decrease when challenged with 1000-fold excess of unlabeled Cbl. Binding of ^{57}Co-Cbl to ethanol-killed *E. coli* could be reversed by the excess of unlabeled Cbl, independently on the pre-incubation with the labeled Cbl (figure 17A). Similar mechanisms were also observed when *S. aureus* was pre-exposed to ^{57}Co-

Cbl or ^{99m}Tc-PAMA(4)-Cbl: the measured binding was only slightly reduced upon later challenge with excess of unlabeled vitamin, both at 37°C and 4°C (figure 17B and 17C).

Biodistribution studies. On the day of tracer injection, the mean ± SD bacterial counts were 9.4 ± 0.82 $\log_{10}$ CFU/ml for *E. coli* and 6.3 ± 0.62 $\log_{10}$ CFU/ml for *S. aureus*. Three days after injection bacterial counts were 8.6 ± 0.2 $\log_{10}$ CFU/ml for *E. coli* and 7.8 ± 0.1 $\log_{10}$ CFU/ml for *S. aureus*. Spontaneous cure was not observed in any infected cage. No clinical or pathological signs of systemic infection were observed during organ dissection.

The results of biodistribution studies of ^{99m}Tc-PAMA(4)-Cbl, ^{99m}Tc-DTPA, ^{57}Co-Cbl and ^{67}Ga-citrate are reported in figure 18 and table 7. The highest concentration of ^{99m}Tc-PAMA(4)-Cbl was measured in sterile cage fluid samples at early time points after injection (figure 18A). The maximum ^{99m}Tc-PAMA(4)-Cbl % ID_{TCF}/ml at 30 min was 2.3 ± 0.39% for sterile cages, 1.33 ± 0.26% for infected cages with *E. coli* and 2.06 ± 0.79% for infected cages with *S. aureus*. Clearance from sterile cages was faster than in infected cages and the % ID_{TCF}/ml was significantly lower in controls than in infected mice with *S. aureus* at 4 h (P = 0.042), and with *E. coli* at 8 h (P = 0.0035). ^{99m}Tc-PAMA(4)-Cbl cage fluid/blood ratios discriminated between non-infected mice (1.53 ± 0.30) and infected mice, both with *S. aureus* (13.48 ± 2.75, P = 0.0036) or *E. coli* (6.31 ± 2.92, P <0.0001), at 24 h p.i. The tracer was rapidly cleared from blood, whereas retention of radioactivity was observed in kidneys up to 24 h after injection. The tracer accumulation measured in explanted cages did not significantly differ in infected and sterile conditions up to 4 h, but it was discriminative at 24 h for *E. coli* infected cages (P = 0.0375), with % ID/g nearly 10-fold higher than in sterile cages (table 7).

^{99m}Tc-DTPA was used in vivo to evaluate the vascularization of sterile and infected cage fluids. The tracer showed an early peak in all sterile and infected cage fluids and cage tissues, ranging between 1.5 and 3%. Following, clearance was fast from all, sterile and infected cages and tissues (figure 18B).

The distribution profile of ^{57}Co-Cbl is shown in figure 18C. ^{57}Co-Cbl displayed a slow penetration into cage fluids, with peaks achieved between 24 and 48 h in sterile and *S. aureus* infected cages. A plateau % ID_{TCF}/ml of ^{57}Co-Cbl into *E. coli* infected cages was not achieved up to 72 h. Clearance from cage fluids was also slow, and was similar in sterile and *S. aureus* infected mice up to 72 h after injection. Only cages infected with *E. coli* at 72 h showed significantly higher tracer retention in the cage fluid, when compared to control mice (P = 0.0032). The cage fluid/blood-ratios in control mice (1.40 ± 0.19) were slightly discriminative for infected cages with *E. coli* (1.72 ± 0.07, P=0.04), but not with *S. aureus* (1.52 ± 0.10, P >0.05). At 72 h ^{57}Co-Cbl remained in high percentage in blood, liver and kidneys.

Similarly to ^{57}Co-Cbl, ^{67}Ga-citrate penetration into cages was slow and peak values were achieved at 12 h. Clearance was faster in sterile compared to infected cages and tissues (figure 18D). The ^{67}Ga-

citrate retention in cage fluid samples became significantly higher in infected than in non-infected animals at 48 h (P=0.029) and 72 h (P=0.0006). At 72 h, accumulation became also significantly higher in explanted cages of infected mice with both, *S. aureus* (P <0.0001) and *E. coli* (P = 0.0019). The cage fluid/blood-ratio of ^{67}Ga-citrate in non-infected animals was 1.14 ± 0.21, which was lower than the one measured in infected cages with *E. coli* (5.41 ± 0.52, P <0.0001) or *S. aureus* (3.56 ± 0.87, P = 0.0003). The distribution in tissues and organs at 72 h after injection showed the highest ^{67}Ga uptake into liver, kidneys and bone, while it was mostly cleared from the remaining tissues.

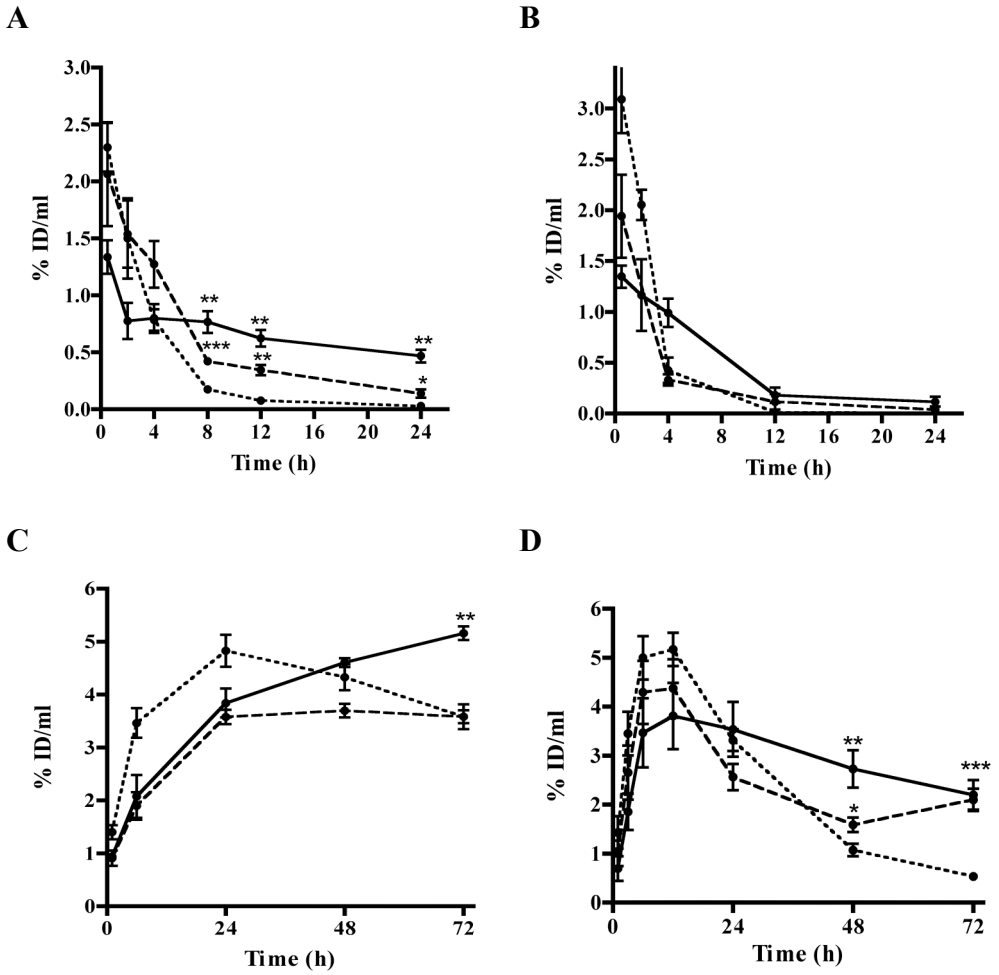

Figure 18. Distribution of: (A) ^{99m}Tc-PAMA(4)-Cbl, (B) ^{99m}Tc-DTPA, (C) ^{57}Co-caynocobalamin and (D) ^{67}Ga-citrate into tissue cage fluids of sterile (dotted line), *S. aureus* (dashed line) and *E. coli* (continuous line) infected cages. Data represent % ID/ml of tissue fluid, expressed as means ± 1 SEM of three to five different mice.

Table 7. Tissue distribution after i.v. injection of ^{99m}Tc-PAMA(4)-cyanocobalamin, ^{99m}Tc-DTPA, ^{57}Co-cyanocobalamin and ^{67}Ga-citrate, expressed as means (±SD) of %ID/g of tissue.

Organ or tissue	**^{99m}Tc-PAMA(4)-Cbl**			**^{99m}Tc-DTPA**			**^{57}Co-vitamin B_{12}**	**^{67}Ga-citrate**
	30 min	4 h	24 h	30 min	4 h	24 h	72 h	72 h
Blood	1.79 (±0.05)	0.15 (±0.02)	0.02 (±0.10)	1.46 (±1.10)	0.02 (±0.10)	0.01 (±0.00)	2.55 (±0.35)	0.46 (±0.20)
Heart	0.90 (±0.07)	0.33 (±0.07)	0.11 (±0.01)	0.15 (±1.10)	0.05 (±0.00)	0.01 (±0.00)	3.60 (±0.68)	1.26 (±0.10)
Liver	5.75 (±0.86)	2.98 (±0.45)	0.92 (±0.90)	0.33 (±0.20)	0.09 (±0.00)	0.02 (±0.00)	15.78 (±1.49)	7.44 (±0.90)
Stomach	1.73 (±0.30)	0.49 (±0.23)	0.44 (±0.14)	1.67 (±1.70)	0.05 (±1.10)	0.02 (±0.00)	4.83 (±0.85)	3.73 (±1.50)
Spleen	1.48 (±0.18)	0.60 (±0.07)	0.22 (±0.03)	0.19 (±0.00)	0.06 (±0.00)	0.02 (±0.00)	9.07 (±1.44)	6.09 (±0.70)
Kidneys	15.66 (±1.88)	13.47 (±1.79)	11.19 (±1.35)	3.92 (±0.80)	0.93 (±0.80)	0.15 (±0.00)	25.91 (±4.64)	10.73 (±1.30)
Lungs	2.81 (±0.51)	1.09 (±0.26)	0.29 (±0.10)	0.40 (±0.20)	0.06 (±0.10)	0.01 (±0.00)	3.72 (±1.75)	2.11 (±0.30)
Intestine	1.81 (±0.14)	1.52 (±0.51)	0.59 (±0.05)	0.90 (±0.50)	0.66 (±0.20)	0.02 (±0.00)	3.63 (±0.89)	2.00 (±0.40)
Bone	0.74 (±0.05)	0.22 (±0.01)	0.08 (±0.01)	0.47 (±0.30)	0.05 (±1.50)	0.01 (±0.00)	3.93 (±0.96)	10.99 (±2.40)
Muscle	0.38 (±0.03)	0.09 (±0.01)	0.03 (±0.01)	0.34 (±0.30)	0.06 (±1.10)	0.00 (±0.00)	1.42 (±0.20)	0.69 (±0.20)
Cage - sterile	2.37 (±0.16)	0.87 (±0.25)	0.04 (±0.01)	2.88 (±0.50)	0.34 (±0.40)	0.01 (±0.00)	4.60 (±0.41)	1.45 (±0.50)
Cage – *S. aureus*	1.80 (±0.91)	1.47 (±0.38)	0.14 (±0.06)	n.d.	0.40 (±0.10)	0.05 (±0.10)	4.88 (±0.55)	9.45 (±2.30)
Cage – *E. coli*	0.76 (±0.21)	0.84 (±0.23)	0.37 (±0.18)	n.d.	0.91 (±0.15)	0.15 (±0.10)	6.52 (±0.17)	3.99 (±1.10)

n.d. = not determined

3.5 Discussion

In vitro studies demonstrated that the bacterial binding of ^{57}Co-Cbl is specific and displaceable by excess of unlabelled Cbl. Higher binding avidity was measured for the *E. coli* strain, which also presented a rapid binding kinetic. On the other hand, ^{57}Co-Cbl binding to *S. aureus* was slow and occurred exclusively with viable bacteria. When *E. coli* and *S. aureus* cultures were pre-exposed to ^{57}Co-Cbl only small fractions of the bound agent could be displaced by unlabeled Cbl, indicating fast internalization mechanisms. In agreement with an energy-dependent uptake mechanism, the internalized fractions were higher at 37°C than at 4°C and they were exclusively measured in viable bacteria.

The in vitro binding of ^{99m}Tc-PAMA(4)-Cbl derivative to *E. coli* was significantly lower than for ^{57}Co-Cbl. Indeed, the techentium chelator of ^{99m}Tc-PAMA(4)-Cbl is linked to the b-acid of the corrin ring A, a functional group previously described as directly involved in the recognition by the *E. coli* outer membrane transporter BtuB [122]. Especially, the amidic and the carboxyl oxygen of the corrin ring A side chains are involved in an hydrogen bond with the amine groups of the residues Leucin 63 and Alanin 231, respectively, in the BtuB binding pocket. In contrast, binding of ^{99m}Tc-PAMA(4)-Cbl to *S. aureus* was specific and only slightly lower than ^{57}Co-Cbl. The *S. aureus* receptor mediating Cbl uptake is evidently less affected by Cbl modifications than the *E. coli* outer membrane transporter BtuB.

In animal studies, ^{99m}Tc-PAMA(4)-Cbl showed a fast penetration into all cages, followed by a slower release in infected cages than in sterile ones. The tracer retention into infected fluids became significantly higher at 4 h p.i. for *S. aureus* infected mice and at 8 h p.i. for *E. coli* infected mice, which is in accordance with a lower receptor affinity of PAMA(4)-Cbl for *E. coli* BtuB receptors. The uptake measured in cage fluid of infected animals was also significantly higher for ^{99m}Tc-PAMA(4)-Cbl than for the non-specific tracer ^{99m}Tc-DTPA. This finding supports a specific interaction with the colonizing bacteria, rather than a non-specific retention due to the morphological differences between infected and sterile cage-fluids.

Differently, ^{57}Co-Cbl and ^{67}Ga-citrate had a slow kinetic of penetration into both infected and sterile cages, explained by their high plasma protein binding and long persistence in blood and organs [136, 137]. ^{57}Co-Cbl was only partially cleared from sterile cages even after 72 h p.i. Significantly higher retention than in sterile mice could be observed in cages infected with *E. coli* at 72 h. The latter result is in accordance to the higher ^{57}Co-Cbl binding measured in vitro to *E. coli* than to *S. aureus*.

The mechanism of the ^{67}Ga-citrate accumulation at infection/inflammation site is associated to the Ga (III) binding to transferrin, lactoferrin and other inflammatory proteins in inflamed sites, internalization into the cells with active metabolic pathway as citrate for citric acid cycle and presumable binding to bacterial siderophores [136, 138]. In our studies ^{67}Ga-citrate discriminated

between infected and sterile cages from 48 h after injection. The retention of the tracer observed in bone, kidneys, liver and spleen is in accordance with data from previous publications [139].

In our cage infection studies, the tracer accumulation was several times higher in the cage fluid than in the tissue surrounding explanted cages. While explanted cages contain residues of low vascularized tissue and adherent bacteria in a stationary-growth phase, the cage fluid represent the active infection site with replicating bacteria in the planktonic growth-phase and exchange with the blood [71]. Sterile cage fluids are characterized by a non-specific low-grade inflammatory response, which is induced by the presence of the foreign body [97].

Conclusion

We demonstrated that the tissue cage mice model of infection is a valid alternative to other experimental models for screening radiotracers targeting infection, such as osteomyelitis, infectious endocarditis and infection of thigh muscles [140]. The model has also the advantage that cage fluid can be sampled several times during the experiment thereby avoiding sacrificing animals for each time-point.

Furthermore, we showed that radiolabeled Cbl has a specific, receptor-mediated binding to *E. coli* and *S. aureus*. In vivo, the ^{99m}Tc-PAMA(4)-Cbl derivative discriminated between infected and non-infected cages in the mouse model within 4 to 8 h after tracer injection, and thus may become a selective tracer for targeting infections in humans.

Chapter 4

Performance of Microcalorimetry for Early Detection of Methicillin-Resistance in Clinical Isolates of *Staphylococcus aureus*

Daniela Baldoni,[1] Heinz Hermann,[1] Reno Frei,[2] Andrej Trampuz,[1,3*] Andrea Steinhuber[1]

[1]Infectious Diseases Research Laboratory, Department of Biomedicine, University Hospital, Basel, Switzerland

[2]Microbiology Laboratory, Laboratory Medicine, University Hospital, Basel, Switzerland

[3]Division of Infectious Diseases and Hospital Epidemiology, University Hospital, Basel, Switzerland

Adapted from: Journal of Clinical Microbiology, 2009 Mar; 47 (3)

Received 11 December 2008/ Returned for modification 8 January 2009/ Accepted 13 January 2009.

4.1 Abstract

Early and accurate detection of methicillin-resistant *Staphylococcus aureus* (MRSA) is essential in the hospital and the outpatient setting. Growing bacterial cultures produce an increasing heat signal that can be measured by isothermal microcalorimetry. We established an assay for discrimination of MRSA from methicillin susceptible *S. aureus* (MSSA) by paired incubation of batch cultures at 37°C in pure medium and in medium supplied with 4 µg/ml cefoxitin. Relative heat was calculated as ratio between the total heat measured in the presence and absence of cefoxitin after 3 h, 4 h and 5 h of incubation in the microcalorimeter. Twenty repeated heat measurements of the two laboratory strains MSSA (ATCC 29213) and MRSA (COL) served to define an optimal cutoff value of relative heat. Subsequently the performance of the assay was evaluated on genetically distinct clinical isolates of *S. aureus*, previously classified with an oxacillin resistance test and PBP2a latex test into MRSA (20 isolates) and MSSA (10 isolates). Using a relative heat cutoff of 0.4, 19 of 20 MRSA (95%) and 10 of 10 MSSA (100%) isolates were correctly identified within 5 h. The relative heat values for correctly identified clinical isolates of MSSA (0.35 - 0.25) and MRSA (0.74 - 0.84) did not overlap. In summary, we developed an assay for the detection of MRSA within 5 hours with high sensitivity, specificity and repeatability. With optimization of the calorimetric assay, the accuracy and speed of MRSA detection could be further increased and potentially extended to other organisms and antimicrobial substances.

4.2 Introduction

Methicillin-resistant *Staphylococcus aureus* (MRSA) is a frequent cause of healthcare- and community-associated infections. Its prevalence continues to increase in hospitals as well as in the outpatient setting, causing a growing problem worldwide. Infection control guidelines combine active surveillance with elaborate patient management, including screening for MRSA, contact isolation and decolonization [141]. Therefore, a rapid and accurate detection of MRSA is essential for both, efficient prevention of spread of resistant bacteria and early-targeted treatment of infections.

Methicillin-resistance in *S. aureus* is mediated by the expression of a low-affinity penicillin-binding protein (PBP2a) encoded by the *mecA* gene, and conferring resistance towards most β-lactam antibiotics. The *mecA* gene is inserted in a mobile genetic element, designated staphylococcal chromosomal cassette *mec* (SCC*mec*) and is present in the chromosome of all MRSA isolates [142, 143]. Thus, MRSA has been traditionally defined as *S. aureus* having the *mecA* gene and an oxacillin MIC >4 μg/ml [144]. Various approaches are used to discriminate between MSSA and MRSA [145-148]. Resistance to oxacillin in staphylococci is usually screened by phenotypic tests, as recommended by the Clinical and Laboratory Standards Institute. In most clinical laboratories, culture methods using selective broth, disc diffusion or chromogenic agar are widely used. In general, a combination of several tests is recommended, as no single test has a 100% sensitivity and specificity for detection of MRSA [145]. The gold standard for the detection of MRSA when screening includes the use of overnight enrichment in salt-containing TSB followed by plating. However, PCR amplification of the *mecA* gene from isolated colonies is largely regarded as one of the most accurate methods to differentiate MRSA from MSSA. Nevertheless, PCR is more expensive.

Calorimetry is a highly sensitive and useful technique that allows measurement of heat generated by biological processes in the living cell [149]. Most of medically relevant microorganisms replicate fast in an appropriate culture medium at 37°C, resulting in an exponential increase of heat that can be recorded in real-time (i.e. heat-flow curve). The time at which the growth-related heat becomes detectable depends on the initial number or organisms, their replication rate and the heat production per cell. Since bacterial growth can be inhibited by exposure to antimicrobials, isothermal calorimetry of bacterial culture can be used to determine antimicrobial susceptibility [150]. This principle for discrimination between an MRSA and MSSA has been recently demonstrated with two laboratory strains of *S. aureus* (ATCC 25923 and ATCC 43300), cultured in the presence of oxacillin or cefoxitin [151]. However, the performance, validity and robustness of this test system have not yet been evaluated with clinical isolates of *S. aureus*. Moreover, genetically diverse strains from various types of patient specimens, existing in different growth and metabolic state may have different thermogenic characteristics than laboratory strains.

Therefore, the aim of this study was to develop a calorimetric assay and optimize it for accurate

detection of methicillin-resistance in clinical isolates of *S. aureus* within few hours. First, we evaluated the assay repeatability in 20 consecutive measurements of two well characterized MSSA and MRSA reference laboratory strains. Subsequently we screened and classified, in a blinded manner, 30 genetically distinct clinical isolates of *S. aureus* (10 MSSA and 20 MRSA strains).

4.3 Materials and Methods

Reference strains and clinical isolates of *S. aureus*. Two laboratory strains of *S. aureus*, ATCC 29213 (MSSA) and COL (MRSA), were used as reference strains [152]. Ten MSSA and 20 MRSA clinical isolates were obtained from the clinical microbiology laboratory at our institution and used for testing the assay performance. The clinical strains were collected from non-related patients between January 2005 and December 2007, without evidence of transmission in the hospital or the community. These strains were isolated from intraoperative tissue specimens (n = 16), blood (n = 6), urine (n = 5) or respiratory aspirates (n = 3). In addition, the commonly used standard laboratory strain ATCC 43300 (MRSA), characterized by delayed expression of methicillin resistance [153], was evaluated by the calorimetric assay.

Susceptibility tests and PFGE-pattern analysis. The clinical isolates were screened for susceptibility to oxacillin using a microdilution broth procedure (Merlin Diagnostika, Bornheim-Hersel, Germany) and interpreted in accordance with the Clinical and Laboratory Standards Institute [144]. Isolates showing an oxacillin MIC >4 μg/ml were confirmed by the presence of PBP2a with a slide latex agglutination test (Denka Seiken, Tokyo, Japan). All clinical isolates were characterized by PFGE-pattern analysis with Pearson correlation, using the Chef DR III system (BioRad) for separating *Sma*I-digested genomic DNA, as previously described [154].

The *S. aureus* reference strains were tested with a macrodilution broth assay to determine the MIC of cefoxitin in TSB, since this growth medium was used in the calorimetric assay. Two-fold dilutions of cefoxitin ranging from 32 to 0.5 μg/ml were prepared in TSB in glass tubes and inoculated with a suspension of the test strain corresponding to 1×10^5 CFU/ml. After static incubation at 37°C for 24 h, samples were checked for turbidity and the lowest concentration of cefoxitin which prevented visible growth was determined as the MIC.

Calorimetry sample preparation. Every strain was tested in parallel in the presence and absence of cefoxitin. Discrete colonies of *S. aureus* freshly grown overnight on Columbia 5% sheep blood agar were resuspended in 0.85% sterile saline to a McFarland turbidity of 5 (corresponding to approximately 1×10^9 CFU/ml). Aliquots of 300 μl were inoculated into sterile calorimetry ampoules prefilled with 2.7 ml tryptic soy broth (TSB) with and without cefoxitin (Sigma, Buchs, Switzerland). A cefoxitin 100× concentrated stock solution, aliquoted and stored at -20°C, served for all the repeats performed. Two-fold dilutions of cefoxitin between 32 and 0.5 μg/ml were tested on both the MSSA and MRSA laboratory strains. The lowest concentration of cefoxitin that inhibited heat production of MSSA was 4 μg/ml (data not shown), which was used for subsequent calorimetric studies.

Calorimetric equipment and measurements. A 48-channel batch calorimeter (Thermal Activity Monitor, Model 3102 TAM III, TA Instruments, New Castle, DE) was used to measure the heat flow at 37°C controlled at ± 0.0001°C and a sensitivity of ± 0.2 μW. Heat generated by each individual sample was measured in an air-tightly sealed 4-ml glass ampoule and plotted over time as a heat-flow curve. The 1-ml gas phase in the ampoule consisted of ambient air. Ampoules were sequentially introduced into the calorimetry channels and remained 15 minutes in the thermal equilibration position before lowering to the measurement position. Heat was then measured in 10 s intervals for up to 24 h and plotted over time as a heat-flow (in Watts [W]). Total heat (in Joules [J]) was defined as heat generated until a time point and was determined by integration of the area below the heat flow-time curve. After measurement was completed, the content of each calorimetry ampoule was assessed for turbidity.

Measurement of relative heat. The relative heat was defined as ratio between the total heat measured in the presence and absence (growth control) of cefoxitin at 3 h, 4 h and 5 h of incubation in the calorimeter. For reference strains, the calorimetric measurement was performed in 20 replicates on consecutive days in order to calculate the inter-day variation of the relative heat, expressed as mean ± standard deviation (SD). Based on these results, a cutoff value of relative heat was set for discrimination of the MSSA and MRSA reference strains. This cutoff value was then applied for the classification of the *S. aureus* clinical isolates. The relative heat of the clinical strains was measured in duplicates. The sensitivity, specificity, positive and negative predictive values and their 95% confidence intervals of the calorimetric assay for detection of methicillin resistance were calculated based on the results of the standard tests. The variability of the relative heat of clinical MSSA or MRSA isolates, reflecting the genetic diversity of these strains, was expressed as mean ± SD.

In addition, the relative heat of the MRSA laboratory strain ATCC 43300 was measured in 20 consecutive repeats.

Data analysis was accomplished using the manufacturer's software (TAM Assistant, TA Instruments) and Prism 4.0a (GraphPad Software, La Jolla, CA).

4.4 Results

Susceptibility tests and PFGE-pattern analysis. The cefoxitin MICs in TSB of the MSSA ATCC 29213, MRSA COL and the ATCC 43300, assessed with a macrodilution method, were 2 µg/ml, 16 µg/ml and 8 µg/ml, respectively. Clinical isolates displayed a Pearson correlation <75% in the PFGE, except for two MRSA isolates (S1771 and T4545) that showed a correlation of 98.2% (figure 19).

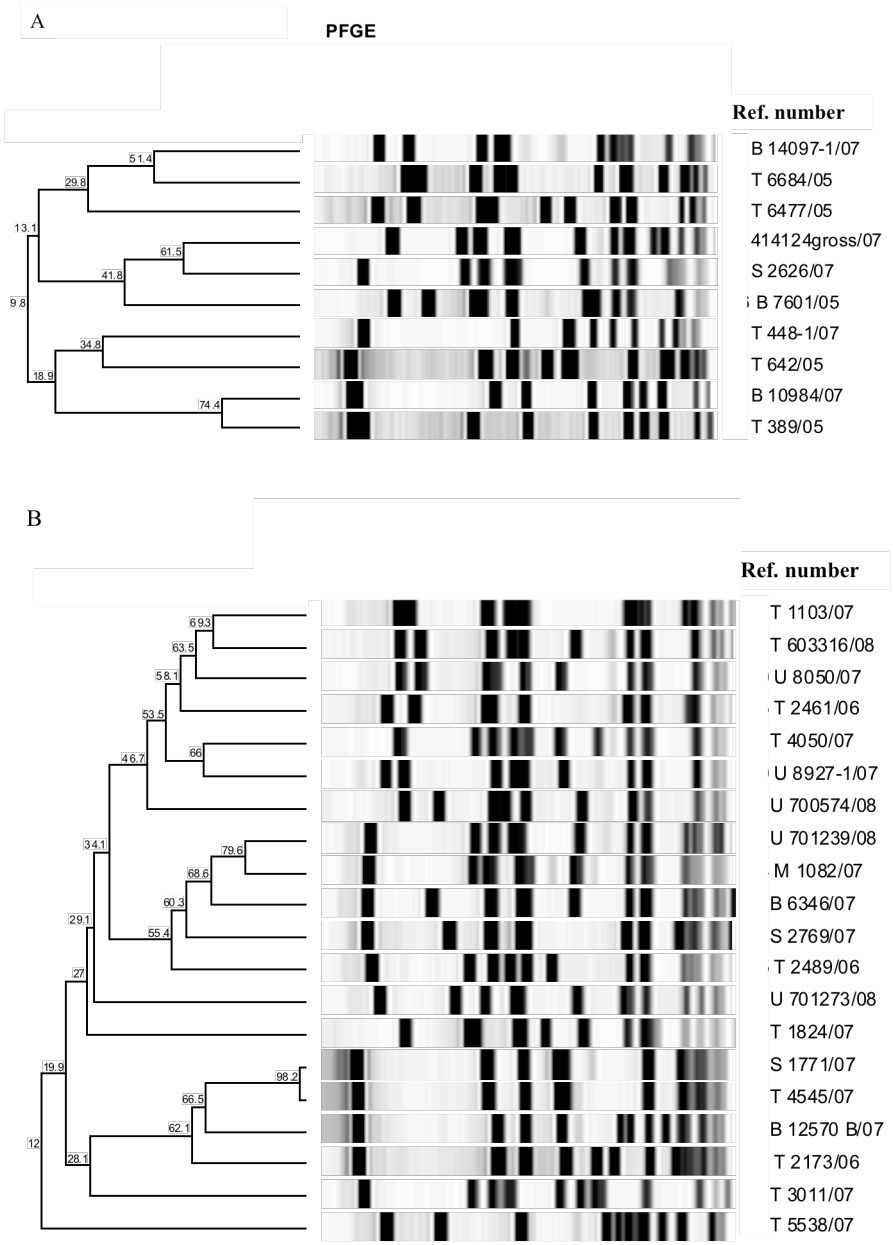

Figure 19. Pulsed-field gel electrophoresis (PFGE) pattern analysis of 10 MSSA (A) and 20 MRSA (B) clinical isolates. The numbers on horizontal lines indicate the percentage of homology by Pearson correlation.

The oxacillin MIC of all 20 MRSA clinical isolates was ≥4 μg/ml, whereas the MIC of all 10 MSSA isolates was ≤1 μg/ml. All clinical MRSA isolates were positive for PBP2a.

Relative heat of reference strains. The lowest concentration of cefoxitin that abrogated heat production of the MSSA was 4 μg/ml. Figure 20 shows the heat-flow (A) and total heat (B) curves in the presence and absence of cefoxitin 4 μg/ml of a representative measurement using both MSSA and MRSA COL strains. In the absence of cefoxitin, the heat-flow curve of the MSSA laboratory strain reached a peak earlier than the one of the MRSA, indicating faster replication of the former. However, the total heat signal from 8 h to 24 h of incubation was higher for the MRSA (independently on the presence or absence of cefoxitin) compared to the MSSA, indicating higher cumulative growth and/or metabolism. Cefoxitin inhibited the heat production of the MSSA during 24 h, whereas only insignificantly affected the heat production of the MRSA strain.

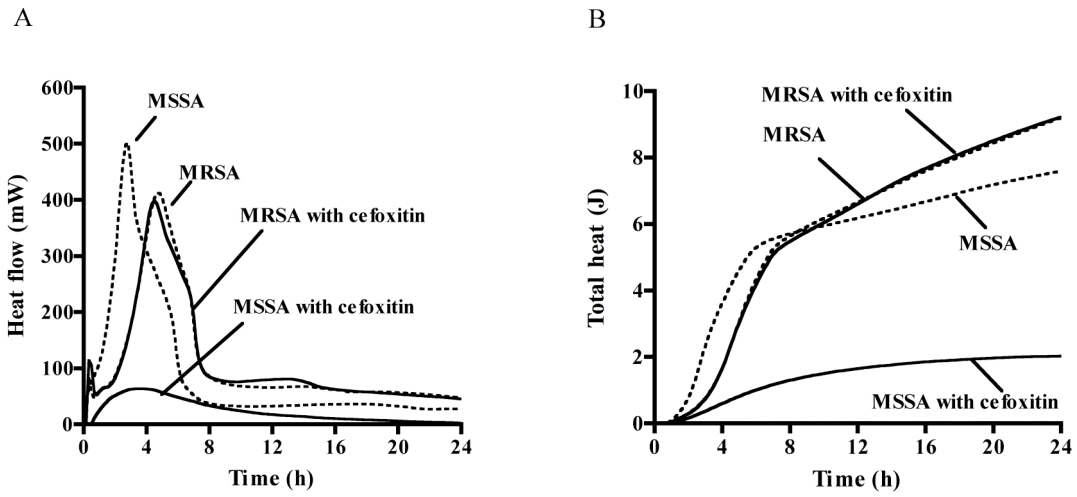

Figure 20. Heat-flow (A) and total heat (B) of reference MSSA (ATCC 29213) and MRSA (COL) strains cultured in the presence of cefoxitin at 4 μg/ml (continued line) or without antibiotic (discontinued line).

We then assessed the repeatability of the reference strains relative heat. Figure 21 shows 20 repeated measurements of relative heat at 3 h, 4 h and 5 h. The standard deviation of the relative heat decreased with prolonged incubation time from 3 h to 5 h. The mean relative heat remained constant for MRSA during 5 h (1.0 – 0.97), while it decreased for MSSA from 0.28 (at 3 h) to 0.22 (at 5 h) (table 9). The 5 h mean relative heat (± SD) for the MSSA and MRSA reference strains was 0.22 (± 0.05) and 1.00 (± 0.09), respectively ($p < 0.001$). Subsequently, based on the distribution of the relative heat values at 5 h, a cutoff of 0.4 was chosen and used for the classification of the clinical isolates.

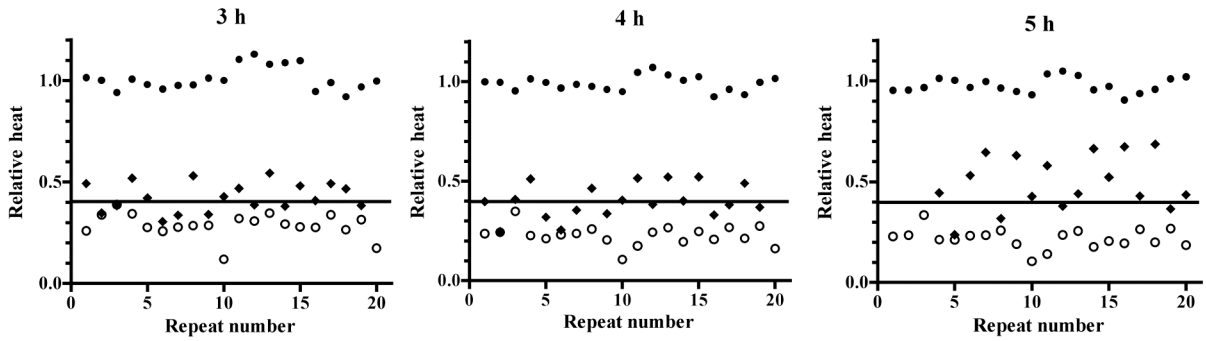

Figure 21. Relative heat distribution in 20 repeated measurements of the reference strains MSSA ATCC 29213 (open circles), MRSA COL (closed circles) and MRSA ATCC 43300 (closed rhombs). Relative heat is calculated as ratio between the total heat in the presence and the absence of 4 μg/ml cefoxitin after 3 h, 4 h and 5 h of incubation. The horizontal line indicates the cutoff value (0.4) of relative heat for discrimination of MSSA and MRSA.

The calorimetric measurements of the MRSA strain ATCC 43300 were characterized by a delay in the peak heat-flow of the cultures in the presence of cefoxitin compared to the growth control. The magnitude of delay varied in the 20 replicates performed on different days, which affected the relative heat distributions around the chosen cutoff. Therefore, the calorimetric measurement for this strain was prolonged. The relative heat (mean ± SD) increased from 0.48 ± 0.14 (at 5 h) to 0.60 ± 0.18 (at 6 h) and 0.80 ± 0.15 (at 8 h) (p for trend <0.05). Of 20 MRSA ATCC 43300 replicates, the relative heat of ≥0.4 was measured in 15, 17 and 20 replicates after 5 h, 6 h and 8 h of incubation, respectively. Thus, prolonged incubation time of 8 h was necessary to detect the MRSA strain ATCC 43300 with 100% accuracy.

Relative heat of clinical isolates. Figure 22 shows the relative heat of 30 clinical isolates at 3 h, 4 h and 5 h of incubation. Cefoxitin at 4 μg/ml inhibited the heat production and the growth of all MSSA clinical isolates cultures in the tested conditions, whereas no inhibition of growth occurred for any of the MRSA isolates. After 24 h, all MSSA and MRSA growth controls and MRSA cultures with cefoxitin showed turbidity, while all of the MSSA cultures with cefoxitin were clear.

Based on the preselected relative heat cutoff of 0.4 for MSSA and MRSA discrimination, 17 of 20 (85%) MRSA clinical isolates were correctly identified after 3 h of incubation. When the incubation was prolonged to 4 h and 5 h, 19 of 20 MRSA isolates (95%) were correctly identified. All MSSA strains had a relative heat <0.4 and were correctly identified after 4 h and 5 h of incubation. At 5 h of incubation, the sensitivity, specificity, positive and negative predictive values (and their 95% confidence intervals) for detection of methicillin resistance were 95% (89%-100%), 100% (92%-100%), 100% (91%-100%) and 91% (85%-97%), respectively.

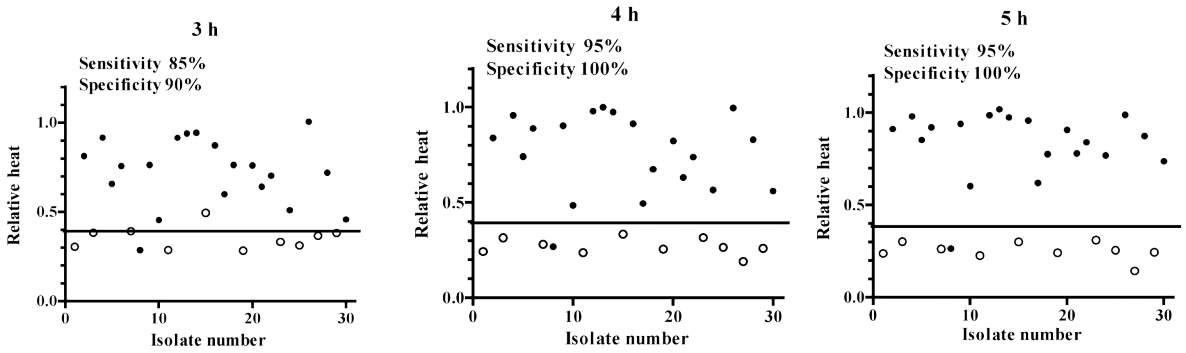

Figure 22. Relative heat distribution of 30 clinical isolates, 10 different MSSA and 20 different MRSA strains. Relative heat is calculated as ratio between the total heat in the presence and the absence of 4 μg/ml cefoxitin after 3 h, 4 h and 5 h of incubation. Open circles indicate MSSA, closed circles MRSA; the horizontal line indicated the cutoff (0.4) value of relative heat for discrimination of MSSA and MRSA.

The mean relative heat after 3 h, 4 h and 5 h ranged between 0.35 and 0.25 for the MSSA isolates, whereas the ones for the MRSA ranged from 0.74 and 0.84 after 3 h and 5 h, respectively. Table 8 summarizes the relative heat means (± SD) of correctly identified clinical isolates.

One of the MRSA clinical isolates (T3011) showed a discrepant result. The relative heat was <0.4 during all 5 h of incubation and the heat-flow curve showed no peak during 24 h of incubation. This clinical isolate was resistant to methicillin by conventional tests (oxacillin MIC ≥4 μg/ml, positive PBP 2a), and had a cefoxitin MIC in TSB of 4 μg/ml when tested with the macrodilution broth method. One MSSA isolate (T 448-1) displayed a relative heat between 0.4 and 0.5 after 3 h of incubation, which decreased below 0.4 thereafter. The unusually high relative heat at 3 h was due to a prolonged lag-phase of the isolates in the growth control.

Table 8. Relative heat of two reference strains (1 MSSA and 1 MRSA) and 30 clinical isolates of *S. aureus* (10 MSSA and 20 MRSA) measured after 3 h, 4 h and 5 h of incubation. Values are means ± SD of 20 repeated measurements (for reference strains) and of 30 clinical isolates (10 MSSA and 20 MRSA).

Strains	**Relative heat at different incubation time, mean (± SD)**		
	3 h	4 h	5 h
Reference strains			
MSSA (ATCC 29213)	0.29 (± 0.06)	0.23 (± 0.05)	0.22 (± 0.05)
MRSA (COL)	1.00 (± 0.08)	0.97 (± 0.08)	0.97 (± 0.05)
Clinical isolates			
MSSA (n = 10)	0.35 (± 0.06)	0.27 (± 0.04)	0.25 (± 0.05)
MRSA (n = 20)	0.76 (± 0.15)	0.80 (± 0.16)	0.84 (± 0.11)

4.5 Discussion

The principle of calorimetric detection of MRSA is based on paired heat measurements of *S. aureus* cultures in the presence and absence of inhibitory concentrations of β-lactam antibiotics in a batch calorimeter. We have chosen cefoxitin since it is a strong inducer of *mecA* expression in both, high-level and low-level methicillin-resistant staphylococci [146, 155]. Cefoxitin is less susceptible to penicillinases than oxacillin and other β-lactams, and is thus more appropriate for correct classification of MRSA, excluding the penicillinase-hyperproducing strains known as borderline oxacillin-resistant *S. aureus* (BORSA) [145]. In our calorimetric MRSA assay, we used cefoxitin at 4 μg/ml since this was the lowest concentration that completely inhibited heat production of the MSSA reference strain and showed only a slight delay of the heat signal of both MRSA reference strains (COL and ATCC 43300). Thus, cefoxitin 4 μg/ml was used in subsequent studies for discrimination of *S. aureus* clinical isolates.

The heat measurements were used to calculate the relative heat, which takes into consideration the strain specific differences in replication rate and minimize the inter-day variability. The assay was highly repeatable when evaluated on 20 consecutive measurements of the reference strains MSSA ATCC 29213 and MRSA COL. In the subsequent testing using clinical isolates, we evaluated the effect of genetic variability on the relative heat. The variability of relative heat for MSSA was similar to the one of the MSSA laboratory strain (SD of relative heat was 0.04 – 0.06), indicating high robustness of the method towards the susceptible strains. On the contrary, the SD of the relative heat of the MRSA clinical isolates ranged between 0.11 – 0.16, reflecting the different phenotypic expression of methicillin-resistance in the 20 MRSA clinical isolates. In a previous study, the majority of MRSA isolates showed a heterogeneous expression of methicillin-resistance, which were categorized into 4 phenotypic expression classes; class 1 was the most hetero-resistant ($\leq$1 in 10^8 cells expressing high-level resistance) and class 4 was homogeneous ($\geq$1 in 10^2 resistant cells) [156]. Therefore, susceptibility results may be misinterpreted, making detection by phenotypic tests challenging [155, 157, 158]. In our assay, high-density bacterial inocula were used to allow early heat measurements and to increase the chances of including highly resistant cells in the detection of heterogeneous MRSA populations [145, 159].

Using the relative heat cutoff of 0.4, clinical isolates showed a sensitivity of 95% (19 of 20 correctly identified MRSA) and a specificity of 100% (10 of 10 correctly identified MSSA) after 5 h of incubation. One MRSA isolate (T 3011) with a relative heat <0.4 had a low growth rate in the presence of cefoxitin during 24 h. This isolate had a cefoxitin MIC in TSB of 4 μg/ml, while the MIC of the MRSA reference strains, was 1- or 2- fold higher. The lower cefoxitin MIC value could be explanatory for the growth inhibition occurred in the cefoxitin cultures of the clinical isoate T 3011. The MRSA ATCC 43300, known to express a heterogeneous methicillin resistance, displayed high variance of

relative heat up to 6 h, with heat ratios <0.4 in 3 of 20 repeated measurements. All measurements led to correct classification of MRSA if the incubation was prolonged to 8 h.

In conclusion, in this report we described a calorimetric assay for rapid and accurate discrimination of clinical MSSA and MRSA isolates, which is highly repeatable, easy to set up, suitable for automation and computer-generated results. The hands-on preparation time is around 15 min and the consumables are inexpensive (two disposable 4 ml glass ampoules with rubber-aluminum lids and 6 ml standard culture medium per test isolate). A prerequisite for a valid test result is normal growth of the isolate in the absence of antibiotic (growth control). With optimization of the calorimetric assay, the accuracy and speed of MRSA detection could be further increased and potentially extended to other organisms and antimicrobial substances. However, a validation study with additional clinical strains from different body sites is needed before introduction in the clinical routine.

Chapter 5

In Vitro Activity of Gallium Maltolate against Staphylococci in Logarithmic, Stationary and Biofilm Growth-Phase: Comparison of Conventional and Calorimetric Susceptibility Testing

Daniela Baldoni[1], Andrea Steinhuber[1], Werner Zimmerli[2], Andrej Trampuz[1,3]

[1]Infectious Diseases, Department of Biomedicine, University Hospital, Basel, Switzerland

[2]University Medical Clinic, Kantonsspital, Liestal, Switzerland

[3]Infectious Diseases Service, Department of Internal Medicine, University Hospital and University of Lausanne, Lausanne, Switzerland

Running title: Antimicrobial activity of gallium maltolate

Adapted from: Antimicrobial Agents and Chemotherapy, 2010 Jan

Received 25 May 2009/Returned for modification 7 September 2009/Accepted 29 September 2009.

5.1 Abstract

Ga^{3+} is a semi-metal element competing for iron-binding sites of transporters and enzymes. We investigated the activity of gallium maltolate (GaM), an organic gallium salt with high solubility, against laboratory and clinical strains of methicillin-susceptible and methicillin-resistant *S. aureus* (MSSA, MRSA) and *S. epidermidis* (MSSE, MRSE) in logarithmic or stationary phase and in biofilm. The MICs of GaM were higher for *S. aureus* (375-2000 µg/ml) than *S. epidermidis* (94-200 µg/ml). Minimal biofilm inhibitory concentrations (MBIC) were 3000-≥6000 (*S. aureus*) and 94-3000 µg/ml (*S. epidermidis*). In time-kill studies, GaM exhibited a slow and dose-dependent killing mechanism, with maximal killing at 24 h against *S. aureus* of 1.9 (MSSA) and 3.3 $\log_{10}$CFU/ml (MRSA) at 3× MIC, and 2.9 (MSSE) and 4.0 $\log_{10}$CFU/ml (MRSE) against *S. epidermidis* at 10× MIC. In calorimetric studies, growth-related heat production was inhibited by GaM sub-inhibitory concentrations and minimal heat inhibitory concentrations (MHIC) were 188-4500 (MSSA), 94-1500 (MRSA), and 94-375 µg/ml (MSSE and MRSE), correlating well with the MIC values. Thus, calorimetry was a fast, accurate and simple method, useful to investigate antimicrobial activity at sub-inhibitory concentrations. In conclusion, GaM exhibited activity against staphylococci in different growth phases, including in stationary phase and biofilms, but high concentrations were required. These data supports the potential use of GaM for topical use, including treatment of wound infections, MRSA decolonization and implant coating. In addition, GaM at sub-inhibitory concentrations may show efficacy against staphylococcal infections, alone or probably tested in combinations to standard antimicrobials.

5.2 Introduction

Staphylococcus aureus continues to represent the major cause of infection in the outpatient and healthcare settings. The therapeutic options for multiresistant strains, including methicillin-resistant *S. aureus* (MRSA) strains, are limited [160, 161]. In addition, coagulase-negative staphylococci often cause chronic low-grade infections associated with implanted devices, on which they can grow embedded in a protective extracellular matrix, known as a biofilm [14]. In the biofilm, bacteria can persist in a low metabolic, stationary growth-phase, in which they resist the killing by the host immune system and antimicrobials [38, 162]. Both the spread of multi-resistant staphylococci and the increased use of temporary implants (vascular catheters, pins from external fixation devices) and permanent implants (e.g. joint prosthesis, breast implants, cardiac or brain pacemakers), drive the need for new antimicrobial agents for innovative therapeutic strategies [39, 160, 163, 164].

The antimicrobial activity of different inorganic salts, such as sodium metabisulfite and copper silicate, was demonstrated in vitro against planktonic and adherent staphylococci [165, 166]. Gallium (Ga^{3+}) is a semi-metal element. The proposed mechanism of action is its competition for Fe^{3+} in the binding to proteins and chelators. Ga^{3+} is virtually irreducible under physiological conditions, while Fe^{3+} participates to redox reaction in which is readily reduced to Fe^{2+}. Thus, when replacing Fe^{3+}, Ga^{3+} could interfere with bacterial DNA and protein synthetic pathways by blocking redox reactions depending on iron electron acquisition [136].

Staphylococci are known to be avid of iron. Previously, several mechanisms of iron recruitment have been studied and described as essential virulence factors [167-171], as consequence, iron uptake and metabolism may constitute a potential target to combat staphylococcal infections.

In the form of nitrate salt, gallium demonstrated bactericidal in-vitro activity against planktonic and adherent *Pseudomonas aeruginosa* and *Burkholderia cepacia* [172, 173]. Gallium maltolate (GaM), a high soluble gallium formulation [174], was effective in vivo against *P. aeruginosa* and *S. aureus* infection after topical subcutaneous injection in thermally injured mice [175]. However, to our knowledge, the in-vitro activity of gallium against staphylococci has not yet been characterized. Gallium was chosen among elements with antibacterial properties due to its theoretical mechanism of action (i.e. competition for Fe^{3+}), selective against bacteria (with low predicted tissue toxicity), in-vitro data on other gram-negative bacilli and previous experience in humans by using it for diagnostic purposes in nuclear medicine.

We investigated the in vitro activity of GaM against staphylococci in the logarithmic, stationary phase and biofilms. Standard in vitro tests for determination of MIC, minimal bactericidal concentration (MBC) in the logarithmic and stationary growth phase [176] and activity against biofilm

were used. To better investigate the activity of GaM at sub-inhibitory concentrations, we studied its effect on bacterial heat production in cultures exposed to GaM using a newly developed calorimetric assay. Antimicrobial assays were performed in a synthetic iron-limited medium. The aim of the study was to investigate the potential use of GaM for systemic or topical application against staphylococci, including treatment of wound infections, MRSA decolonization and the coating of implants.

5.3 Materials and methods

Laboratory bacterial strains. *S. aureus* ATCC 29213 (MSSA), *S. aureus* ATCC 43300 (MRSA), *S. epidermidis* 1457 (MSSE) and *S. epidermidis* B3972 (MRSE) were used. Bacteria were stored at -70°C using a cryovial bead preservation system (Microbank, Pro-Lab Diagnostics, Richmond Hill, ON, Canada). Single cryovial beads were cultured overnight on Columbia sheep blood agar plates (Becton Dickinson, Heidelberg, Germany). Inocula were prepared from the sub-culture of two to three colonies resuspended in trypticase soy broth (TSB) and incubated overnight at 37°C without shaking. The overnight cultures were diluted with the appropriate medium to an inoculum of $\approx 1 \times 10^6$ CFU/ml.

Clinical isolates. For susceptibility screening, 20 genotypically distinct clinical isolates, 5 per bacterial susceptibility group, were used. The clinical strains were collected from non-related patients admitted to our hospital (University Hospital, Basel) between January 2005 and December 2008, isolated from intraoperative tissue specimens (n = 3), blood (n = 6), urine (n = 8) or synovial fluid (n = 3). The *S. aureus* isolates were characterized by PFGE-pattern analysis with Pearson correlation using the Chef DR III system (BioRad) for separating *Sma*I-digested genomic DNA, as previously described [154], displaying a Pearson correlation <75% [177]. The clinical isolates were screened for susceptibility to methicillin using a microdilution broth procedure (Merlin Diagnostika, Bornheim-Hersel, Germany), interpreted in accordance with the Clinical and Laboratory Standards Institute. Inocula of clinical isolates were prepared from bacterial overnight cultures on Columbia sheep blood agar plates resuspended to a McF of 0.5, and further diluted in the appropriate medium to inocula of $\approx 1 \times 10^6$ CFU/ml.

Chemicals. Susceptibility assays were performed in iron-limited media, including RPMI 1640 (Invitrogen, Basel, Switzerland) supplemented with 5% pyruvate and 5% glutamate (RPMI), or 0.01 M phosphate-buffered saline (PBS), pH 7.4. GaM was kindly provided by Titan Pharmaceuticals (South San Francisco, CA, USA). Stock solutions were freshly prepared and sterile filtered on the day of the assays.

Doubling time. Bacterial doubling time of laboratory strains in Mueller-Hinton broth (MHB) and RPMI were investigated. 1:100 diluted overnight cultures were further grown in MHB and in RPMI until mid-logarithmic phase. From the mid-phase each culture was diluted 1:100 (*S. aureus*) or 1:10 (*S. epidermidis*) in either MHB or RPMI and incubated at 37°C at 180 rpm (for MSSA, MRSA, MRSE) or without shaking (for MSSE to avoid clot formation induced by shaking). OD_{600} was measured every 30 minutes during 10 h (MSSA, MRSA, MRSE) or every 60 minutes during 12 h (MSSE). The $\log_2$ of OD_{600} values were plotted versus time and the linear regression equation determined for the

logarithmic growth phase. The inverse of the slope was defined as the bacterial doubling time (in minutes). Experiments were performed in triplicate and results expressed as mean ± SD. Comparisons in doubling time were performed using the Student's t-test. Differences were considered significant when *P* values were <0.05.

Antimicrobial susceptibility of planktonic bacteria. The MIC and MBC in the logarithmic growth phase (MBC_{log}) were evaluated in RPMI with a broth macrodilution method according to the Clinical Laboratory Standards Institute (CLSI) (formerly the NCCLS) guidelines [176]. The MBC in the stationary growth phase (MBC_{stat}) was assayed in PBS, as previously described [41]. In this medium, bacterial counts remained within ± 15% of the initial inoculum within 24 h. Ten 2-fold serial dilutions were prepared from GaM stock solution of 6000 µg/ml. The MIC was defined as the lowest GaM concentration that prevented visible bacterial growth and the MBC as the lowest GaM concentration that reduced the CFU/ml by ≥ 99.9% of the initial inoculum. MIC and MBC of laboratory strains were repeated three times and results were expressed as medians. Following, the MIC values of GaM against the clinical isolates were determined.

Antimicrobial susceptibility of biofilm bacteria. The activity of GaM against staphylococcal biofilms was tested with a broth microdilution assay, as previously described [178, 179] and modified by Sandoe *et al*. [82]. Briefly, 200 µl of overnight cultures diluted in 1% glucose supplemented RPMI (inoculum ≈1 × 10^6 CFU/ml) were distributed into 96-wells microtiter plates (Nuclon Delta, Nunc). Frame wells were filled with medium only, serving as negative growth control. Biofilms were formed on pegs of modified polystyrene microtiter lids (TSP system, Nunc, Roskilde, Denmark), immersed into the wells and cultured for 20 h at 37°C. Following, pegged lids were rinsed with PBS and transferred to a second microtiter plate (antimicrobial susceptibility plate) containing 2-fold serial dilutions of GaM between 6000 µg/ml and 10 µg/ml, six wells were filled with medium only and served as positive growth control. Plates were incubated for further 20 h at 37°C. On the third day, peg-lids were rinsed again with PBS and transferred to recovery plates, where 200 µl of RPMI had been distributed to all wells. Plates were shaken for 5 minutes at 250 rpm to enhance bacterial re-growth from biofilms and incubated at 37°C without shaking. After 48 h of incubation bacterial growth occurring on the recovery plates was measured as turbidity using an ELISA-reader at OD_{600}. The lowest concentration of GaM, which prevented biofilm re-growth in the recovery plate, was defined as the minimal biofilm inhibitory concentration (MBIC). Experiments were performed in triplicate, four times in different days and results were reported as median values. Screening of clinical isolates was performed in triplicate and MBIC medians reported.

As control, strain-dependent biofilm formation was evaluated as previously described [180, 181].

Briefly, 200 µl of bacterial inocula, prepared as described above, were distributed in six replicates in polystyrene, 96-well, flat-bottomed tissue culture plates (Becton Dickinson, Falcon, France). Plates were incubated for 20 h at 37°C. Following, medium was gently aspirated from each well. Bacteria adhering on the plate bottoms were washed with 200 µl PBS and air dried for around 2 h. Biofilms were stained for 15 minutes with a solution of 0.5% crystal violet in 70% methanol. Then, the stain was removed and wells were rinsed twice with 300 µl of PBS. Stained adherent bacteria were re-suspended from each well with 200 µl of 70% methanol and transferred to a new plate. OD_{490} of the latter was measured, each value was subtracted by the mean absorbance of the blank wells (negative control) and the mean of 6 well per each strain was calculated. The value derived from three standard deviations above the mean OD_{490} of the blank was used as breakpoint for classifying the strain as able or not able to form biofilms in the in vitro tested conditions [180].

Time-kill studies. Killing profile of four GaM concentrations were assessed in parallel with growth controls against laboratory strains. Samples were incubated at 37°C without shaking during 24 h (for *S. aureus*) and 48 h (for *S. epidermidis*). Bacterial concentrations (CFU/ml) were determined by plating aliquots of appropriate dilutions on Muller-Hinton agar plates at 0 h, 2 h, 4 h, 6 h, 8 h, 24 h and 48 h (the 48 h time points was tested only with the *S. epidermidis* strains). Bacterial colonies were enumerated after 24 h incubation at 37°C. Each strain was tested three times on different days and results were analyzed using GraphPad Prism 4.0 (GraphPad Software, La Jolla, CA). Results were plotted as means ± SD of reduction of $\log_{10}$ CFU/ml, defined as $\log_{10}(CFU/ml)_t - \log_{10}(CFU/ml)_0$, over time (t).

Inhibition of growth-related heat production by GaM. Viable and growing microorganisms produce heat, which can be measured in a calorimeter [182, 183]. This property allows measuring the antimicrobial potency against bacterial growth [183]. We evaluated the inhibition of bacterial heat production at different concentrations of GaM during 24 h. From a GaM stock solution of 6000 µg/l, nine 2-fold serial dilutions were performed in RPMI and 2 ml were transferred into sterile 4-ml glass ampoules. Ampoules were then inoculated under meniscus with the adjusted bacterial cultures, air-tightly sealed and sequentially introduced into the calorimetry channels.

A 48-channel batch calorimeter (Thermal Activity Monitor, Model 3102 TAM III, TA Instruments, New Castle, DE) was used to measure the heat flow at 37°C controlled at ± 0.0001°C and an analytical sensitivity of ± 0.2 µW. Heat-flow (in µWatts) was measured for 24 h in 10 s intervals. The curve of total heat (in Joules) versus time was determined by integration of the area below the heat flow-time curve. After the heat measurement was completed, the content of each ampoule was assessed for visual growth. The minimal heat inhibitory concentrations (MHIC) was defined as the lowest GaM

concentration leading to a growth-related heat production < 0.25 Joule after 24 h. Bacterial cultures without GaM were used as positive (growth) controls. Experiments were performed in duplicates, for two times in different days, for the laboratory strains. Following, the clinical isolates were screened and the MHIC values collected.

5.4 Results

Doubling time in iron-limited medium. The replication of *S. epidermidis* was slower than of *S. aureus* laboratory strains, with doubling times in RPMI (mean ± SD) of 46 ± 10 min (MSSA) and 55 ± 8 min (MRSA) versus 114 ± 27 min (MSSE) and 108 ± 17 min (MRSE). No significant differences in doubling time were observed between strains cultured in RPMI or MHB ($P > 0.05$).

Antimicrobial susceptibility of planktonic bacteria. Table 9 summarizes the in vitro susceptibility of GaM against laboratory strains. Against the laboratory *S. aureus* strains, MIC values were about 10-fold higher than the *S. epidermidis* strains. GaM in concentrations up to 6000 µg/ml was not bactericidal against MSSA, whereas a 3-$\log_{10}$ CFU reduction was reached against the other strains. MBC_{log} values were between 6× and 20× the respective MICs. In the stationary phase GaM exhibited bactericidal activity only against *S. epidermidis*; the MBC_{stat} was 60× the MIC for the MSSE and 7.5× the MIC for the MRSE. Table 10 shows the results for clinical isolates. GaM inhibited growth of all tested strains. Clinical isolates of MSSA and *S. epidermidis* exhibited similar MIC values to the correspondent laboratory strain, whereas MRSA isolates had median MIC values about 4-times lower than the correspondent laboratory strain.

Antimicrobial susceptibility of biofilm bacteria. In biofilm susceptibility studies, GaM MBIC values for laboratory strains were 3× MIC for MSSA, 6× MIC for MRSA and 2.8× MIC for MSSE and MRSE (table 9). The biofilm formation on pegged lids was confirmed by growth of positive control biofilm cultures in the recovery plates. Three of the five MSSA clinical isolates screened for MBIC (table 10) resulted in MBIC >6000 µg/ml. The MRSA isolates displayed better susceptibility, with 2 strains only having MBIC >6000 µg/ml. The median MBICs for the MSSE and MRSE isolates were respectively 375 and 750 µg/ml, with all isolates displaying biofilm susceptibility to GaM. The strain DJ192 did not grow in the recovery plate during the 48 h of incubation both in wells with and without GaM. Therefore, for this strain, MBIC value could not be measured.

Both laboratory strains and clinical isolates resulted positive for biofilm formation after crystal violet staining of bacteria adhering on the bottom of polystyrene 96-well tissue culture plates. The OD_{490} breakpoint was 0.08, calculated as three standard deviations (3× 0.009) above the mean OD_{490} (0.053) of the blank wells. The OD_{490} means ± SD (laboratory strain and clinical isolates) were 0.104 ± 0.044 (MSSA), 0.184 ± 0.074 (MRSA), 0.244 ± 0.077 (MSSE) and 0.187 ± 0.070 (MRSE).

Time-kill studies. Figure 23 shows the reduction $\log_{10}$ CFU/ml of the laboratory strains in the presence of GaM over 24 h (*S. aureus*) or 48 h (*S. epidermidis*) of incubation.

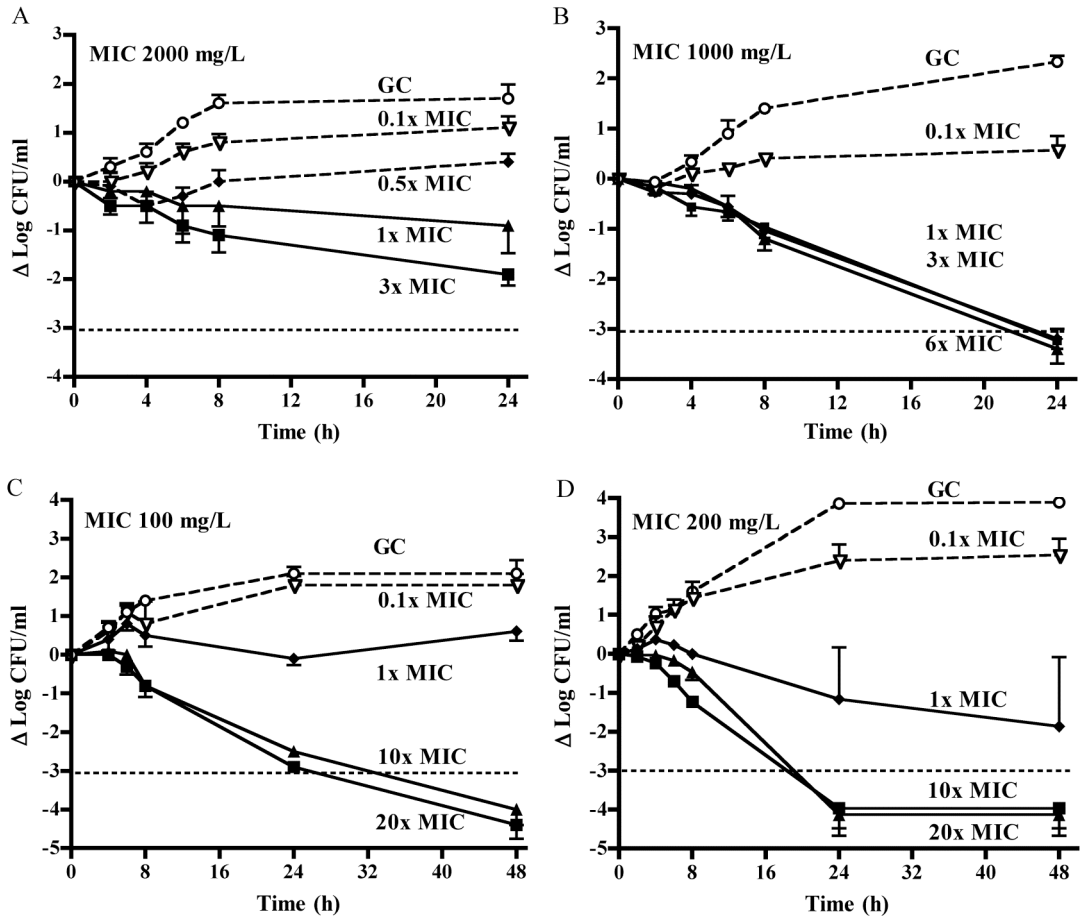

Figure 23. Time-kill curves of GaM in RPMI against MSSA (A), MRSA (B), MSSE (C) and MRSE (D). Values are mean CFU/ml ± SD of three measurements. GC indicates growth controls performed in RPMI without GaM. Horizontal dotted line indicates the 3-log10 CFU/m reductions. Note that the X- and Y-axis scales are adapted for *S. aureus* and *S. epidermidis*.

For all tested strains, GaM inhibited bacterial growth in a time-dependent and dose-dependent manner. At sub-inhibitory concentrations, only a slight reduction and a delay in net bacterial counts were detected when compared to growth controls. Against MSSA and MRSA the highest killing after 24 h, achieved with GaM at 3× MIC, was by 1.9 and 3.3 $\log_{10}$ CFU/ml, respectively. Against the MSSE GaM at 10× MIC reduced bacterial viability by 2.9 and 4.4 $\log_{10}$ CFU/ml after 24 h and 48 h, respectively, while MRSE was reduced by 4.0 $\log_{10}$ CFU/ml already at 24 h. A bactericidal activity was demonstrated against the MRSA, MSSE and MRSE, and was time-dependent.

Inhibition of growth-related heat production. Figure 24 shows representative calorimetry curves

of total heat generated by each of the laboratory strains cultured at 37°C in RPMI over 24 h. The inhibition of growth-related total heat produced by the strains in the presence and absence of GaM was measured. The total heat generated over 24 h without GaM was similar for all strains and ranged between 4 and 5 Joules. The curves of laboratory strains were analyzed and followed a two-phase course: an initial rapid increase of heat, corresponding to the logarithmic growth phase, occurred in MSSA between 0 and 4 h, in MRSA and MSSE between 3 and 7 h, and in MRSE between 4 and 9 h of incubation. In the second phase, the increase of heat production was slower but continuous up to 24 h (except for MSSA, which reached a plateau at ≈16 h of incubation).

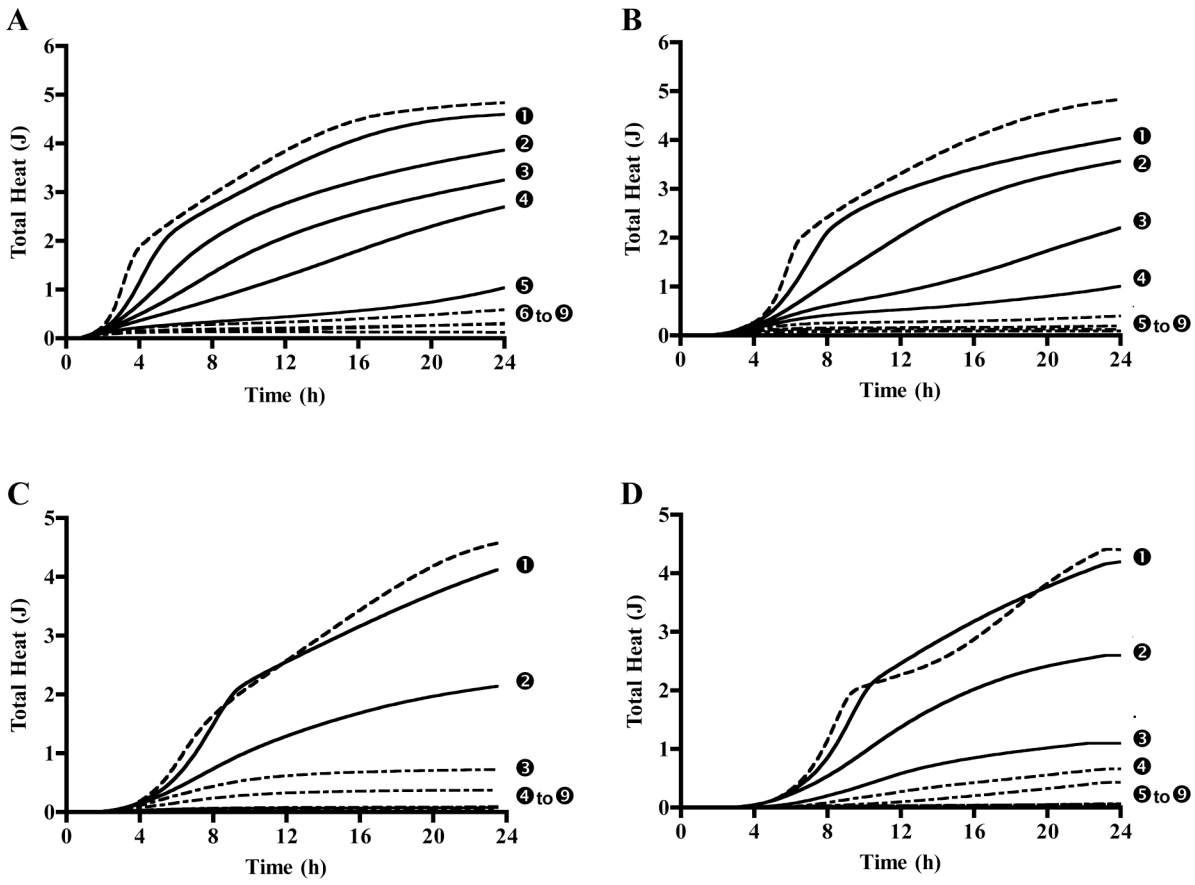

Figure 24. Calorimetry curves representing the total heat generated by MSSA (A), MRSA (B), MSSE (C) and MRSE (D) at 37°C for 24 h in presence of 2-fold dilutions of GaM in RPMI. Dashed lines represent growth controls without GaM, continuous lines indicate GaM concentrations below the MIC and dashed-dot lines indicate GaM concentrations above the MIC of the corresponding test strain. NOTE: GC = growth control; ❶ = 23 µg/ml, ❷ = 46 µg/ml, ❸ = 94 µg/ml, ❹ = 188 µg/ml, ❺ = 375 µg/ml, ❻ = 750 µg/ml, ❼ = 1500 µg/ml, ❽ = 3000 µg/ml, ❾ = 6000 µg/ml GaM. Note Y-axis scales are adapted for *S. aureus* and *S. epidermidis*.

At sub-inhibitory concentrations, GaM reduced the production of heat in a dose-dependent manner, in comparison to the growth controls. Cultures associated to a 24 h total heat <0.25 Joule did not display any visual turbidity and thus 0.25 Joule was used as total heat breakpoint for MHIC evaluation. The MHICs of laboratory and clinical isolates (table 9 and 10) correlated with the MICs for all strains,

with values ± 4× the respective MICs, except for one MSSE isolate (DJ134) where the MHIC was 6× higher than the MIC value.

Table 9. In-vitro susceptibility of 4 laboratory strains of staphylococci against GaM (in the logarithmic, stationary and biofilm growth phase) with corresponding calorimetry parameters.

Organism (strain)	MIC (µg/ml)	MBC_{log}[a] (µg/ml)	MBC_{stat}[b] (µg/ml)	MBIC[c] (µg/ml)	MHIC[d] (µg/ml)
MSSA (ATCC 29213)	2000	>6000	>6000	6000	4500
MRSA (ATCC 43300)	1000	6000	>6000	6000	1500
MSSE (1457)	100	2000	6000	280	375
MRSE (B3972)	200	1500	1500	560	375

[a]MBC_{log}, minimal bactericidal concentration in the logarithmic growth phase.

[b]MBC_{stat}, minimal bactericidal concentration in the stationary growth phase.

[c]MBIC, minimal biofilm inhibitory concentration.

[d]MHIC, minimal heat inhibitory concentration.

Table 10. In-vitro susceptibility of 20 clinical isolates of staphylococci against GaM (in the logarithmic and biofilm growth phase) with corresponding calorimetry parameters.

Organism	MIC (µg/ml)	MBIC[a] (µg/ml)	MHIC[b] (µg/ml)
MSSA			
B14097/07	750	>6000	375
T6477/05	1500	6000	750
S2626/07	1500	>6000	375
T642/05	750	>6000	188
B10984/07	750	3000	188
MRSA			
T3011	375	>6000	94
U8927-1/07	375	3000	94
M1082/07	375	3000	94
S1771.07	375	6000	375
B12570/07	375	>6000	375
MSSE			
DJ 67	188	1500	188
DJ 134	188	3000	1500
DJ 169	188	750	94
DJ 198	94	3000	94
DJ 254	94	3000	188
MRSE			
DJ 146	94	3000	188
DJ 192	94	-[c]	375
B 102285	94	94	375
B 102534	188	750	375
B 103110	94	750	188

[a]MBIC, minimal biofilm inhibitory concentration.

[b]MHIC, minimal heat inhibitory concentration.

[c]Biofilm susceptibility not available due to absent growth in the growth control.

5.5 Discussion

Gallium exhibits its antimicrobial action by targeting iron metabolism and interfering thereby with an important virulence factor for infection and persistence of staphylococci [170, 171]. We evaluated the antimicrobial activity of gallium in the form of GaM against four staphylococci laboratory strains and twenty distinct clinical isolates. Assays were performed in a defined synthetic iron-limited medium (RPMI). By determination of bacterial doubling time, we could assume the appropriateness of the iron-restricted medium RPMI to be used instead of the standard medium (MHB) for susceptibility testing. Indeed, in our assay RPMI supported staphylococcal growth as well as MHB.

Against laboratory strains and using the criteria applied for conventional antimicrobial substances, *S. epidermidis* was more susceptible to GaM than *S. aureus*. Moreover, bactericidal activity was detected against staphylococci in logarithmic phase, except for MSSA, and also against *S. epidermidis* in the stationary growth-phase. The time-kill studies demonstrated that the killing mechanism of GaM occur in a time-dependent and dose-dependent fashion. Since *S. epidermidis* strains had longer doubling times than *S. aureus* (both in RPMI and MHB), time-kill studies were prolonged to 48 h for MSSE and MRSE. Indeed, killing of MSSE was improved at 48 h compared to 24 h. A higher killing was achieved with GaM in time-kill curves than with the MIC/MBC macrodilution assay. This discrepancy was mainly observed with the MRSA strain, where a 3-log reduction was achieved in the time-kill curves already at the MIC value. The reason of the better killing action may be correlated to the different conditions in which bacteria are cultured for the MBC test and for the kill curves. The MBC assay requires incubation in static conditions, whereas killing curves are performed with repetitive shaking at each sampling time point. By shaking, bacteria get access to more oxygen in the growth medium and thus, they may maintain a better metabolic activity also at late times of incubation. Since GaM displayed a better efficacy against replicating bacteria, in killing curves the 3-log reduction may occur already at concentrations lower than the MBC.

The activity of GaM against biofilm embedded bacteria was measured by determining the MBIC for laboratory strains and 20 clinical isolates. All isolates were classified as able to form biofilms by the crystal violet staining assay. However, one of the MRSE isolates could not be further evaluated for biofilm susceptibility to GaM because of the lack of re-growth from sub-cultured pegged lids. For the remaining strains, GaM exhibited inhibitory activity against biofilms with MBIC values between 3000 and 6000 µg/ml (for *S. aureus*) and between 280 and 3000 µg/ml (for *S. epidermidis*). In 5 of 10 tested clinical *S. aureus* isolates no inhibition of biofilms were observed up to 6000 µg/ml.

By measurement of bacterial heat production, we compared this novel calorimetric method with

conventional susceptibility tests and we evaluated the effect on bacterial metabolism and growth of GaM at sub-inhibitory concentrations. The concentrations of GaM for heat inhibition correlated well with MICs, confirming the direct link between heat measurement and bacterial growth. Eventual discrepancies in absolute values of MHIC and MIC could possibly have occurred because of the culture conditions. Indeed, for heat measurement, bacteria were cultured in sealed ampoules with limited oxygen availability, while broth macrodilution assays were performed in snap-lid tubes with sufficient oxygen availability. However, differences of 2 to 4-fold may still represent good correlation of the two parameters. Thus, we suggest the potential use of calorimetry as a fast, accurate and simple method to investigate antimicrobial activity of new substances at sub-inhibitory concentrations. The major finding was that, in accordance to the results of the kill studies performed, also the GaM mechanism of inhibition of heat production was dose-dependent and time- dependent, and a reduction in heat production comparing to controls was measured up to 23 µg/ml of GaM.

The in vitro activity of GaM against laboratory and clinical strains of staphylococci occurred at MICs ranging from 100 to 2000 µg/ml. After a single oral dose of 500 mg of GaM in three healthy volunteers, the median peak concentration of gallium in serum was 1 µg/ml, which is 100- to 2000-fold lower than the measured MICs [174]. These data suggest that, systemic application of GaM will probably not achieve therapeutic concentrations in humans. However, a subcutaneous injection of GaM (25 mg/kg) was highly protective against a wound infection induced with *P. aeruginosa* and *S. aureus* in a thermally injured infection mouse model [175]. The latter study would support, together with our in vitro results, the potentials of GaM for local administration in the prevention and treatment of wound infections. Moreover, due to its activity at sub-inhibitory concentrations, low doses of GaM may be investigated in combination with standard antimicrobials to elucidate potential synergistic effects or prevention of resistance development. Also, GaM is a promising candidate for topical use, where high local concentrations can be achieved. In the view of the increasing resistance of *S. aureus* to oxacillin and mupirocin, GaM may become an option (alone or in combination with other agents) for skin and mucosal decolonization. Finally, the displayed anti-biofilm activity may suggest the gallium use in coating of implants as preventive strategy against staphylococcal adherence. Animal and clinical studies are needed to further characterize the therapeutic and preventive potentials of gallium, followed by toxicity studies. A safe and efficacious Ga-containing formulation to treat a broad spectrum of biofilm-forming or multi-resistant microbes would be highly desirable.

Chapter 6

Linezolid Alone or Combined with Rifampin against Methicillin-Resistant *Staphylococcus aureus* in Experimental Foreign-Body Infection

Daniela Baldoni[1], Manuel Haschke[2], Zarko Rajacic[1], Werner Zimmerli[3], Andrej Trampuz[1,4]*

[1]Infectious Diseases Research Laboratory, Department of Biomedicine, University Hospital, Basel, Switzerland

[2]Division of Clinical Pharmacology and Toxicology, University Hospital, Basel, Switzerland

[3]Basel University Medical Clinic, Kantonsspital, Liestal, Switzerland

[4]Division of Infectious Diseases and Hospital Epidemiology, University Hospital, Basel, Switzerland

Adapted from: Antimicrobial Agents and Chemotherapy, 2009 Mar; 53 (3)

Received 13 June 2008/ Returned for modification 29 September 2008/ Accepted 3 December 2008

6.1 Abstract

We investigated the activity of linezolid, alone and in combination with rifampin (rifampicin), against a methicillin-resistant *Staphylococcus aureus* (MRSA) strain in vitro and in a guinea pig model of foreign-body infection. The MIC, minimal bactericidal concentration (MBC) in logarithmic phase and MBC in stationary growth phase for linezolid, rifampin and levofloxacin were 2.5, >20 and >20 μg/ml, respectively, for linezolid; 0.01, 0.08 and 2.5 μg/ml, respectively, for rifampin; and 0.16, 0.63 and >20 μg/ml, respectively, for levofloxacin. In time-kill studies, bacterial re-growth and development of rifampin resistance were observed after 24 h with rifampin alone at 1× or 4× MIC, and were prevented by the addition of linezolid. After the administration of single intraperitoneal doses of 25, 50 and 75 mg/kg of body weight, linezolid peak concentrations of 6.8, 12.7 and 18.1 μg/ml, respectively, were achieved in sterile cage fluid at ≈3 h. The linezolid concentration remained above the MIC of the test organism during 12 h with all doses. Antimicrobial treatments of animals with cage implant infections were given twice daily for 4 days. Linezolid alone at 25, 50 and 75 mg/kg reduced the planktonic bacteria in cage fluid during treatment by 1.2-1.7 $\log_{10}$ CFU/ml; only linezolid at 75 mg/kg prevented bacterial re-growth 5 days after end of treatment. Linezolid used in combination with rifampin (12.5 mg/kg) was more effective than linezolid used as monotherapy, reducing the planktonic bacteria by ≥3 $\log_{10}$ CFU ($P < 0.05$). Efficacy in eradication of cage-associated infection was achieved only when linezolid was combined with rifampin, with cure rates being between 50% and 60%, whereas the levofloxacin-rifampin combination demonstrated the highest cure rate (91%) against the strain tested. The linezolid-rifampin combination is a treatment option for implant-associated infections caused by quinolone-resistant MRSA.

6.2 Introduction

Implanted devices are increasingly used in modern medicine to alleviate pain or improve a compromised function. Implant-associated infections represent an emerging complication, caused by organisms which adhere to the implant surface and grow embedded in a protective extracellular polymeric matrix, known as a biofilm [4, 9, 184]. In addition, the microorganisms in biofilms enter a stationary growth phase and become phenotypically resistant to most antimicrobials, frequently causing treatment failure. In such cases, surgical removal of the implant is often required, causing high morbidity and substantial healthcare costs [38, 185, 186].

Staphylococcus aureus is the most common pathogen causing implant-associated infections [184, 185]. Successful treatment of these infections includes early surgical intervention and antimicrobial treatment with bactericidal drugs that also act on surface-adhering microorganisms. Rifampin (rifampicin) is bactericidal against stationary-growth-phase staphylococci, as demonstrated in vitro, in experimental animal models, and in clinical studies [43, 187]. However, when it is used as single agent, the rapid emergence of rifampin resistance occurs [83, 188]. Therefore, the use of antimicrobial combinations to prevent the development of rifampin resistance during treatment has been investigated [41, 72, 83]. Rifampin in combination with quinolones has successfully been used for the treatment of orthopedic implant-related infections [189-191]. However, the increasing prevalence of quinolone-resistant staphylococci has urged investigations for alternative drugs to use in combination with rifampin [192, 193]. In particular, methicillin-resistant staphylococci represent an increasing challenge due to their resistance to a broad variety of antimicrobials [194, 195].

The oxazolidinone linezolid is active against gram-positive cocci, including methicillin-resistant *Staphylococcus aureus* (MRSA) [196-199]. Limited data on the use of the linezolid-rifampin combination for the treatment of MRSA implant-associated infections are available. In vitro time-kill experiments showed a potential additive effect between linezolid and rifampin against MRSA [200]. However, only case reports or small case series describing the treatment of implant-associated infections with linezolid and rifampin exist [52, 54, 201, 202].

In the study described here, we investigated the activity of linezolid, alone and in combination with rifampin, against one reference MRSA strain in vitro and in an established foreign-body infection model. The cage-associated infection model in guinea pigs has been validated for testing the activities of antimicrobial agents and their combinations against implant-associated infections in pre-clinical studies [71, 203].

(Part of the results of this study was presented at the 47th Interscience Conference of Antimicrobiaal Agents and Chemotherapy, Chicago, IL, 17th to 20th September 2007, abstr. B-811)

6.3 Materials and Methods

Study organism. MRSA strain ATCC 43300, which is susceptible to levofloxacin and rifampin, was used for in vitro and in vivo antimicrobial testing. Methicillin-susceptible *S. aureus* strain ATCC 29213 was used as the indicator organism for the agar diffusion bioassay. The strains were stored at -70°C by use of a cryovial bead preservation system (Microbank, Pro-Lab Diagnostics, Richmond Hill, ON, Canada). One cryovial bead was cultured overnight on Columbia sheep blood agar plates (Becton Dickinson, Heidelberg, Germany). Inocula were prepared from the sub-culture of two to three colonies, which were resuspended in 5 ml of trypticase soy broth (TSB) and incubated overnight at 37°C without shaking.

Antimicrobial agents. Linezolid was provided as purified powder by the manufacturer (Pfizer AG, Zurich, Switzerland); stock solutions of 2.5 mg/ml were prepared in sterile pyrogen-free water. Levofloxacin hemihydrate injectable solution (5 mg/ml; Aventis Pharma AG, Zurich, Switzerland) and rifampin (Sandoz AG, Steinhausen, Switzerland) were purchased from the respective manufacturers.

In vitro antimicrobial susceptibility. The in vitro susceptibility of the MRSA strain to linezolid, levofloxacin and rifampin was determined in triplicate by using a standard inoculum of 1-5 × 10^5 CFU/ml, adjusted from overnight cultures. The MIC was determined in Mueller-Hinton broth (MHB) by the macrodilution method, according to guidelines of the Clinical Laboratory Standards Institute (CLSI) (formerly the National Committee for Clinical Laboratory Standards) [176]. In brief, ten twofold serial dilutions of the test drug were prepared in 2 ml MHB in sterile boro-silicate glass tubes. Two milliliters of the antimicrobial dilutions were inoculated below the meniscus and incubated for 18 h at 37°C without shaking. The MIC was the lowest drug concentration that inhibited visible bacterial growth. Tubes without visible growth were then vigorously vortexed, incubated for 4 h at 37°C without shaking, and assessed for viable bacteria by plating the contents of the tubes on agar. The lowest antimicrobial concentration, which killed ≥99.9% of the initial bacterial count (i.e. ≥3 $\log_{10}$ CFU/ml) was defined as the minimum bactericidal concentration (MBC) during logarithmic growth (MBC_{log}), as described in the Manual of Clinical Microbiology [204]. Killing of bacteria during stationary growth phase (MBC_{stat}) was assayed in nutrient-restricted medium (0.01 M phosphate-buffered saline, pH 7.4), as described previously [41]. In this medium, bacterial counts remained within ±15% of the initial inoculum in the antimicrobial-free culture for >36 h.

In vitro time-kill studies. The antimicrobial activities of linezolid and rifampin, alone and in

combination, against the MRSA strain were evaluated by time-kill studies with inocula of 1×10^6 to 5×10^6 CFU/ml, as described previously [144]. Antibiotic solutions with 1× and 4× the MIC of the test strain were prepared in 10 ml of MHB. Growth in the absence of antibiotics served as the control. Colony counts were determined after 0, 6 and 24 h of incubation at 37°C by plating aliquots of appropriate dilutions on Muller-Hinton agar (MHA). The ≥10-fold dilutions allowed accurate colony-counts in the range of 10-250 CFU per plate and minimized the effects of drug carry-over. The quantification limit was set equal to 200 CFU/ml (>10 CFU in 50 μl of a 10-fold dilution). Killing over time was expressed as the mean reduction in the $\log_{10}$ CFU/ml ± the standard deviation (SD). Synergism was defined as a 100-fold increase in the level of killing at 24 h with the combination in comparison with the level of killing achieved with the most active single drug. Antagonism was defined as a 100-fold decrease in the level of killing at 24 h with the combination of both drugs, compared to the level of killing achieved with the most active single drug [144]. Cultures of the MRSA strain that were exposed to rifampin alone or in combination with linezolid and that showed visible growth after 24 h of incubation were tested for rifampin resistance. The cultures were adjusted to a standardized inoculum corresponding to a McFarland 0.5, spread on MHA containing rifampin (1 μg/ml), and assessed for growth. Experiments were performed in triplicate.

In vitro antimicrobial resistance studies. An assay was developed to evaluate the rate of in vitro emergence of rifampin resistance. The ratio of resistant to total colony counts was assessed after 24 h of incubation of the MRSA strain in 10 ml MHB containing rifampin alone or rifampin and linezolid at 1× the MIC. The 24-h bacterial cultures were serially diluted 10-fold, 50 μl aliquots were plated on MHA containing rifampin (1 μg/ml) or no antibiotic, and the colonies were counted after 48 h of incubation at 37°C. The results were expressed as a ratio between the rifampin-resistant $\log_{10}$ CFU/ml and the total $\log_{10}$ CFU/ml. Experiments were performed in triplicate.

Animal model. A foreign-body infection model in guinea pigs was used, as previously described [6, 71, 78, 203]. Guinea pigs were kept under specific-pathogen-free conditions in the Animal House of the Department of Biomedicine, University Hospital Basel, and animal experimentation guidelines according to the regulations of Swiss veterinary law were followed. The study protocol was approved by the Institutional Animal Care and Use Committee. In brief, four sterile polytetrafluorethylene (Teflon) cages (32 mm x 10 mm), perforated by 130 regularly spaced holes of 1 mm diameter (Angst-Pfister AG, Zurich, Switzerland) were subcutaneously implanted in the flanks of male albino guinea pigs (Charles River, Sulzfeld, Germany) under aseptic conditions. Animals weighing 550 to 600 g were anesthetized with an intramuscular injection of ketamine (20 mg/kg) and xylazine (4 mg/kg). Two weeks after surgery and healing of the surgical wounds, the sterility of the cages was verified by culture of the aspirated cage fluid. The cages, which resulted being contaminated, were excluded from

further studies. Sterile cages were used for the pharmacokinetic studies. For the treatment studies, the cages were infected by percutaneous inoculation of 200 μl containing 2×10^4 CFU MRSA (day 0). Before inoculation, overnight bacterial cultures were washed twice, resuspended in 5 ml of sterile pyrogen-free normal saline and diluted 1:1,000. The establishment of infection was confirmed 24 h later by quantitative culture of aspirated cage fluid.

Pharmacokinetic studies. Cage fluid was aspirated from non-infected animals during 24 h (1, 2, 4, 6, 8, 10, 12 and 24 h) following intraperitoneal administration of a single dose of linezolid at 25, 50, and 75 mg/kg. Each dose was tested in three guinea pigs; therefore, 12 cages were used to relate the pharmacokinetic parameters to the antimicrobial treatment efficacy results. At each time point, 150-μl aliquots of cage fluid were aspirated from two cages from each animal (i.e., six replicates per time point and drug dose). The collected fluid was centrifuged (2100 × g for 7 min), and the supernatant was stored at -20°C until further analysis.

Determination of drug concentrations. Linezolid concentrations in cage fluid were determined by an agar plate diffusion bioassay with *S. aureus* strain ATCC 29213 as the indicator organism. Antibiotic medium 1 (Difco, BD, Le Pont de Claix, France) was suspended with sterile pyrogen-free water, and the mixture was boiled at 100°C in water bath for 30 min. After the medium was boiled, it was cooled down to 50°C, inoculated with the overnight culture of the indicator organism (300 μl/400 ml medium) and poured into large assay plates (30 by 30 cm). Calibration curves were plotted for each of the assay plates, and the regression fitting equation was extrapolated. The standard solutions were prepared in 31% guinea pig serum (corresponding to linezolid-albumin binding ratio in humans) by preparing twofold serial dilutions of the 20-mg/liter linezolid solution [205]. One hundred microliters of the cage fluid samples and duplicates of the linezolid standard solutions were spotted into holes punched into the assay plates, and the plates were incubated overnight. The diameter of the inhibition zone was measured with calipers. The bioassay detection limit corresponded to the linezolid MIC of the indicator organism (i.e., 1.25 μg/ml).

Pharmacokinetic parameters. The concentration-time data were analyzed individually for each animal by using the WinNonlin software package (Pharsight Corp., Mountain View, CA). Mean ± SD values of the peak concentration (C_{max}), the time to reach C_{max} (T_{max}), the trough concentration at 12 h after dosing (C_{min}), half-life ($t_{½}$), and the area under the concentration-time curve from time zero to 24 h (AUC_{0-24}) were calculated from three animals receiving the same linezolid dose.

Antimicrobial treatment studies. Antimicrobial treatment was initiated 24 h after infection (day 1). At least three animals were randomized into each of the following treatment groups: control

(saline), linezolid at 25, 50 and 75 mg/kg (alone or in combination with rifampin at 12.5 mg/kg), and levofloxacin at 10 mg/kg in combination with rifampin at 12.5 mg/kg [84]. All antibiotics were administered intraperitoneally every 12 h over 4 days (i.e., total of eight doses).

Efficacy of treatment against planktonic bacteria. The planktonic bacteria in aspirated cage fluid were enumerated before initiation of antimicrobial treatment (day 1), on the fourth day of treatment and before administration of the last antimicrobial dose (day 4), and 5 days after end of treatment (day 10). Bacterial counts were expressed as the median and interquartile range (IQR) of the $\log_{10}$ CFU/ml. The quantification limit of the planktonic bacteria was set at 1000 CFU/ml (>10 CFU in 50 μL from dilutions ≥10- fold). Thus, negative cage fluid cultures were assigned a value of 3 $\log_{10}$ CFU/ml for calculation of the $\log_{10}$ CFU/ml reduction and for statistical analysis. The efficacy of the treatment against planktonic bacteria was expressed as (i) the difference in bacterial counts in cage fluid (Δ $\log_{10}$ CFU/ml = $\log_{10}$ CFU/ml [day 4 or 10] - $\log_{10}$ CFU/ml [day 1]) and (ii) the rate of culture-negative cage fluid samples, i.e., the number of cage fluid samples without detectable growth of the MRSA strain divided by the total number of cages in the treatment group.

Efficacy of treatment against adherent bacteria. To determine the efficacy of the treatment against adherent bacteria, the animals were sacrificed on day 10. The cages were removed under aseptic conditions, placed in 5 ml TSB, vortexed for 30 s and incubated at 37°C. After 48 h, 100-μl aliquots of the cage cultures were plated on Columbia sheep blood agar plates (Becton Dickinson) and assessed for bacterial growth. Cultures displaying growth were tested by the *S. aureus* latex test (Staphytect Plus; Oxoid, Basel, Switzerland). Cage cultures negative in this test were considered contaminated and were not used for the evaluation of treatment efficacy. The efficacy of the treatment against adherent bacteria was expressed as the cure rate, defined as the number of cage cultures without MRSA growth divided by the total number of cages in the treatment group.

In vivo antimicrobial resistance studies. MRSA isolates from positive cultures in TSB containing explanted cages (i.e. treatment failures) were screened for the in vivo development of rifampin resistance. For this purpose, multiple colonies of each morphologically distinct colony type were collected from an agar subculture, suspended in saline to a standardized inoculum corresponding to the turbidity of a McFarland 0.5, and plated on MHA containing 1 μg/ml rifampin. The plates were incubated at 37°C and screened for growth after 48 h.

Statistics. Comparisons were performed by using the Man-Whitney U-test for continuous variables and a two-sided χ^2 or Fisher's exact tests for categorical variables, as appropriate. For all tests, differences were considered significant when *P* values were <0.05. Figures were plotted using GraphPad Prism (version 4.0) software (GraphPad Software, La Jolla, CA).

6.4 Results

In vitro antimicrobial susceptibility. Table 11 shows the in vitro susceptibility of the MRSA strain to linezolid, rifampin and levofloxacin. Linezolid inhibited bacterial growth at 2.5 μg/ml, whereas a bactericidal effect was not achieved up to 20 μg/ml either in the logarithmic or in the stationary growth phase. Rifampin exerted a low MIC (0.01 μg/ml) and was bactericidal in the logarithmic and the stationary growth phase. Levofloxacin had a MIC of 0.16 μg/ml and exhibited bactericidal activity only against bacteria in the logarithmic growth phase, and not those in the stationary phase.

Table 11. In vitro susceptibility of MRSA ATCC 43300

Antibiotic	MIC	MBC_{log}[a]	MBC_{stat}[b]
	(μg/ml)		
Linezolid	2.5	>20	>20
Rifampin	0.01	0.08	2.5
Levofloxacin	0.16	0.63	>20

[a] MBC_{log}, minimal bactericidal concentration in the logarithmic growth phase.

[b] MBC_{stat}, minimal bactericidal concentration in the stationary growth phase.

In vitro time-kill studies. In vitro time-kill studies were performed with inocula of 1×10^6 to 5×10^6 CFU/ml to investigate the synergism or antagonism of linezolid and rifampin. In the controls, the bacterial counts increased by 1.7 $\log_{10}$ CFU/ml after 24 h. In the presence of linezolid at 1× the MIC, the bacterial counts remained unchanged, while at 4× MIC they decreased by 1.7 $\log_{10}$ CFU/ml at 24 h. Rifampin at both 1× and 4× the MIC similarly decreased the bacterial counts after 6 h (0.5 $\log_{10}$ CFU/ml), however, regrowth to counts similar to those for the growth controls occurred after 24 h (figure 25). Bacteria exposed to rifampin alone showed regrowth after 24 h and were resistant to rifampin. When rifampin was combined with linezolid at either 1× or 4× the MIC, the bacterial counts at 24 h were decreased by 1.6 and 1.8 $\log_{10}$ CFU/ml, respectively. Due to the development of rifampin resistance during exposure to rifampin alone, it was not possible to evaluate whether a potential synergistic or antagonistic interaction between rifampin and linezolid existed, as described above.

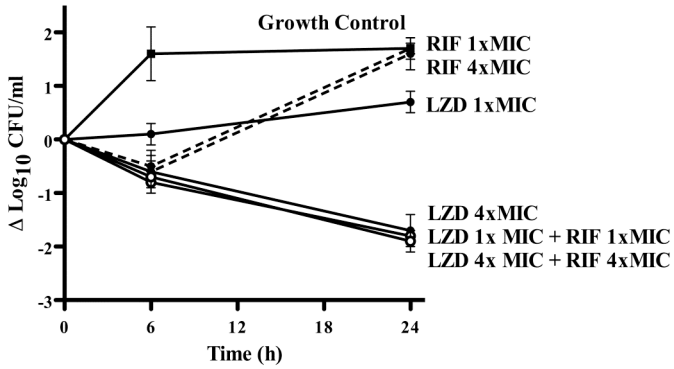

Figure 25. Time-kill curves of 1× and 4× MIC linezolid (closed circles), 1x and 4x MIC rifampin (closed circle, dashed line), and their combination (open circles), against MRSA. Values are means ± SD. LZD, linezolid; RIF, rifampin.

In vitro antimicrobial resistance. With MRSA inocula of 1× 10^6 to 5 × 10^6 CFU/ml, the ratio of rifampin-resistance developed after 24 h from cultures exposed to rifampin alone at 1× the MIC was 94% ± 3%. In contrast, no rifampin-resistant strains colonies were detected after 24 h incubation with the rifampin-linezolid combination at 1× the MIC.

Pharmacokinetic studies. Figure 26 shows the concentration-time profile in cage fluid after the administration of a single intraperitoneal dose in noninfected animals. The calculated values of the pharmacokinetic parameters are summarized in table 12. The C_{max}s of linezolid at 25, 50 or 75 mg/kg i.p. dose, were achieved at ≈3 h after dosing. The linezolid concentration remained above the MIC of the test organism for 12 h, as did the rifampin and levofloxacin concentration. The C_{max} of rifampin in the cage fluid reached almost 100× the MIC, whereas this ratio was considerably lower for linezolid and levofloxacin (5× and 9× the MIC, respectively).

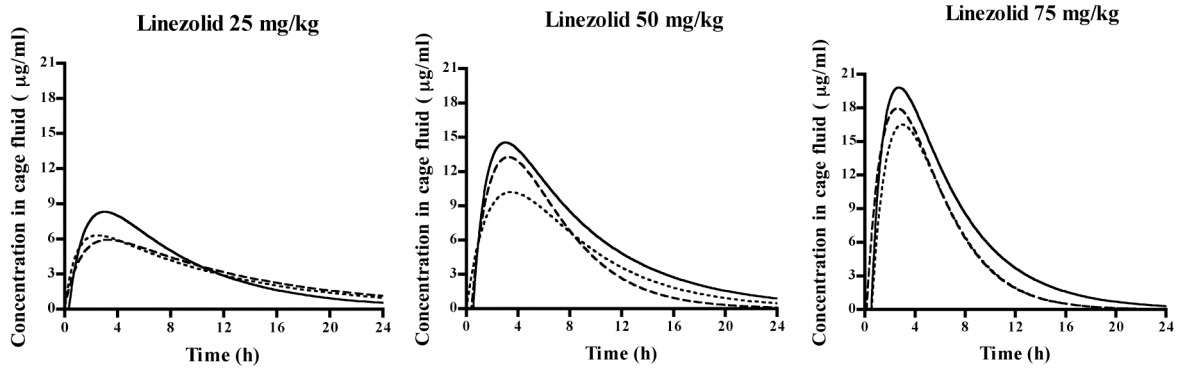

Figure 26. Pharmacokinetic of linezolid in cage fluid after a single intraperitoneal dose of 25 mg/kg (left), 50 mg/kg (center) and 75 mg/kg (right). Graphs represent WinNonLin individual fitting curves per animal, of three animal per linezolid dose.

Table 12. Pharmacokinetic parameters in cage fluid after a single intraperitoneal administration in non-infected animals, linked to pharmacokinetic parameters in cage fluid [a]

Antibiotic	Dose (mg/kg)	C_{max} (µg/ml)	C_{min} (µg/ml)[b]	T_{max} (h)	$T_{1/2}$ (h)	AUC_{0-24} (h×µg/ml)	C_{max}[c]/MIC	AUC_{0-24}[c]/MIC (h)
Linezolid	25	6.8 ± 1.3	3.0 ± 0.2	3.0 ± 0.4	6.8 ± 1.7	87.8 ± 2.7	2.7	35.1
Linezolid	50	12.7 ± 2.2	3.7 ± 1.1	3.3 ± 0.2	3.5 ± 1.7	118.7 ± 23.0	5.1	47.5
Linezolid	75	18.1 ± 1.7	2.5 ± 1.0	2.8 ± 0.2	2.6 ± 0.9	125.8 ± 20.5	7.2	50.3
Rifampin	12.5	1.0 ± 0.3	0.1 ± 0.1	2.1 ± 0.3	2.5 ± 1.3	4.6 ± 0.5	100.0	460
Levofloxacin	10	1.5 ± 0.2	0.3 ± 0.1	2.5 ± 0.3	4.2 ± 1.4	6.1 ± 0.8	9.4	38.1

[a] Values are means ± SD from 3 animals, as predicted by WinNonlin software package.

[b] C_{min} (trough concentration) at 12 h after dosing.

[c] Mean values of C_{max} and AUC_{0-24} in cage fluid after a single intraperitoneal dose. Pharmacokinetic data for rifampin and levofloxacin were described previously [42]

Antimicrobial treatment studies. Cage fluid sterility was confirmed prior to infection. At 24 h after infection, the median concentration of the bacteria enumerated in the cage fluid was 6.5 $\log_{10}$ CFU/ml. In control animals receiving saline, the bacterial counts in the cage fluid were 7.1 and 7.9 $\log_{10}$ CFU/ml after 4 and 10 days, respectively, which correspond to increases of 0.6 and 1.4 $\log_{10}$ CFU/ml, respectively. No spontaneous cure of the cage-associated infection occurred in untreated animals.

Efficacy of treatment against planktonic bacteria. Table 13 shows the counts of planktonic bacteria and the rates of culture-negative cage fluid samples during and after treatment. During treatment (day 4), the bacterial counts in the cage fluid of animals treated with linezolid alone at 25, 50 and 75 mg/kg were decreased by a median values of 1.4, 1.2 and 1.7 $\log_{10}$ CFU/ml, respectively. No differences in treatment efficacy were observed between the three linezolid doses (P >0.05). Linezolid achieved culture-negativity in 8% of cage fluid samples when it was used at 25 mg/kg and 17% of cage fluid samples when it was used at 50 and 75 mg/kg. When the three linezolid regimens were combined with rifampin, they reduced the bacterial counts by >3.0 $\log_{10}$ CFU/ml, which was significantly better than the results achieved with linezolid alone (P <0.05) (figure 27A). A total of 55% to 65% of the cage fluid samples from animals treated with rifampin-linezolid combinations were culture negative on day 4.

Five days after the end of treatment (day 10), the planktonic bacteria in the cage fluid of animals treated with linezolid at 25 and 50 mg/kg showed regrowth to 7.3 and 7.1 $\log_{10}$ CFU/ml, respectively (table 13), which correspond to increases of 1.0 and 0.8 $\log_{10}$ CFU/ml compared to the level of growth on day 1 (figure 27B). Linezolid at 75 mg/kg prevented bacterial regrowth in cage fluid on day 10, and the bacterial counts remained comparable to the values on day 4. In animals treated with the combination of linezolid and rifampin, the bacterial counts remained at the levels measured on day 4,

independent of the linezolid dose (P >0.05). No differences in treatment efficacy were observed between the three-linezolid doses (P >0.05) when they were combined with rifampin. The cure rates for animals treated with the linezolid-rifampin combination ranged from 75% to 95%, and rifampin-resistance did not emerge.

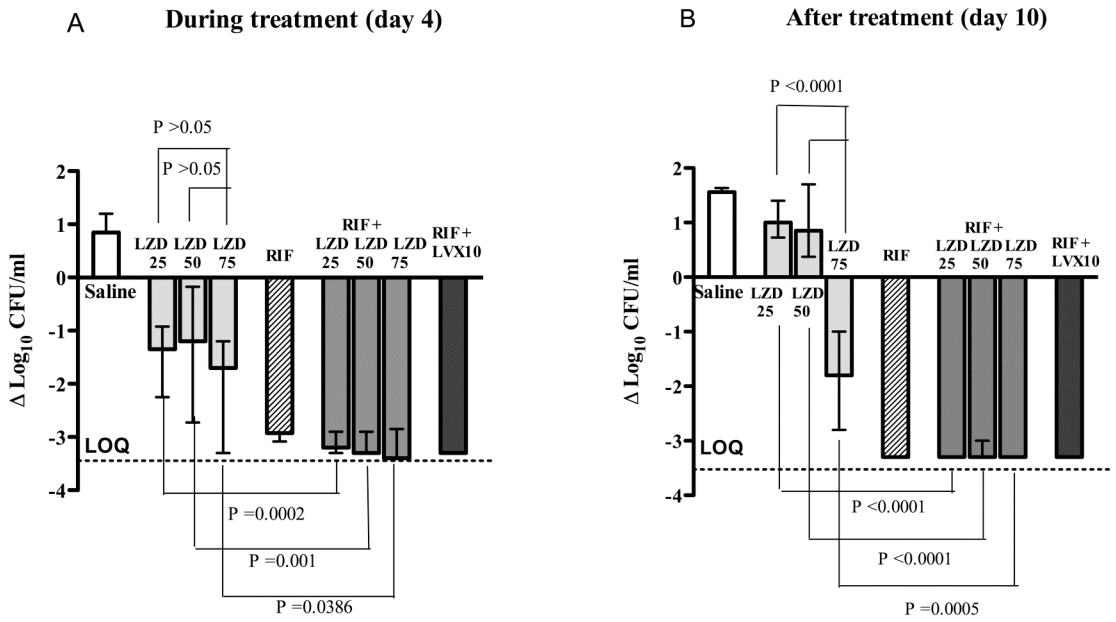

Figure 27. Treatment efficacy against planktonic bacteria in cage fluid (Δ $\log_{10}$ CFU/ml) during treatment – day 4 (A) and 5 days after the end of treatment – day 10 (B). Dashed horizontal line indicates the limit of quantification (LOQ). LZD25, linezolid 25 mg/kg; LZD50, linezolid 50 mg/kg; LZD75, linezolid 75 mg/kg; RIF, rifampin 12.5 mg/kg and LVX10, levofloxacin 10 mg/kg.

Table 13. Counts of planktonic bacteria in cage fluid and rate of culture-negative cage fluid samples during treatment (day 4) and 5 days after end of treatment (day 10)

Treatment group, dose (N cages)	**Bacterial counts in cage fluid ($\log_{10}$ CFU/ml)[a]**		**No. culture-negative / total no. cage fluid samples (%)**	
	Day 4	Day 10	Day 4	Day 10
Control (12)	7.1 (7.0 - 7.5)	7.9 (7.6 – 8.1)	0/12 (0%)	0/12 (0%)
Linezolid, 25 mg/kg (12)	4.5 (4.1 – 5.0)	7.3 (7.1 - 7.7)	1/12 (8%)	0/12 (0%)
Linezolid, 50 mg/kg (12)	5.1 (4.1 – 6.0)	7.1 (6.8 – 8.0)	2/12 (17%)	0/12 (0%)
Linezolid, 75 mg/kg (12)	4.6 (3.2 – 5.0)	4.5 (4.0 – 5.2)	3/12 (25%)	2/12 (17%)
Rifampin, 12.5 mg/kg (12)	3.1 (3.0 – 3.4)	<3.0	6/12 (50%)	11/12 (92%)
Linezolid, 25 mg/kg + rifampin, 12.5 mg/kg (20)	<3.0	<3.0	13/20 (65%)	19/20 (95%)
Linezolid, 50 mg/kg + rifampin, 12.5 mg/kg (20)	<3.0	<3.0	13/20 (65%)	15/20 (75%)
Linezolid, 75 mg/kg + rifampin, 12.5 mg/kg (20)	<3.0	<3.0	11/20 (55%)	17/20 (85%)
Levofloxacin, 10 mg/kg + rifampin, 12.5 mg/kg (24)	<3.0	<3.0	7/11 (75%)	11/11 (100%)

[a] Values are medians and interquartile ranges.

Efficacy of treatment against adherent bacteria. No cure of cage-associated infections was observed with linezolid alone (figure 28). The use of linezolid in combination with rifampin showed cure rates of 50% to 60%. All linezolid-rifampin combinations exhibited significantly better activities than linezolid alone against adherent bacteria (P <0.001). For comparison, the efficacy of the combination levofloxacin plus rifampin was tested and demonstrated a cure rate of 91%.

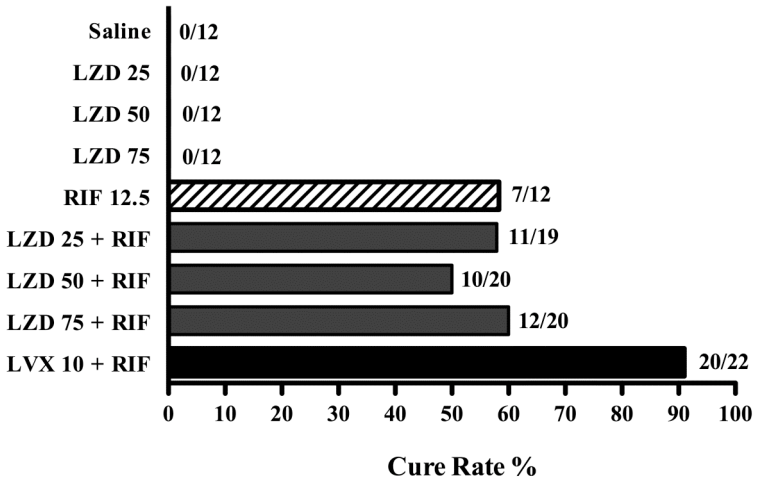

Figure 28. Cure rates of cage-associated infection at day 10. The values indicate the number of cage cultures without growth of MRSA / the total number of cages in the treatment group. LZD25, linezolid 25 mg/kg; LZD50, linezolid 50 mg/kg; LZD75, linezolid 75 mg/kg; RIF, rifampin 12.5 mg/kg and LVX, levofloxacin 10 mg/kg.

In vivo antimicrobial resistance studies. No rifampin-resistant MRSA strains were detected within positive cultures of cages from animals treated with rifampin alone or in combination with linezolid.

6.5 Discussion

In this study, we investigated the activity of linezolid alone and in combination with rifampin against MRSA in vitro and in a guinea pig implant-associated infection model. The test organism was inhibited by linezolid at 2.5 μg/ml. However, a reduction of ≥99.9% CFU/ml was not achieved at concentrations up to 20 μg/ml in either the logarithmic or the stationary growth phase. This is in agreement with the bacteriostatic activity of linezolid against staphylococci [206]. On the basis of this characteristic, linezolid monotherapy does not seem to be appropriate for the treatment of staphylococcal implant-associated infections.

In the in vitro time kill-curve studies, rifampin-resistance was detected after 24 h of incubation in all cultures exposed to rifampin alone (1× and 4× the MIC). In contrast, the use of rifampin in combination with linezolid never resulted in the emergence of rifampin resistance [196, 200, 207]. Thus, we can conclude that in vitro the combination linezolid-rifampin did not display any synergism or antagonism against the strain tested, and it was difficult to interpret whether there was any additive effect because of bacterial regrowth at 24 h of incubation with rifampin alone, due to resistance selection. However, the combination was effective in completely preventing the development of rifampin resistance.

In the pharmacokinetic studies, linezolid peak concentrations in cage fluid increased linearly with increasing doses between 25 and 75 mg/kg, whereas the increase in the AUC_{0-24} was not proportional to the dose due to the faster elimination of linezolid from the cage fluid at higher doses. The peak linezolid concentration and AUC_{0-24} reached in the cage fluid with the 75-mg/kg dose were comparable to the values reported by Gee T. et al. [208] in the inflammatory blister fluid of healthy volunteers receiving 600 mg linezolid, every 12 h. The 25-mg/kg and the 50-mg/kg linezolid doses administered to guinea pigs more likely simulate the 400 mg and 600 mg single-dose regimens, respectively. The three doses of linezolid chosen guaranteed that the antimicro bial concentration in cage fluid remained above its MIC for the test organism (2.5 μg/ml) for 12 h, and, thus, during the entire treatment. Andes et al. [209], showed that a plasma AUC_{0-24}/ MIC ratio of linezolid between 50 and 100 was predictive of a successful outcome of staphylococcal infections in the thigh muscle model. In our studies, the AUC_{0-24}/ MIC was only approximately 50 and was achieved with the highest linezolid dose (75 mg/kg). However, these values are difficult to interpret since we investigated a different compartment (cage fluid) and a different type of infection (an infection associated with an implant) comparing to those used by Andes et al..

The rifampin dose of 12.5 mg/kg was chosen as described previously [42, 72]. The peak levels in tissue fluid were equal or less than the maximal concentrations reached in humans [210], and the

rifampin concentration in cage fluid was greater than the MIC for 12 h after administration.

The cage fluid from the MRSA-infected cages implanted in guinea pigs demonstrated continuous bacterial growth for 10 days and no spontaneous cure. Linezolid induced a significant reduction in the counts of planktonic bacteria during treatment (day 4) both when it was given alone and when it was given in combination with rifampin (P <0.05). During treatment, no difference between the linezolid monotherapies was observed, but in combination with rifampin, bacterial killing was significantly improved (P <0.05). Five days after the end of treatment (day 10), bacterial regrowth occurred with linezolid doses 25 and 50 mg/kg, whereas the counts remained suppressed after the linezolid dose of 75 mg/kg, even though the AUC_{0-24} was only slightly higher. As previously shown [197], linezolid is able to induce a postantibiotic effect in *S. aureus* in a dose-dependent manner in vitro. Thus, it is likely that the postantibiotic effect was induced by the highest linezolid dose (75 mg/kg) but not by the two lower doses. In addition, the accumulation of linezolid may have occurred with the highest dose, delaying its time of clearance from the cage fluid. All combinations of linezolid with rifampin inhibited bacterial regrowth five days after the last dose.

None of the treatment regimens with linezolid monotherapies eradicated the cage-associated MRSA infections, while the combinations of linezolid with rifampin achieved cure rates between 50% and 60%, which is not significantly different from that achieved with rifampin monotherapy. The combination of rifampin and levofloxacin showed the highest cure rate (91%). Treatment failures were related to lack of efficacy in the killing of bacteria when they were embedded into the biofilm matrix. The emergence of rifampin resistance did not occur in vivo with any of the rifampin regimens tested.

In conclusion, linezolid monotherapies showed a bacteriostatic activity against the MRSA strain tested and were not able to eradicate the adhering bacteria. Thus, linezolid should not be used alone for the eradication of implant-associated infections caused by MRSA. In vitro studies demonstrated the potential of linezolid-rifampin combination for the treatment of MRSA infections, and these findings were confirmed in the animal foreign-body infection model. However, levofloxacin-rifampin combinations achieved higher cure rates than the linezolid-rifampin combination against the quinolone-susceptible MRSA strain tested (91% and 50 to 60%, respectively). In contrast to our previous recommendations [4], the quinolone-rifampin combination seems to be a valid option for the treatment of MRSA infections, whereas linezolid-rifampin regimens may be used for the treatment of quinolone-resistant MRSA implant-associated infections.

Chapter 7

Conclusions and Outlook

In the present study we described in vitro and in vivo innovative methods developed and evaluated for improving the diagnosis and treatment of prosthetic joint infections.

Diagnosis of infection (nuclear medicine). Nuclear medicine studies were performed in order to evaluate novel radiopharmaceuticals targeting bacterial infections. We established experimental protocols for measuring the radiotracers' binding in vitro to bacterial cells and accumulation in vivo at infection sites, in a mouse tissue cage model of infection.

In our studies, we compared published formulated kits of ^{99m}Tc-UBI, ^{99m}Tc-ciprofloxacin, ^{99m}TcN-ciproCS$_2$ and ^{111}In-DTPA-biotin with the aim to define their in vitro labelling stability, in vitro binding to different bacteria, and the in vivo biodistribution in our experimental settings.

All tested radiotracers showed high labelling resolutions and a high stability, both in saline and serum. The in vitro binding to the *E. coli* and *S. aureus* test strains was for ^{99m}Tc-UBI, ^{99m}Tc-ciprofloxacin and ^{111}In-DTPA-biotin lower than 1%, independently on the temperature and non-displaceable by an 100-fold excess of unlabeled compound. ^{99m}TcN-ciproCS$_2$ showed high in vitro binding, but no specificity could be demonstrated. However, it is known that, with the exception of biotin, the binding of the remaining agents to bacteria is non-receptor mediated, and thus non-displaceable [108, 109, 112].

In vivo ^{99m}Tc-UBI, ^{99m}Tc-ciprofloxacin and ^{111}In-DTPA-biotin showed a rapid kinetic of accumulation into cage fluids, followed by an exponential clearance, slower in infected than in sterile cages. Differently behaved the tracer ^{99m}TcN-ciproCS$_2$, which gradually entered the cages, and persisted during 24 h. All radiotracers were fast eliminated from blood and non-target organs. The T/NT ratios, calculated between target (infected) and non-target (sterile) cages, were at 4 h p.i. higher for ^{99m}Tc-ciprofloxacin and ^{111}In-DTPA-biotin than for ^{99m}Tc-UBI 29-41 and ^{99m}TcN-CiproCS$_2$. Whereas, at 24 h T/NT ratios > 2 where observed with ^{99m}Tc-UBI 29-41, ^{99m}Tc-ciprofloxacin and ^{99m}TcN-CiproCS$_2$ and were generally higher in *E. coli* than in *S. aureus* infected cages. Differently, ^{111}In-DTPA-biotin was manily cleared at 24 h p.i. from all organs and tissues. The observation that T/NT ratio >3 were not achieved at any time and with any bacteria, in our opinion may constitute a limiting factor for their application in humans.

In a separate study but with an experimental set up similar to the one described above, we evaluated the novel transcobalamin II non-binder ^{99m}Tc-PAMA(4) derivative of the vitamin B_{12} for targeting *S. aureus* and *E. coli* implant infections. Due to the lack of binding to the transcobalamin II transporter, in vivo the ^{99m}Tc-PAMA(4) derivative of the vitamin B_{12} is not accumulated systemically, but only by malignant cells and, eventually, bacteria. The derivative had been previously developed by Waibel et al. [85] and had brought successful results in targeting tumor cells in vivo.

We performed in vitro binding studies and we demonstrated that radiolabeled Cbl (^{57}Co-Cbl) has a receptor-mediated and displaceable binding to *E. coli* and *S. aureus*. Temperature dependency of the

binding was more evident for *S. aureus* than for *E. coli*. In addition, no binding could be measured to heat killed bacteria. The binding internalization was measured by pre-incubation of the bacterial cultures with the labeled vitamin, followed by addition of excesses of the unlabeled Cbl. Differently from the results gathered when incubating labeled and unlabeled Cbl simultaneously, when bacteria were pre-incubated with the labeled Cbl no more displacement could be measured. The latter result may indicate either an internalization mechanism or a maturation of the binding, which would prevent further displacement. Interestingly, ethanol *E. coli* fixed bacteria, which preserved the binding properties towards ^{57}Co-Cbl, showed equal displacement in both the competition assays.

When testing the ^{99m}Tc-PAMA(4)-Cbl derivative in vitro, the binding to *S. aureus* did not differ from the one measured with ^{57}Co-Cbl. Whereas, when testing *E. coli*, the binding ratio of the ^{99m}Tc-PAMA(4)-Cbl derivative was approximately 100-fold lower than the ^{57}Co-Cbl.

In the mouse tissue cage model of infection, the distribution of the agent ^{99m}Tc-DTPA served as negative control, and confirmed the tissue cages to be filled with a richly vascularized granulation tissue. Indeed, the tracer displayed an early uptake followed by rapid clearance from all cages fluids.

^{99m}Tc-PAMA(4)-Cbl showed a fast penetration into both infected and sterile cage-fluids but a slower release from infected cages. The tracer retention into infected fluids became significantly higher at 4 h p.i. for *S. aureus* infected mice and 8 h p.i. for *E. coli* infected mice, in accordance with the lower in vitro binding of PAMA(4)-Cbl to *E. coli*. In addition, the uptake of ^{99m}Tc-PAMA(4)-Cbl in infected fluids was significantly higher than the one of the non-specific tracer ^{99m}Tc-DTPA, in both *S. aureus* and *E. coli* infected cages. The latter result suggested a specific interaction of ^{99m}Tc-PAMA(4)-Cbl with the colonizing bacteria, rather than a non-specific retention due to the morphological differences between infected and sterile cages. Further studies should be addressed to determine an optimal SPECT/CT imaging time after i.v. injection of ^{99m}Tc-PAMA(4)-Cbl. From our data, we could suggest a delay of 8 h to 12 h p.i. in order to achieve a discriminative accumulation in both *S. aureus* and *E.coli* infected rather than sterile cages.

Differently, ^{57}Co-Cbl was not discriminative for *S. aureus* infected cages, and it became discriminative for *E. coli* infected mice at 72 h p.i. In addition, high background retention in non-target tissues was measured up to 72 h p.i..

When the infection-inflammation non-specific tracer, ^{67}Ga-citrate, was tested (positive control), a discriminative accumulation of the tracer in infected rather than sterile cages was achieved from 48 h until 72 h p.i.. Thus, our studies demonstrated the validity of the tissue cage mouse model of infection for screening in vivo the radiotracer's targeting of bacterial infections. Importantly, further studies should be addressed to better characterize the predictive value of our in vivo model towards diagnosis of infections in humans.

Diagnosis of infection (calorimetry). Calorimetry is a high-potential method for sensitive measurements of bacterial heat production related to their growth and metabolism in culture. We

aimed to prove the use of calorimetry for early and accurate detection of methicillin-resistance, using laboratory strains and clinical isolates of *S. aureus*. Relative heat was calculated as ratio between the total heat measured for bacterial cultures in the presence and absence of 4 µg/ml cefoxitin. A cutoff of relative heat was generated on the basis of 20 repeated measurements performed with MSSA and MRSA laboratory strains at 3 h, 4 h and 5 h of incubation in the microcalorimeter. Based on the relative heat cutoff of 0.4, 17 of 20 (85%) MRSA clinical isolates were correctly identified after 3 h of incubation. When the incubation was prolonged to 5 h, 19 of 20 (95%) MRSA isolates were correctly identified. The relative heat of all MSSA strains remained <0.4 up to 5 h of incubation. At 5 h of incubation, the sensitivity, specificity, positive and negative predictive values (and their 95% confidence intervals) for detection of methicillin resistance were 95% (89%-100%), 100% (92%-100%), 100% (91%-100%) and 91% (85%-97%), respectively. 19

The calorimetric protocol has the advantages of being rapid, inexpensive, easy to set up, suitable for automation and the processing of computer-generated results. Thus, calorimetry is a promising tool for the rapid discrimination between MSSA and MRSA strains. Our protocol may be further optimized to increase the accuracy and speed of MRSA detection. In addition, the use of calorimetry measurements for screening of bacterial resistance patterns could be extended to other organisms and antibiotic substances.

Antimicrobial prophylaxis and treatment of infection. The introduction in the clinical practice of antimicrobials with an unconventional mechanism of action may become an innovative approach for prophylaxis and treatment of prosthetic joint infection. Indeed, the spread of multi-resistant organisms or the emergence of acquired resistance during antimicrobial treatment raises the urgency for new pharmaceuticals. We investigated the in vitro activity of Gallium Maltolate (GaM) against laboratory and clinical staphylococci in the logarithmic, stationary phase and biofilms. Gallium (III) acts against bacteria by substituting Iron (III) at its enzyme binding-sites, and thus, blocking all iron-dependent metabolic reactions. Standard in vitro tests for determination of MIC, minimal bactericidal concentration (MBC) in the logarithmic and stationary growth phase, showed a bactericidal activity of GaM against *S. epidermidis* strains at concentrations ranging between 1500 and 6000 µg/ml (MICs between 94 and 200 µg/ml). Whereas, GaM was mostly bacteriostatic against *S. aureus* (MICs between 375 and 2000 µg/ml). Also when testing eradication of pre-formed biofilm, GaM showed higher efficacy against *S. epidermidis* than *S. aureus* strains. In addition, methicillin-resistant strains showed a tendency of higher susceptibility to GaM than the methicillin-susceptible strains. At sub-inhibitory concentrations, GaM inhibited in a dose-dependent manner the bacterial heat production, measured using a newly developed calorimetric assay.

The high concentrations of GaM associated with in vitro anti-staphylococcal activity would suggest that, the systemic application of GaM for therapeutic use in humans is rather improbable. However in previous studies, the subcutaneous injection of GaM (25 mg/kg) showed prevention of

colonization by *P. aeruginosa* and *S. aureus* in a thermally injured infection mouse model, suggesting potential applications in local therapy of wound infections [175]. Moreover, due to its activity at sub-inhibitory concentrations, low doses of GaM may be investigated in combination with standard antimicrobials to elucidate potential synergistic effects or prevention of resistance development.

Alternatively, GaM could be a promising candidate for MRSA skin and mucosal decolonization. Finally, the displayed anti-biofilm activity may suggest gallium use in implant coating as preventive strategy against staphylococcal adherence. Animal and clinical studies are needed to further characterize the therapeutic and preventive potentials of gallium, together with toxicity studies.

Antimicrobial treatment of infection. The combination rifampin/ levofloxacin is one of the most effective antimicrobial regimens against MRSA prosthetic infection. However, the diffusion of strains resistant to fluoroquinolones stimulated the search of novel anti-staphylococcal agents to be administered in combination with rifampin. Linezolid has been reported for the high activity against soft-tissue MRSA infections [211]. However, only case reports have been published regarding the potential of linezolid in combination with rifampin against MRSA prosthetic infections. Thus we tested linezolid alone and in combination with rifampin, against one reference MRSA strain in vitro and in the established guinea pig foreign-body infection model.

The test MRSA strain was susceptible to linezolid, but only bacteriostatic concentrations of the antimicrobials could be achieved in vitro. In kill curve studies we demonstrated the efficacy of linezolid-rifampin combination to completely prevent the development of rifampin resistance, observed in cultures exposed to rifampin alone.

In the animal foreign-body infection model, linezolid monotherapies showed only a slight reduction of planktonic MRSA and were not able to eradicate the adhering bacteria, against which bactericidal activity is mandatory. Thus, linezolid should not be used alone for the eradication of implant-associated infections caused by MRSA.

The linezolid-rifampin combinations achieved cure rates of adherent MRSA of 50 to 60%. In comparison, levofloxacin-rifampin combinations displayed higher cure rates (91%) than the linezolid-rifampin combination against the quinolone-susceptible MRSA strain tested.

In contrast to our previous recommendations [4], the quinolone-rifampin combination seems to be a valid option for the treatment of MRSA infections, whereas linezolid-rifampin regimens may be used for the treatment of quinolone-resistant MRSA implant-associated infections.

References

1. Washingtom Winn, J., Stephen Allen, William Janda, Elmer Koneman, Gary Procop, Paul Schreckenberger, Gail Woods, *Color Atlas and Texrbook of Diagnostic Microbiology.* Lippincott Williams & Wilkins, 2006. Sixth Edition(Chapter 1).
2. Connie R. Mahon, D.C.L., George Manuselis, *Textbook of Diagnostic Microbiology.* Saunders Elsevier, 2007. Third Edition(Chapter 1).
3. Francis A. Waldvogel, A.L.B., *Infections Associated with Indwelling Medical Devices.* ASM Press Washington, DC, 2000. Third Edition.
4. Zimmerli, W., A. Trampuz, and P.E. Ochsner, *Prosthetic-joint infections.* N Engl J Med, 2004. 351(16): p. 1645-54.
5. Trampuz, A. and W. Zimmerli, *Antimicrobial agents in orthopaedic surgery: Prophylaxis and treatment.* Drugs, 2006. 66(8): p. 1089-105.
6. Zimmerli, W., P.D. Lew, and F.A. Waldvogel, *Pathogenesis of foreign body infection. Evidence for a local granulocyte defect.* J Clin Invest, 1984. 73(4): p. 1191-200.
7. Harris, L.G. and R.G. Richards, *Staphylococci and implant surfaces: a review.* Injury, 2006. 37 Suppl 2: p. S3-14.
8. Trampuz, A. and W. Zimmerli, *Prosthetic joint infections: update in diagnosis and treatment.* Swiss Med Wkly, 2005. 135(17-18): p. 243-51.
9. Donlan, R.M., *Biofilms: microbial life on surfaces.* Emerg Infect Dis, 2002. 8(9): p. 881-90.
10. Darouiche, R.O., *Device-associated infections: a macroproblem that starts with microadherence.* Clin Infect Dis, 2001. 33(9): p. 1567-72.
11. Campoccia, D., L. Montanaro, and C.R. Arciola, *The significance of infection related to orthopedic devices and issues of antibiotic resistance.* Biomaterials, 2006. 27(11): p. 2331-9.
12. Sendi, P., et al., *Staphylococcus aureus small colony variants in prosthetic joint infection.* Clin Infect Dis, 2006. 43(8): p. 961-7.
13. Trampuz, A. and A.F. Widmer, *Infections associated with orthopedic implants.* Curr Opin Infect Dis, 2006. 19(4): p. 349-56.
14. Costerton, J.W., P.S. Stewart, and E.P. Greenberg, *Bacterial biofilms: a common cause of persistent infections.* Science, 1999. 284(5418): p. 1318-22.
15. Maderazo, E.G., S. Judson, and H. Pasternak, *Late infections of total joint prostheses. A review and recommendations for prevention.* Clin Orthop Relat Res, 1988(229): p. 131-42.
16. Andrej Trampuz, J.M.S., Douglas R. Osmon, Franklin R. Cockerill, Arlen D. Hanssen, Robin Patel, *Advances in the laboratory diagnosis of prosthetic joint infection.* Reviews in Medical Microbiology, 2003. 14(1): p. 1 - 14.
17. Love, C., S.E. Marwin, and C.J. Palestro, *Nuclear medicine and the infected joint replacement.* Semin Nucl Med, 2009. 39(1): p. 66-78.
18. Bauer, T.W., et al., *Diagnosis of periprosthetic infection.* J Bone Joint Surg Am, 2006. 88(4): p. 869-82.
19. Trampuz, A., et al., *Synovial fluid leukocyte count and differential for the diagnosis of prosthetic knee infection.* Am J Med, 2004. 117(8): p. 556-62.
20. Trampuz, A., et al., *Sonication of removed hip and knee prostheses for diagnosis of infection.* N Engl J Med, 2007. 357(7): p. 654-63.

21. Boerman, O.C., et al., *Radiopharmaceuticals for scintigraphic imaging of infection and inflammation.* Inflamm Res, 2001. 50(2): p. 55-64.

22. Palestro, C.J., C. Love, and T.T. Miller, *Diagnostic imaging tests and microbial infections.* Cell Microbiol, 2007. 9(10): p. 2323-33.

23. Signore, A., et al., *Receptor targeting agents for imaging inflammation/infection: where are we now?* Q J Nucl Med Mol Imaging, 2006. 50(3): p. 236-42.

24. Love, C. and C.J. Palestro, *Radionuclide imaging of infection.* J Nucl Med Technol, 2004. 32(2): p. 47-57; quiz 58-9.

25. Becker, W. and J. Meller, *The role of nuclear medicine in infection and inflammation.* Lancet Infect Dis, 2001. 1(5): p. 326-33.

26. Palestro, C.J. and M.A. Torres, *Radionuclide imaging of nonosseous infection.* Q J Nucl Med, 1999. 43(1): p. 46-60.

27. Lucignani, G., *The many roads to infection imaging.* Eur J Nucl Med Mol Imaging, 2007. 34(11): p. 1873-7.

28. Pakos, E.E., et al., *Prosthesis infection: diagnosis after total joint arthroplasty with antigranulocyte scintigraphy with 99mTc-labeled monoclonal antibodies--a meta-analysis.* Radiology, 2007. 242(1): p. 101-8.

29. Signore, A., et al., *Radiolabelled lymphokines and growth factors for in vivo imaging of inflammation, infection and cancer.* Trends Immunol, 2003. 24(7): p. 395-402.

30. Love, C., et al., *5. Utility of F-18 FDG Imaging for Diagnosing the Infected Joint Replacement.* Clin Positron Imaging, 2000. 3(4): p. 159.

31. Signore, A., et al., *Can we produce an image of bacteria with radiopharmaceuticals?* Eur J Nucl Med Mol Imaging, 2008. 35(6): p. 1051-5.

32. Palestro, C.J., *Radionuclide imaging of infection: in search of the grail.* J Nucl Med, 2009. 50(5): p. 671-3.

33. Wadsö, I., *Microcalorimetric techniques for characterization of living cellular systems. Will there be any important practical applications?* Thermochimica Acta, 1995. 269/270: p. 337-350.

34. Beezer, A.E., *Biological Microcalorimetry.* Academic Press, Chelsea College, University of London, 1980.

35. A.M. James, M., DPhil, DSc, CChem, *Thermal and Energetic studies of cellular biologicas systems.* FRSC-WRIGHT, Bristol, 1987.

36. Schmidmaier, G., et al., *Prophylaxis and treatment of implant-related infections by antibiotic-coated implants: a review.* Injury, 2006. 37 Suppl 2: p. S105-12.

37. Hetrick, E.M. and M.H. Schoenfisch, *Reducing implant-related infections: active release strategies.* Chem Soc Rev, 2006. 35(9): p. 780-9.

38. Trampuz, A. and W. Zimmerli, *New strategies for the treatment of infections associated with prosthetic joints.* Curr Opin Investig Drugs, 2005. 6(2): p. 185-90.

39. Aksoy, D.Y. and S. Unal, *New antimicrobial agents for the treatment of Gram-positive bacterial infections.* Clin Microbiol Infect, 2008. 14(5): p. 411-20.

40. Zimmerli, W., O. Zak, and K. Vosbeck, *Experimental hematogenous infection of subcutaneously implanted foreign bodies.* Scand J Infect Dis, 1985. 17(3): p. 303-10.

41. Zimmerli, W., et al., *Microbiological tests to predict treatment outcome in experimental device-related infections due to Staphylococcus aureus.* J Antimicrob Chemother, 1994. 33(5): p. 959-67.

42. Trampuz, A., et al., *Efficacy of a novel rifamycin derivative, ABI-0043, against Staphylococcus aureus in an experimental model of foreign-body infection.* Antimicrob Agents Chemother, 2007. 51(7): p. 2540-5.

43. Zimmerli, W., et al., *Role of rifampin for treatment of orthopedic implant-related staphylococcal infections: a randomized controlled trial. Foreign-Body Infection (FBI) Study Group.* Jama, 1998. 279(19): p. 1537-41.

44. Bryskier, A., *Antimicrobial Agents, Antibacterials and Antifungals.* ASM Press, Washington, DC, 2005.

45. Wimer, S.M., L. Schoonover, and M.W. Garrison, *Levofloxacin: a therapeutic review.* Clin Ther, 1998. 20(6): p. 1049-70.

46. Robicsek, A., G.A. Jacoby, and D.C. Hooper, *The worldwide emergence of plasmid-mediated quinolone resistance.* Lancet Infect Dis, 2006. 6(10): p. 629-40.

47. Owens, R.C., Jr. and P.G. Ambrose, *Antimicrobial safety: focus on fluoroquinolones.* Clin Infect Dis, 2005. 41 Suppl 2: p. S144-57.

48. Ball, P., et al., *Comparative tolerability of the newer fluoroquinolone antibacterials.* Drug Saf, 1999. 21(5): p. 407-21.

49. Brickner, S.J., et al., *Synthesis and antibacterial activity of U-100592 and U-100766, two oxazolidinone antibacterial agents for the potential treatment of multidrug-resistant gram-positive bacterial infections.* J Med Chem, 1996. 39(3): p. 673-9.

50. Saager, B., et al., *Molecular characterisation of linezolid resistance in two vancomycin-resistant (VanB) Enterococcus faecium isolates using Pyrosequencing.* Eur J Clin Microbiol Infect Dis, 2008. 27(9): p. 873-8.

51. Besier, S., et al., *Linezolid resistance in Staphylococcus aureus: gene dosage effect, stability, fitness costs, and cross-resistances.* Antimicrob Agents Chemother, 2008. 52(4): p. 1570-2.

52. Manfredi, R., *Update on the appropriate use of linezolid in clinical practice.* Ther Clin Risk Manag, 2006. 2(4): p. 455-64.

53. Bassetti, M., et al., *Linezolid in the treatment of Gram-positive prosthetic joint infections.* J Antimicrob Chemother, 2005. 55(3): p. 387-90.

54. Soriano, A., et al., *Efficacy and tolerability of prolonged linezolid therapy in the treatment of orthopedic implant infections.* Eur J Clin Microbiol Infect Dis, 2007. 26(5): p. 353-6.

55. Slatter, J.G., et al., *Pharmacokinetics, toxicokinetics, distribution, metabolism and excretion of linezolid in mouse, rat and dog.* Xenobiotica, 2002. 32(10): p. 907-24.

56. Gebhart, B.C., B.C. Barker, and B.A. Markewitz, *Decreased serum linezolid levels in a critically ill patient receiving concomitant linezolid and rifampin.* Pharmacotherapy, 2007. 27(3): p. 476-9.

57. Wynalda, M.A., M.J. Hauer, and L.C. Wienkers, *Oxidation of the novel oxazolidinone antibiotic linezolid in human liver microsomes.* Drug Metab Dispos, 2000. 28(9): p. 1014-7.

58. McKee, E.E., et al., *Inhibition of mammalian mitochondrial protein synthesis by oxazolidinones.* Antimicrob Agents Chemother, 2006. 50(6): p. 2042-9.

59. Falagas, M.E., et al., *Comparison of antibiotics with placebo for treatment of acute sinusitis: a meta-analysis of randomised controlled trials.* Lancet Infect Dis, 2008. 8(9): p. 543-52.

60. Narita, M., B.T. Tsuji, and V.L. Yu, *Linezolid-associated peripheral and optic neuropathy, lactic acidosis, and serotonin syndrome.* Pharmacotherapy, 2007. 27(8): p. 1189-97.

61. Van Bambeke, F., *Glycopeptides in clinical development: pharmacological profile and clinical perspectives.* Curr Opin Pharmacol, 2004. 4(5): p. 471-8.

62. Chen, A.Y., M.J. Zervos, and J.A. Vazquez, *Dalbavancin: a novel antimicrobial.* Int J Clin Pract, 2007. 61(5): p. 853-63.

63. Anderson, V.R. and G.M. Keating, *Dalbavancin.* Drugs, 2008. 68(5): p. 639-48; discussion 649-51.

64. Billeter, M., et al., *Dalbavancin: a novel once-weekly lipoglycopeptide antibiotic.* Clin Infect Dis, 2008. 46(4): p. 577-83.

65. Lin, S.W., P.L. Carver, and D.D. DePestel, *Dalbavancin: a new option for the treatment of gram-positive infections.* Ann Pharmacother, 2006. 40(3): p. 449-60.

66. Seaton, R.A., *Daptomycin: rationale and role in the management of skin and soft tissue infections.* J Antimicrob Chemother, 2008. 62 Suppl 3: p. iii15-23.

67. John, A.K., et al., *Efficacy of daptomycin in implant-associated infection due to methicillin-resistant Staphylococcus aureus: importance of combination with rifampin.* Antimicrob Agents Chemother, 2009. 53(7): p. 2719-24.

68. Eisenstein, B.I., *Treatment of staphylococcal infections with cyclic lipopeptides.* Clin Microbiol Infect, 2008. 14 Suppl 2: p. 10-6.

69. Sande, O.Z.a.M.A., *Handbook of Animal Models of Infections.* Academic Press, 1999. Chapter 47: p. 409-418.

70. Baldoni, D., et al., *Linezolid alone or combined with rifampin against methicillin-resistant Staphylococcus aureus in experimental foreign-body infection.* Antimicrob Agents Chemother, 2009. 53(3): p. 1142-8.

71. Zimmerli, W., et al., *Pathogenesis of foreign body infection: description and characteristics of an animal model.* J Infect Dis, 1982. 146(4): p. 487-97.

72. Widmer, A.F., et al., *Correlation between in vivo and in vitro efficacy of antimicrobial agents against foreign body infections.* J Infect Dis, 1990. 162(1): p. 96-102.

73. Dayer, E., et al., *Quantitation of retroviral gp70 antigen, autoantibodies, and immune complexes in extravascular space in arthritic MRL-lpr/lpr mice. Use of a subcutaneously implanted tissue cage model.* Arthritis Rheum, 1987. 30(11): p. 1274-82.

74. McCallum, N., et al., *In vivo survival of teicoplanin-resistant Staphylococcus aureus and fitness cost of teicoplanin resistance.* Antimicrob Agents Chemother, 2006. 50(7): p. 2352-60.

75. Schaad, H.J., et al., *Comparative efficacies of imipenem, oxacillin and vancomycin for therapy of chronic foreign body infection due to methicillin-susceptible and -resistant Staphylococcus aureus.* J Antimicrob Chemother, 1994. 33(6): p. 1191-200.

76. Lucet, J.C., et al., *Treatment of experimental foreign body infection caused by methicillin-resistant Staphylococcus aureus.* Antimicrob Agents Chemother, 1990. 34(12): p. 2312-7.

77. Kristian, S.A., et al., *The ability of biofilm formation does not influence virulence of Staphylococcus aureus and host response in a mouse tissue cage infection model.* Microb Pathog, 2004. 36(5): p. 237-45.

78. Blaser, J., et al., *In vivo verification of in vitro model of antibiotic treatment of device-related infection.* Antimicrob Agents Chemother, 1995. 39(5): p. 1134-9.

79. Maglio, D. and D.P. Nicolau, *The integration of pharmacokinetics and pathogen susceptibility data in the design of rational dosing regimens.* Methods Find Exp Clin Pharmacol, 2004. 26(10): p. 781-8.

80. Jacobs, M.R., *How can we predict bacterial eradication?* Int J Infect Dis, 2003. 7 Suppl 1: p. S13-20.

81. Jacobs, M.R., *Optimisation of antimicrobial therapy using pharmacokinetic and pharmacodynamic parameters.* Clin Microbiol Infect, 2001. 7(11): p. 589-96.

82. Sandoe, J.A., et al., *Measurement of ampicillin, vancomycin, linezolid and gentamicin activity against enterococcal biofilms.* J Antimicrob Chemother, 2006. 57(4): p. 767-70.

83. Widmer, A.F., et al., *Killing of nongrowing and adherent Escherichia coli determines drug efficacy in device-related infections.* Antimicrob Agents Chemother, 1991. 35(4): p. 741-6.

84. Schwank, S., et al., *Impact of bacterial biofilm formation on in vitro and in vivo activities of antibiotics.* Antimicrob Agents Chemother, 1998. 42(4): p. 895-8.

85. Waibel, R., et al., *New derivatives of vitamin B12 show preferential targeting of tumors.* Cancer Res, 2008. 68(8): p. 2904-11.

86. Andrej Trampuz, J.M.S., Douglas R. Osmon, Franklin R. Cockerill, Arlen D. Hanssen, Robin Patel, *Advances in the laboratory diagnosis of prosthetic joint infection.* Reviews in Medical Microbiology, 2003. 14(1): p. 1-14.

87. Prandini, N., et al., *Nuclear medicine imaging of bone infections.* Nucl Med Commun, 2006. 27(8): p. 633-44.

88. Pakos, E.E., et al., *Use of (99m)Tc-sulesomab for the diagnosis of prosthesis infection after total joint arthroplasty.* J Int Med Res, 2007. 35(4): p. 474-81.

89. Ferro-Flores, G., et al., *In vitro and in vivo assessment of 99mTc-UBI specificity for bacteria.* Nucl Med Biol, 2003. 30(6): p. 597-603.

90. G. Ferro-Flores, C.A.d.M., P. Palomares-Rodriguez, L. Meléndez-Alafort and M. Pedraza-Lopez, *Kit for instant 99mTc labeling of the antimicrobial peptide ubiquicidin.* Journal of Radioanalytical and Nuclear Chemistry, 2005. 266(2): p. 307-311.

91. Melendez-Alafort, L., et al., *Detection of sites of infection in mice using 99mTc-labeled PN(2)S-PEG conjugated to UBI and 99mTc-UBI: a comparative biodistribution study.* Nucl Med Biol, 2009. 36(1): p. 57-64.

92. Welling, M.M., et al., *Radiochemical and biological characteristics of 99mTc-UBI 29-41 for imaging of bacterial infections.* Nucl Med Biol, 2002. 29(4): p. 413-22.

93. Akhtar, M.S., et al., *99mTc-labeled antimicrobial peptide ubiquicidin (29-41) accumulates less in Escherichia coli infection than in Staphlococcus aureus infection.* J Nucl Med, 2004. 45(5): p. 849-56.

94. Sarda-Mantel, L., et al., *Evaluation of 99mTc-UBI 29-41 scintigraphy for specific detection of experimental Staphylococcus aureus prosthetic joint infections.* Eur J Nucl Med Mol Imaging, 2007. 34(8): p. 1302-9.

95. Malamitsi, J., et al., *Infecton: a 99mTc-ciprofloxacin radiopharmaceutical for the detection of bone infection.* Clin Microbiol Infect, 2003. 9(2): p. 101-9.

96. Britton, K.E., et al., *Imaging bacterial infection with (99m)Tc-ciprofloxacin (Infecton).* J Clin Pathol, 2002. 55(11): p. 817-23.

97. Sarda, L., et al., *Evaluation of (99m)Tc-ciprofloxacin scintigraphy in a rabbit model of Staphylococcus aureus prosthetic joint infection.* J Nucl Med, 2002. 43(2): p. 239-45.

98. Appelboom, T., et al., *Evaluation of technetium-99m-ciprofloxacin (Infecton) for detecting sites of inflammation in arthritis.* Rheumatology (Oxford), 2003. 42(10): p. 1179-82.

99. Sonmezoglu, K., et al., *Usefulness of 99mTc-ciprofloxacin (infecton) scan in diagnosis of chronic orthopedic infections: comparative study with 99mTc-HMPAO leukocyte scintigraphy.* J Nucl Med, 2001. 42(4): p. 567-74.

100. De Winter, F., et al., *99mTc-ciprofloxacin planar and tomographic imaging for the diagnosis of infection in the postoperative spine: experience in 48 patients.* Eur J Nucl Med Mol Imaging, 2004. 31(2): p. 233-9.

101. Larikka, M.J., et al., *Comparison of 99mTc ciprofloxacin, 99mTc white blood cell and three-*

phase bone imaging in the diagnosis of hip prosthesis infections: improved diagnostic accuracy with extended imaging time. Nucl Med Commun, 2002. 23(7): p. 655-61.

102. Zhang, J., et al., *Synthesis and biodistribution of a novel (99m)TcN complex of ciprofloxacin dithiocarbamate as a potential agent for infection imaging.* Bioorg Med Chem Lett, 2008. 18(19): p. 5168-70.

103. Lazzeri, E., et al., *Scintigraphic imaging of vertebral osteomyelitis with 111in-biotin.* Spine, 2008. 33(7): p. E198-204.

104. Kristian, S.A., et al., *Alanylation of teichoic acids protects Staphylococcus aureus against Toll-like receptor 2-dependent host defense in a mouse tissue cage infection model.* J Infect Dis, 2003. 188(3): p. 414-23.

105. Sierra, J.M., et al., *Accumulation of 99mTc-ciprofloxacin in Staphylococcus aureus and Pseudomonas aeruginosa.* Antimicrob Agents Chemother, 2008. 52(7): p. 2691-2.

106. Rodriguez-Puig D., C.P., D. Fuster, A. Soriano, J.M. Sierra, S. Rub, J. Suades, *A new method of [99mTc]-ciprofloxacin preparation and quality control.* J. Labelled Comp. Radiopharm, 2006. 49: p. 1171-1176.

107. Ferro-Flores, G., et al., *Molecular recognition and stability of 99mTc-UBI 29-41 based on experimental and semiempirical results.* Appl Radiat Isot, 2004. 61(6): p. 1261-8.

108. Yeaman, M.R. and N.Y. Yount, *Mechanisms of antimicrobial peptide action and resistance.* Pharmacol Rev, 2003. 55(1): p. 27-55.

109. McCaffrey, C., et al., *Quinolone accumulation in Escherichia coli, Pseudomonas aeruginosa, and Staphylococcus aureus.* Antimicrob Agents Chemother, 1992. 36(8): p. 1601-5.

110. Siaens, R.H., et al., *Synthesis and comparison of 99mTc-enrofloxacin and 99mTc-ciprofloxacin.* J Nucl Med, 2004. 45(12): p. 2088-94.

111. Alexander, K., et al., *Binding of ciprofloxacin labelled with technetium Tc 99m versus 99mTc-pertechnetate to a live and killed equine isolate of Escherichia coil.* Can J Vet Res, 2005. 69(4): p. 272-7.

112. Piffeteau, A. and M. Gaudry, *Biotin uptake: influx, efflux and countertransport in Escherichia coli K12.* Biochim Biophys Acta, 1985. 816(1): p. 77-82.

113. Akhtar, M.S., et al., *Antimicrobial peptide 99mTc-ubiquicidin 29-41 as human infection-imaging agent: clinical trial.* J Nucl Med, 2005. 46(4): p. 567-73.

114. Melendez-Alafort, L., et al., *Biokinetics of (99m)Tc-UBI 29-41 in humans.* Nucl Med Biol, 2004. 31(3): p. 373-9.

115. Gandomkar, M., et al., *Clinical evaluation of antimicrobial peptide [(99m)Tc/Tricine/HYNIC(0)]ubiquicidin 29-41 as a human-specific infection imaging agent.* Nucl Med Biol, 2009. 36(2): p. 199-205.

116. Annovazzi, A., et al., *Nuclear medicine imaging of inflammatory/infective disorders of the abdomen.* Nucl Med Commun, 2005. 26(7): p. 657-64.

117. Capriotti, G., M. Chianelli, and A. Signore, *Nuclear medicine imaging of diabetic foot infection: results of meta-analysis.* Nucl Med Commun, 2006. 27(10): p. 757-64.

118. Cascini, G.L., et al., *Fever of unknown origin, infection of subcutaneous devices, brain abscesses and endocarditis.* Nucl Med Commun, 2006. 27(3): p. 213-22.

119. Chianelli, M., et al., *Receptor binding ligands to image infection.* Curr Pharm Des, 2008. 14(31): p. 3316-25.

120. Rusckowski, M., et al., *Investigations of a (99m)Tc-labeled bacteriophage as a potential infection-specific imaging agent.* J Nucl Med, 2004. 45(7): p. 1201-8.

121. Akhtar, M.S., et al., *An imaging analysis of (99m)Tc-UBI (29-41) uptake in S. aureus infected thighs of rabbits on ciprofloxacin treatment.* Eur J Nucl Med Mol Imaging, 2008. 35(6): p. 1056-64.

122. Rodionov, D.A., et al., *Comparative genomics of the vitamin B12 metabolism and regulation in prokaryotes.* J Biol Chem, 2003. 278(42): p. 41148-59.

123. Chimento, D.P., R.J. Kadner, and M.C. Wiener, *The Escherichia coli outer membrane cobalamin transporter BtuB: structural analysis of calcium and substrate binding, and identification of orthologous transporters by sequence/structure conservation.* J Mol Biol, 2003. 332(5): p. 999-1014.

124. Roth, J.R., J.G. Lawrence, and T.A. Bobik, *Cobalamin (coenzyme B12): synthesis and biological significance.* Annu Rev Microbiol, 1996. 50: p. 137-81.

125. Weng, J., et al., *The conformational coupling and translocation mechanism of vitamin B12 ATP-binding cassette transporter BtuCD.* Biophys J, 2008. 94(2): p. 612-21.

126. Giannella, R.A., S.A. Broitman, and N. Zamcheck, *Vitamin B12 uptake by intestinal microorganisms: mechanism and relevance to syndromes of intestinal bacterial overgrowth.* J Clin Invest, 1971. 50(5): p. 1100-7.

127. Omori, H., et al., *Correlation between the level of vitamin-B12-dependent methionine synthetase and intracellular concentration of vitamin B12 in some bacteria.* Eur J Biochem, 1974. 47(1): p. 207-18.

128. Christensen, E.I. and H. Birn, *Megalin and cubilin: synergistic endocytic receptors in renal proximal tubule.* Am J Physiol Renal Physiol, 2001. 280(4): p. F562-73.

129. Christensen, E.I. and H. Birn, *Megalin and cubilin: multifunctional endocytic receptors.* Nat Rev Mol Cell Biol, 2002. 3(4): p. 256-66.

130. Burger, R.L., C.S. Mehlman, and R.H. Allen, *Human plasma R-type vitamin B12-binding proteins. I. Isolation and characterization of transcobalamin I. TRANSCOBALAMIN III. and the normal granulocyte vitamin B12-binding protein.* J Biol Chem, 1975. 250(19): p. 7700-6.

131. Burger, R.L., et al., *Human plasma R-type vitamin B12-binding proteins. II. The role of transcobalamin I, transcobalamin III, and the normal granulocyte vitamin B12-binding protein in the plasma transport of vitamin B12*. J Biol Chem, 1975. 250(19): p. 7707-13.

132. Fellows, R.E., *The Schilling test in the diagnosis of pernicious anemia.* McGill Med J, 1958. 27(1): p. 53-8.

133. Flodh, H. and S. Ullberg, *Accumulation of labelled vitamin B12 in some transplanted tumours.* Int J Cancer, 1968. 3(5): p. 694-9.

134. Collins, D.A., et al., *Biodistribution of radiolabeled adenosylcobalamin in patients diagnosed with various malignancies.* Mayo Clin Proc, 2000. 75(6): p. 568-80.

135. Stichelberger, A., et al., *Versatile synthetic approach to new bifunctional chelating agents tailor made for labeling with the fac-[M(CO)(3)](+) core (M = Tc, (99m)Tc, Re): synthesis, in vitro, and in vivo behavior of the model complex [M(APPA)(CO)(3)] (APPA = [(5-amino-pentyl)-pyridin-2-yl-methyl-amino]-acetic acid).* Nucl Med Biol, 2003. 30(5): p. 465-70.

136. Bernstein, L.R., *Mechanisms of therapeutic activity for gallium.* Pharmacol Rev, 1998. 50(4): p. 665-82.

137. van Asselt, D.Z., et al., *Cobalamin-binding proteins in normal and cobalamin-deficient older subjects.* Ann Clin Biochem, 2003. 40(Pt 1): p. 65-9.

138. Lavender, J.P., et al., *Gallium 67 citrate scanning in neoplastic and inflammatory lesions.* Br J Radiol, 1971. 44(521): p. 361-6.

139. Palestro, C.J., *The current role of gallium imaging in infection.* Semin Nucl Med, 1994. 24(2):

p. 128-41.

140. Oyen, W.J., O.C. Boerman, and F.H. Corstens, *Animal models of infection and inflammation and their role in experimental nuclear medicine.* J Microbiol Methods, 2001. 47(2): p. 151-7.

141. Tomic, V., et al., *Comprehensive strategy to prevent nosocomial spread of methicillin-resistant Staphylococcus aureus in a highly endemic setting.* Arch Intern Med, 2004. 164(18): p. 2038-43.

142. Ito, T., et al., *Structural comparison of three types of staphylococcal cassette chromosome mec integrated in the chromosome in methicillin-resistant Staphylococcus aureus.* Antimicrob Agents Chemother, 2001. 45(5): p. 1323-36.

143. McKinney, T.K., et al., *Transcription of the gene mediating methicillin resistance in Staphylococcus aureus (mecA) is corepressed but not coinduced by cognate mecA and beta-lactamase regulators.* J Bacteriol, 2001. 183(23): p. 6862-8.

144. Lorian, V., *Antibiotics in Laboratory Medicine, V Edition.* 2005.

145. Brown, D.F., et al., *Guidelines for the laboratory diagnosis and susceptibility testing of methicillin-resistant Staphylococcus aureus (MRSA).* J Antimicrob Chemother, 2005. 56(6): p. 1000-18.

146. Fang, H. and G. Hedin, *Use of cefoxitin-based selective broth for improved detection of methicillin-resistant Staphylococcus aureus.* J Clin Microbiol, 2006. 44(2): p. 592-4.

147. Felten, A., et al., *Evaluation of three techniques for detection of low-level methicillin-resistant Staphylococcus aureus (MRSA): a disk diffusion method with cefoxitin and moxalactam, the Vitek 2 system, and the MRSA-screen latex agglutination test.* J Clin Microbiol, 2002. 40(8): p. 2766-71.

148. von Eiff, C., et al., *Microbiological evaluation of a new growth-based approach for rapid detection of methicillin-resistant Staphylococcus aureus.* J Antimicrob Chemother, 2008. 61(6): p. 1277-80.

149. Wiley, J., *Methods in Biochemical Analysis.* New York, 1976. 24.

150. Mardh, P., et al., *Kinetics of the actions of tetracyclines on Escherichia coli as studied by microcalorimetry.* Antimicrob Agents Chemother, 1976. 10(4): p. 604-9.

151. von Ah, U., D. Wirz, and A.U. Daniels, *Rapid differentiation of methicillin-susceptible Staphylococcus aureus from methicillin-resistant S. aureus and MIC determinations by isothermal microcalorimetry.* J Clin Microbiol, 2008. 46(6): p. 2083-7.

152. Hartman, B.J. and A. Tomasz, *Low-affinity penicillin-binding protein associated with beta-lactam resistance in Staphylococcus aureus.* J Bacteriol, 1984. 158(2): p. 513-6.

153. Mackenzie, A.M., et al., *Evidence that the National Committee for Clinical Laboratory Standards disk test is less sensitive than the screen plate for detection of low-expression-class methicillin-resistant Staphylococcus aureus.* J Clin Microbiol, 1995. 33(7): p. 1909-11.

154. Stranden, A., R. Frei, and A.F. Widmer, *Molecular typing of methicillin-resistant Staphylococcus aureus: can PCR replace pulsed-field gel electrophoresis?* J Clin Microbiol, 2003. 41(7): p. 3181-6.

155. Jana M. Swenson, R.S., Jean Patel, *The Cefoxitin Disk Test - What a Clinical Microbiologist Need To Know.* Clinical Microbiology Newsletter, 2007. 29(5): p. 33-40.

156. Tomasz, A., S. Nachman, and H. Leaf, *Stable classes of phenotypic expression in methicillin-resistant clinical isolates of staphylococci.* Antimicrob Agents Chemother, 1991. 35(1): p. 124-9.

157. Witte, W., et al., *Methicillin-resistant Staphylococcus aureus ST398 in humans and animals, Central Europe.* Emerg Infect Dis, 2007. 13(2): p. 255-8.

158. de Lencastre, H., et al., *Molecular aspects of methicillin resistance in Staphylococcus aureus.* J Antimicrob Chemother, 1994. 33(1): p. 7-24.

159. Niemeyer, D.M., et al., *Role of mecA transcriptional regulation in the phenotypic expression of methicillin resistance in Staphylococcus aureus*. J Bacteriol, 1996. 178(18): p. 5464-71.

160. Casey, A.L., P.A. Lambert, and T.S. Elliott, *Staphylococci.* Int J Antimicrob Agents, 2007. 29 Suppl 3: p. S23-32.

161. Haddadin, A.S., S.A. Fappiano, and P.A. Lipsett, *Methicillin resistant Staphylococcus aureus (MRSA) in the intensive care unit.* Postgrad Med J, 2002. 78(921): p. 385-92.

162. Donlan, R.M., *Biofilms and device-associated infections.* Emerg Infect Dis, 2001. 7(2): p. 277-81.

163. Proctor, R.A. and A. von Humboldt, *Bacterial energetics and antimicrobial resistance.* Drug Resist Updat, 1998. 1(4): p. 227-35.

164. Witte, W., et al., *Emergence and spread of antibiotic-resistant Gram-positive bacterial pathogens.* Int J Med Microbiol, 2008. 298(5-6): p. 365-77.

165. Carson, K.C., et al., *In Vitro susceptibility of methicillin-resistant Staphylococcus aureus and methicillin-susceptible Staphylococcus aureus to a new antimicrobial, copper silicate.* Antimicrob Agents Chemother, 2007. 51(12): p. 4505-7.

166. Frank, K.L. and R. Patel, *Activity of sodium metabisulfite against planktonic and biofilm Staphylococcus species.* Diagn Microbiol Infect Dis, 2007. 57(4): p. 355-9.

167. Dale, S.E., M.T. Sebulsky, and D.E. Heinrichs, *Involvement of SirABC in iron-siderophore import in Staphylococcus aureus.* J Bacteriol, 2004. 186(24): p. 8356-62.

168. Modun, B., J. Morrissey, and P. Williams, *The staphylococcal transferrin receptor: a glycolytic enzyme with novel functions.* Trends Microbiol, 2000. 8(5): p. 231-7.

169. Modun, B.J., et al., *The Staphylococcus aureus and Staphylococcus epidermidis transferrin-binding proteins are expressed in vivo during infection.* Microbiology, 1998. 144 (Pt 4): p. 1005-12.

170. Ratledge, C. and L.G. Dover, *Iron metabolism in pathogenic bacteria.* Annu Rev Microbiol, 2000. 54: p. 881-941.

171. Rouault, T.A., *Microbiology. Pathogenic bacteria prefer heme.* Science, 2004. 305(5690): p. 1577-8.

172. Kaneko, Y., et al., *The transition metal gallium disrupts Pseudomonas aeruginosa iron metabolism and has antimicrobial and antibiofilm activity.* J Clin Invest, 2007. 117(4): p. 877-88.

173. Peeters, E., H.J. Nelis, and T. Coenye, *Resistance of planktonic and biofilm-grown Burkholderia cepacia complex isolates to the transition metal gallium.* J Antimicrob Chemother, 2008. 61(5): p. 1062-5.

174. Bernstein, L.R., et al., *Chemistry and pharmacokinetics of gallium maltolate, a compound with high oral gallium bioavailability.* Met Based Drugs, 2000. 7(1): p. 33-47.

175. DeLeon, K., et al., *Gallium maltolate treatment eradicates Pseudomonas aeruginosa infection in thermally injured mice.* Antimicrob Agents Chemother, 2009. 53(4): p. 1331-7.

176. Clinical Laboratory Standards Institute, W., PA, *Methods for dilution antimicrobial susceptibility tests for bacteria that grow aerobically, 7th ed. NCCLS document M7-A7.* 2003.

177. Baldoni, D., et al., *Performance of microcalorimetry for early detection of methicillin resistance in clinical isolates of Staphylococcus aureus.* J Clin Microbiol, 2009. 47(3): p. 774-6.

178. Ceri, H., et al., *The Calgary Biofilm Device: new technology for rapid determination of antibiotic susceptibilities of bacterial biofilms.* J Clin Microbiol, 1999. 37(6): p. 1771-6.

179. Moskowitz, S.M., et al., *Clinically feasible biofilm susceptibility assay for isolates of Pseudomonas aeruginosa from patients with cystic fibrosis.* J Clin Microbiol, 2004. 42(5): p. 1915-22.

180. Christensen, G.D., et al., *Adherence of coagulase-negative staphylococci to plastic tissue culture plates: a quantitative model for the adherence of staphylococci to medical devices*. J Clin Microbiol, 1985. 22(6): p. 996-1006.

181. Ziebuhr, W., et al., *Detection of the intercellular adhesion gene cluster (ica) and phase variation in Staphylococcus epidermidis blood culture strains and mucosal isolates.* Infect Immun, 1997. 65(3): p. 890-6.

182. Boling, E.A., G.C. Blanchard, and W.J. Russell, *Bacterial identification by microcalorimetry.* Nature, 1973. 241(5390): p. 472-3.

183. Per-Anders Mardh, T.R., Karl-Erik Andersson, Ingemar Wadso, *Kinetics of the Actions of Tetracyclines on Escherichia coli as Studied by Microcalorimetry.* Antimicrobial Agents and Chemotherapy, 1976. 10(4): p. 604-609.

184. Donlan, R.M. and J.W. Costerton, *Biofilms: survival mechanisms of clinically relevant microorganisms.* Clin Microbiol Rev, 2002. 15(2): p. 167-93.

185. Brandt, C.M., et al., *Staphylococcus aureus prosthetic joint infection treated with prosthesis removal and delayed reimplantation arthroplasty.* Mayo Clin Proc, 1999. 74(6): p. 553-8.

186. Laffer, R.R., et al., *Outcome of prosthetic knee-associated infection: evaluation of 40 consecutive episodes at a single centre.* Clin Microbiol Infect, 2006. 12(5): p. 433-9.

187. Drancourt, M., et al., *Oral treatment of Staphylococcus spp. infected orthopaedic implants with fusidic acid or ofloxacin in combination with rifampicin.* J Antimicrob Chemother, 1997. 39(2): p. 235-40.

188. Zavasky, D.M. and M.A. Sande, *Reconsideration of rifampin: a unique drug for a unique infection.* Jama, 1998. 279(19): p. 1575-7.

189. Murillo, O., et al., *Efficacy of high doses of levofloxacin in experimental foreign-body infection by methicillin-susceptible Staphylococcus aureus.* Antimicrob Agents Chemother, 2006. 50(12): p. 4011-7.

190. Soriano, A., et al., *Treatment of acute post-surgical infection of joint arthroplasty.* Clin Microbiol Infect, 2006. 12(9): p. 930-3.

191. Widmer, A.F., et al., *Antimicrobial treatment of orthopedic implant-related infections with rifampin combinations.* Clin Infect Dis, 1992. 14(6): p. 1251-3.

192. Bonomo, R.A., *Multiple antibiotic-resistant bacteria in long-term-care facilities: An emerging problem in the practice of infectious diseases.* Clin Infect Dis, 2000. 31(6): p. 1414-22.

193. Thomson, C.J., *The global epidemiology of resistance to ciprofloxacin and the changing nature of antibiotic resistance: a 10 year perspective.* J Antimicrob Chemother, 1999. 43 Suppl A: p. 31-40.

194. Shams, W.E. and R.P. Rapp, *Methicillin-resistant staphylococcal infections: an important consideration for orthopedic surgeons.* Orthopedics, 2004. 27(6): p. 565-8.

195. Tverdek, F.P., C.W. Crank, and J. Segreti, *Antibiotic therapy of methicillin-resistant Staphylococcus aureus in critical care.* Crit Care Clin, 2008. 24(2): p. 249-60, vii-viii.

196. Grohs, P., M.D. Kitzis, and L. Gutmann, *In vitro bactericidal activities of linezolid in combination with vancomycin, gentamicin, ciprofloxacin, fusidic acid, and rifampin against Staphylococcus aureus.* Antimicrob Agents Chemother, 2003. 47(1): p. 418-20.

197. Rybak, M.J., et al., *Comparative in vitro activities and postantibiotic effects of the oxazolidinone compounds eperezolid (PNU-100592) and linezolid (PNU-100766) versus vancomycin against Staphylococcus aureus, coagulase-negative staphylococci, Enterococcus faecalis, and Enterococcus faecium.* Antimicrob Agents Chemother, 1998. 42(3): p. 721-4.

198. Shinabarger, D.L., et al., *Mechanism of action of oxazolidinones: effects of linezolid and eperezolid on translation reactions.* Antimicrob Agents Chemother, 1997. 41(10): p. 2132-6.

199. Swaney, S.M., et al., *The oxazolidinone linezolid inhibits initiation of protein synthesis in bacteria.* Antimicrob Agents Chemother, 1998. 42(12): p. 3251-5.

200. Jacqueline, C., et al., *In vitro activity of linezolid alone and in combination with gentamicin, vancomycin or rifampicin against methicillin-resistant Staphylococcus aureus by time-kill curve methods.* J Antimicrob Chemother, 2003. 51(4): p. 857-64.

201. Bassetti, M., et al., *Linezolid treatment of prosthetic hip Infections due to methicillin-resistant Staphylococcus aureus (MRSA).* J Infect, 2001. 43(2): p. 148-9.

202. Prugger, V., et al., *Treatment with linezolid and rifampicin for 18 months for recurrent infection of a megaprosthesis in a patient with Ewing's sarcoma.* Int J Antimicrob Agents, 2004. 24(6): p. 628-30.

203. Zimmerli, W., *Experimental models in the investigation of device-related infections.* J Antimicrob Chemother, 1993. 31 Suppl D: p. 97-102.

204. Murray, P.R., E. J. Baron, J. H. Jorgensen, M. A. Pfaller, and R. H. Yolken, *Manual of clinical microbiology.* 2003.

205. Stalker, D.J. and G.L. Jungbluth, *Clinical pharmacokinetics of linezolid, a novel oxazolidinone antibacterial.* Clin Pharmacokinet, 2003. 42(13): p. 1129-40.

206. Jorgensen, J.H., M.L. McElmeel, and C.W. Trippy, *In vitro activities of the oxazolidinone antibiotics U-100592 and U-100766 against Staphylococcus aureus and coagulase-negative Staphylococcus species.* Antimicrob Agents Chemother, 1997. 41(2): p. 465-7.

207. Sweeney, M.T. and G.E. Zurenko, *In vitro activities of linezolid combined with other antimicrobial agents against Staphylococci, Enterococci, Pneumococci, and selected gram-negative organisms.* Antimicrob Agents Chemother, 2003. 47(6): p. 1902-6.

208. Gee, T., et al., *Pharmacokinetics and tissue penetration of linezolid following multiple oral doses.* Antimicrob Agents Chemother, 2001. 45(6): p. 1843-6.

209. Andes, D., et al., *In vivo pharmacodynamics of a new oxazolidinone (linezolid).* Antimicrob Agents Chemother, 2002. 46(11): p. 3484-9.

210. Scherwood L. Gorbach, J.G.B., Neil R. Blacklow, *Infectious Diseases.* 2003.

211. Ament, P.W., N. Jamshed, and J.P. Horne, *Linezolid: its role in the treatment of gram-positive, drug-resistant bacterial infections.* Am Fam Physician, 2002. 65(4): p. 663-70.

Publications and Presentations

Publications

Linezolid alone or combined with rifampin against methicillin-resistant Staphylococcus aureus in experimental foreign-body infection.
Baldoni D, Haschke M, Rajacic Z, Zimmerli W, Trampuz A.
Antimicrob. Agents Chemother. 2009 Mar;53(3):1142-8. Epub 2008 Dec 15.

Performance of microcalorimetry for early detection of methicillin resistance in clinical isolates of Staphylococcus aureus.
Baldoni D, Hermann H, Frei R, Trampuz A, Steinhuber A.
J. Clin. Microbiol. 2009 Mar;47(3):774-6. Epub 2009 Jan 21.

Efficacy of daptomycin in implant-associated infection due to methicillin-resistant Staphylococcus aureus: importance of combination with rifampin.
John AK, Baldoni D, Haschke M, Rentsch K, Schaerli P, Zimmerli W, Trampuz A.
Antimicrob. Agents Chemother. 2009 Jul;53(7):2719-24. Epub 2009 Apr 13.

In Vitro Activity of Gallium Maltolate against Staphylococci in Logarithmic, Stationary and Biofilm Growth-Phase: Comparison of Conventional and Calorimetric Susceptibility Testing.
Baldoni D, Steinhuber A, Zimmerli W and Trampuz A.
Antimicrob Agents Chemother. Jan 2010.

Poster Presentations

Combination of Linezolid and Rifampin against Methicillin-Resistant *Staphylococcus aureus* (MRSA) in Experimental Foreign-Body Infection
D. Baldoni, Z. Rajacic, W. Zimmerli, A. Trampuz
47th Interscience Conference of Antimicrobial Agents and Chemotherapy, Chicago, IL, 17 to 20 September 2007 (B-811).

Radiolabeled Drivatives of Vitamin B_{12} for Potential Diagnosis of Implant Associated Infections
D. Baldoni, R. Waibel, R. Schibli, A. Trampuz
4th Swiss Experimental Surgery Symposium, Geneva, January 2008.

Dalbavancin (DAL) and Rifampin (RIF) against Methicillin-resistant *Staphylococcus aureus* (MRSA) in Experimental Foreign-body Infection
D. Baldoni, A. K. John, S. Aeppli, E. Angevaare, Z. Rajacic, W. Zimmerli, A. Trampuz
19th European Congress of Clinical Microbiology and Infectious Diseases, Helsinki, May 2009 (1024).

Activity of gallium maltolate against meticillin susceptible and methicillin resistant *Staphylococcus aureus* and *S. epidermidis*
D. Baldoni, A. Steinhuber, W. Zimmerli, A. Trampuz
Swiss ID Meeting, March 2009, Geneva.

Tc-99m Ciprofloxacin for Imaging of *Staphylococcus aureus* and *Escherichia coli* Infection in a Mouse Model of Foreign Body Infection
D. Baldoni, F. Galli, H. Maecke, A. Trampuz, A. Signore
4th European Molecular Imaging Meeting (EMIM), Barcelona, May 2009 (P-062).

Oral Presentations

Radiolabeled Vitamin B12: a Potential Marker for Implant Associated Infections?
D. Baldoni, R. Waibel, R. Schibli, A. Trampuz
Mayo Clinic Research Day, Basel, August 2007.

Radiolabeled Vitamin B_{12} – A Promising Tool for Diagnosing Infections?
D. Baldoni, R. Waibel, R. Schibli, A. Trampuz
Club de Pathologie, Bern March 2008.

In vitro Activity of Gallium against Methicillin-susceptible and Methicillin-resistant *Staphylococcus aureus* and *S. epidermidis*
D. Baldoni, A. Steinhuber, W. Zimmerli, A. Trampuz
18th European Congress of Clinical Microbiology and Infectious Diseases (ECCMID) in Barcelona, Spain, 19-22 April 2008 (presentation O 99).

Dalbavancin and Rifampin against MRSA in Experimental Foreign Body Infections
D. Baldoni, A. K. John, S. Aeppli, W. Zimmerli, A. Trampuz
Club De Pathologie, Bern, August 2009.

Curriculum Vitae

Name: Daniela Baldoni
Gempenstrasse 56
4053 Basel
Switzerland

Email: Daniela.baldoni@unibas.ch; danybaldoni@interfree.it

1982: Born on 22nd January in L'Aquila, Itlay

1987 - 1995: Primary and middle school, Avezzano (AQ), Italy

1995 - 2000: Scientific High School, Avezzano (AQ), Italy

2000: Federal Matura (94/ 100), Avezzano (AQ), Italy

2000 - 2005: Pharmaceutical Chemistry and Technology, University of Bologna, Italy

2005: From January to August, thesis research project entitled "Spectroscopic Techniques Applied to Study the Complexation Processes of Diazepam with Cyclodextrins and Human Albumin", supervision of Prof. Alex Drake, department of Pharmaceutical Sciences, King's College of London, UK

2005: University Master Degree in Pharmaceutical Chemistry and Technology (110/ 100 cum laude) University of Bologna, Italy

2005 – 2006: From October to July, pre-registration training in to private Pharmacy, Pharmacy S. Domenico, Bologna, Italy

2006: July, Federal Examination for Pharmacists, University of Bologna, Italy

2006 – 2009: PhD Student in the Infectious Disease research group at the Department of Biomedicine, University Hospital of Basel, Switzerland

2006: Federal Certificate for the Official Legitimation to Direct Animal Experiments, University of Basel, Switzerland

2007: Course in Molecular Biology, Rochester Mayo Clinic, USA

2007: Federal Certificate for Legitimation to Handle and Work with Radioactive Tracers, University of Basel, Switzerland

2009: January, Course Certificate "Key Issues in Drug Discovery and Development", Department of Pharmaceutical Sciences, Basel

2009: October, Final Examination to Obtain the Degree of Doctor of Natural Sciences (6/6 summa cum laude), with the thesis "Innovative Methods for the Diagnosis and Treatment of Implant-associated Infections", University of Basel, Switzerland